UNIVERSIDADE FEDERAL DO PARANÁ

ADRIANO ÁVILA GOULART

TAXAS DE DENUDAÇÃO E FERRAMENTAS MORFOMÉTRICAS APLICADAS NA ANÁLISE DA EVOLUÇÃO DE LONGO TERMO DO RELEVO DO SUL DA BACIA SEDIMENTAR BAURU

CURITIBA

2020

ADRIANO ÁVILA GOULART

TAXAS DE DENUDAÇÃO E FERRAMENTAS MORFOMÉTRICAS APLICADAS NA ANÁLISE DA EVOLUÇÃO DE LONGO TERMO DO RELEVO DO SUL DA BACIA SEDIMENTAR BAURU

Tese apresentada ao curso de Pós-Graduação em Geografia, Setor de Ciências da Terra, Universidade Federal do Paraná, como requisito parcial à obtenção do título de Doutor em Geografia.

Orientador: Prof. Dr. Leonardo José Cordeiro Santos

Coorientador: Prof. Dr. Lionel Siame

CURITIBA

2020

Catalogação na Fonte: Sistema de Bibliotecas, UFPR
Biblioteca de Ciência e Tecnologia

G694t Goulart, Adriano Ávila
Taxas de denudação e ferramentas morfométricas aplicadas na análise da evolução de longo termo do relevo do sul da bacia sedimentar Bauru [recurso eletrônico] / Adriano Ávila Goulart. – Curitiba, 2020.

Tese - Universidade Federal do Paraná, Setor de Ciências da Terra, Programa de Pós-Graduação em Geografia, 2020.

Orientador: Leonardo José Cordeiro Santos.
Coorientador: Lionel Siame.

1. Bacias sedimentares. 2. Nuclídeos cosmogênicos. 3. Morfometria. I. Universidade Federal do Paraná. II. Santos, Leonardo José Cordeiro. III. Siame, Lionel. IV. Título.

CDD: 551.44

Bibliotecária: Vanusa Maciel CRB- 9/1928

MINISTÉRIO DA EDUCAÇÃO
SETOR DE CIENCIAS DA TERRA
UNIVERSIDADE FEDERAL DO PARANÁ
PRÓ-REITORIA DE PESQUISA E PÓS-GRADUAÇÃO
PROGRAMA DE PÓS-GRADUAÇÃO GEOGRAFIA - 40001016035P1

TERMO DE APROVAÇÃO

Os membros da Banca Examinadora designada pelo Colegiado do Programa de Pós-Graduação em GEOGRAFIA da Universidade Federal do Paraná foram convocados para realizar a arguição da tese de Doutorado de **ADRIANO ÁVILA GOULART** intitulada: **TAXAS DE DENUDAÇÃO E FERRAMENTAS MORFOMÉTRICAS APLICADAS NA ANÁLISE DA EVOLUÇÃO A LONGO TERMO DO RELEVO DO SUDESTE DA BACIA SEDIMENTAR BAURU.** , sob orientação do Prof. Dr. LEONARDO JOSÉ CORDEIRO SANTOS, que após terem inquirido o aluno e realizada a avaliação do trabalho, são de parecer pela sua APROVAÇÃO no rito de defesa.
A outorga do título de doutor está sujeita à homologação pelo colegiado, ao atendimento de todas as indicações e correções solicitadas pela banca e ao pleno atendimento das demandas regimentais do Programa de Pós-Graduação.

CURITIBA, 30 de Outubro de 2020.

Assinatura Eletrônica
04/11/2020 14:00:10.0
LEONARDO JOSÉ CORDEIRO SANTOS
Presidente da Banca Examinadora

Assinatura Eletrônica
03/11/2020 16:28:05.0
CLAUDINEI TABORDA DA SILVEIRA
Avaliador Interno (UNIVERSIDADE FEDERAL DO PARANÁ)

Assinatura Eletrônica
11/11/2020 17:13:41.0
DANIEL PEIFER BEZERRA
Avaliador Externo (UNIVERSIDADE FEDERAL DE MINAS GERAIS)

Assinatura Eletrônica
25/11/2020 16:47:03.0
LUIS FELIPE SOARES CHEREM
Avaliador Externo (UNIVERSIDADE FEDERAL DE GOIÁS)

Assinatura Eletrônica
05/11/2020 09:25:41.0
PEDRO FONSECA DE ALMEIDA E VAL
Avaliador Externo (UNIVERSIDADE FEDERAL DE OURO PRETO)

Dedico esta tese ao meu irmão, Tiago Ávila Goulart.

AGRADECIMENTOS

O trabalho acadêmico muitas vezes parece ser um ato individual, um trabalho um tanto quanto solitário, contudo eu não poderia deixar de citar e agradecer algumas pessoas e instituições que, de maneira direta ou indireta, me auxiliaram a fazer esta pesquisa:

Primeiramente gostaria de agradecer à minha família, meus pais Gil Dumont e Filomena Ávila e meu irmão Tiago Goulart, pelo apoio incondicional em todos os momentos da minha vida.

Em seguida, deixo meus agradecimentos:

Ao professor Leonardo Santos (UFPR), pela orientação e confiança, e por ter me dado a oportunidade de trabalharmos juntos durante todo o período do doutorado. Ao professor Lionel Siame (AMU/CEREGE), pela coorientação, pelo acolhimento e suporte durante o período sanduíche na França, além das inúmeras contribuições que permitiram a conclusão desta tese. E ao professor Luis Cherem (UFGO) pelas conversas e trabalhos em conjunto durante a estadia fora do país.

Aos amigos, àqueles que de diversas formas, presentes ou não, acabaram por contribuir muito na elaboração desse trabalho.

Ao Departamento de Geografia e o Programa de Pós-Graduação em Geografia da Universidade Federal do Paraná, pelo apoio institucional, assim como os funcionários (da secretaria) Alexandra Gama, Luiz Zen, Adriana Oliveira e (do Labsed) Daniel Paredes, pela atenção e solicitude.

Aos colegas da Aix-Marseille Université, do CEREGE, (do laboratório de preparo das amostras) Laëtitia Leanni, Valéry Guillou, (do SIGéo) Jules Fleury e Philippe Dussouillez pela orientação e ajuda no desenvolvimento do doutorado durante o período sanduíche. Aos colegas de Équipe Terre et Planètes Brice Lebrun, Léa Pousse, Jesus Diaz e Clément Desormeaux, além dos colegas de pesquisa Romano Clementucci, Irene Puliti e Kamal Agrroud, por me fazerem sentir bem, mesmo longe de casa.

Por último, quero agradecer ao CNPQ e ao Programa CAPES/COFECUB pelo apoio financeiro e pelas bolsas concedidas ao longo do desenvolvimento deste estudo.

“It was the work of the quiet mountains, this torrent of purity at my feet.”

Jack Kerouac

RESUMO

Estudos que analisam a morfodinâmica a longo termo no Brasil utilizando mensurações de ^{10}Be in situ totalizaram 20 publicações até o final de 2019. Uma porção específica do território brasileiro, o sul da Bacia Sedimentar Bauru, já havia sido investigado por do Couto (2014), porém algumas lacunas ainda estavam abertas, como a generalização das taxas de denudação para uma área maior, assim como o grau de influência de feições geomorfológicas específicas remanescentes de outros períodos geológicos, como as paleovoçorocas e os inselbergs internos à essa bacia sedimentar. Diante desse contexto, o objetivo da tese foi compreender a evolução geomorfológica de longo-termo da porção sul da Bacia Sedimentar Bauru. A metodologia aplicada se baseou na aplicação de algoritmos sofisticados para a extração de informações quantitativas da topografia digital (ICR; χ; K_{sn}; HI; perfis topográficos longitudinais de rios e perfis swath), e na aplicação de ferramentas isotópicas (mensuração de concentrações de ^{10}Be em amostras de sedimentos fluviais extraídas de 20 bacias hidrográficas diferentes). A taxa de denudação de fundo calculada foi de 12.9 ±2.1 m/My, o que é consistente com os valores esperados para regiões relativamente planas, como é a área de estudo, oriunda de um paleodeserto. Correlações entre *low relief surfaces* e ciclos erosivos também confirmaram essa lenta evolução desde o Cretáceo até o modelado atual do relevo. A diferença da magnitude dos processos visualizada por trabalhos anteriores que analisaram as margens norte e sul do Rio Ivaí não se confirmou, visto que os erros acabaram por homogeneizar os valores norte (11.4 ±1.9 m/My) e sul (14.0 ±2.3 m/My). Assim, notou-se que a diferença observada por do Couto (2014) refletiu processos ocorridos nas cabeceiras de drenagem e não na região como um todo, o que acabou por superestimar os valores. Apesar de individualmente as paleovoçorocas apresentarem valores médios 3 vezes maiores que os regionais (PG, 42.7 ±3.7 m/My), essas feições mostraram-se integradas aos processos regionais de denudação, pois não elevam a média da taxa de denudação das bacias onde ocorrem. O que levou a conjectura de que a morfodinâmica da região pode ter evoluído a partir da formação e coalescência dessas paleovoçorocas, formadas durante o Plio-Pleistoceno, segundo os resultados de idade aproximada do início do processo de denudação. Por sua vez, os inselbergs se mostraram influentes nos processos regionais, já que esses atuaram diminuindo os valores de denudação nas bacias onde são encontrados. Sendo assim, notou-se que as feições de relevo relictuais na verdade são parte integrante da evolução regional, pois essas controlam processos locais, mas essa influência acaba homogeneizada/dissolvida, quando as escalas espacial e temporal são amplificadas.

Palavras-chave: Nuclídeos cosmogênicos ^{10}Be. Morfodinâmica. Bacia Sedimentar Bauru. Morfometria. Paleovoçorocas.

ABSTRACT

Studies that analyze long-term morphodynamics in Brazil using in situ ^{10}Be measurements totaled 20 publications until the end of 2019. A specific portion of the Brazilian territory, the southern Bauru Sedimentary Basin, had already been investigated by do Couto (2014), however, some gaps were still open, such as the generalization of denudation rates for a larger area, as well as the influence magnitude of specific geomorphological features remaining from other geological periods, such as paleogullies and inselbergs into this sedimentary basin. Given this context, the goal of the thesis was to understand the long-term geomorphological evolution of the the Bauru Sedimentary Basin southern portion. The applied methodology was based on morphometric (ICR; χ; K_{sn}; HI; longitudinal topographic profiles of rivers and swath profiles) and isotopic (measurement of ^{10}Be in situ of 20 hydrographic basins) tools. The background denudation rate calculated was 12.9 ± 2.1 m / My-1, which corroborated with the expected values for relatively flat regions, such as the study area, made from a paleodesert. Correlations between low relief surfaces and erosive cycles also confirmed these low values of evolution from the Cretaceous to the current relief model. The difference in the process's magnitude visualized by previous works that analyzed the north and south banks of the Ivaí River was not confirmed, since the uncertainties ended up homogenizing the north (11.4 ± 1.9 m / My-1) and south (14.0 ± 2.3 m / My-1) values. Thus, it was noted that the difference visualized by do Couto (2014) reflected processes that occurred at the drainage headwaters and not in the whole region, which ended up overestimating the values. Although the paleogullies individually present average values of 3 times higher than the regional ones (PG, 42.7 ± 3.7 m / My-1), these features were shown to be integrated with the regional denudation processes, as they do not increase the average denudation rate of the watersheds where they occur. This led to the conjecture that the region's morphodynamics may have evolved from the formation and coalescence of these paleogullies, formed during the Plio-Pleistocene, according to the approximate age of the denudation process beginning results. The inselbergs proved to be influential in regional processes since they acted by reducing the denudation values of the watersheds where they are found. Thus, it was noted that the relictual relief features are actually an integral part of regional evolution, as these control local processes, but this influence was being homogenized/dissolved, when the spatial and temporal scales are amplified.

Keywords: Cosmogenic nuclides ^{10}Be. Morphodynamics. Bauru Sedimentary Basin. Morphometry. Paleogullies.

SUMÁRIO

1 INTRODUÇÃO GERAL

As escalas, temporal e espacial, são fundamentais para a delimitação de um objeto de pesquisa na Geomorfologia. No contexto da morfodinâmica[1], são elas que definem os limites espaciais e a janela temporal que o pesquisador irá abordar ao longo da pesquisa. Com o desenvolvimento das técnicas de campo, para coleta de amostras, e de laboratório/gabinete, para a geração de dados primários, a tendência é que possamos cada vez mais expandir essas escalas, permitindo aos pesquisadores análises de grandes áreas com correlações cada vez mais antigas.

Um termo clássico e que vem sendo cada vez mais empregado nas pesquisas de Geomorfologia após esse aperfeiçoamento das técnicas é a evolução de longo-termo do relevo (Granger et al., 1996; Brocard et al., 2003; Bishop, 2007; Inkpen et al., 2010; Kirby e Whipple, 2012; Scuderi, 2017; Sembroni e Molin, 2018; Van Binh et al., 2019). A evolução de longo-termo refere-se a processos distintos mais lentos e duradouros, geralmente relacionados a processos erosivos, que moldaram os padrões de relevo encontrados atualmente em uma área predefinida, geralmente no interior de uma placa tectônica, longe da interferência de tectonismos que interfiram de maneira pontual e intensa na morfodinâmica em um curto período de tempo. Os trabalhos com ^{10}Be são exemplos dessa evolução metodológica que permitiu correlações de evolução do relevo de longo-termo, associando taxas de denudação às bacias hidrográficas.

No Brasil os estudos que se apoiam em metodologias de longo-termo, embasados pela análise isotópica do ^{10}Be, têm ganhado relevância nos últimos anos (Barreto et al., 2013; Cherem et al., 2012; do Couto et al., 2018; Gonzalez et al., 2016a; 2016b; Salgado et al., 2014; 2016; Sordi et al., 2018; Souza et al., 2019; Vasconcelos et al., 2019).

Esses trabalhos, mensuram isótopos cosmogênicos, como o ^{10}Be, para o cálculo da taxa de denudação. No Brasil, sem uma ação tectônica significativa desde o final do Cretáceo, 66 My, a evolução do relevo vem ocorrendo majoritariamente pela ação dos processos denudacionais, principalmente pela ação do clima atual e de paleoclimas, e das dinâmicas da rede de drenagem.

---

[1] Entende-se como morfodinâmica a análise dos processos de gênese e evolução do modelado (Tricart, 1977). Portanto, deve-se atentar não apenas para a morfologia do relevo, mas também para os processos que permitiram a formação e todo o histórico dinâmico que formou a paisagem analisada atualmente.

O fator climático é relevante para o entendimento no modelado do relevo de bacias intracratrônicas, não somente o clima atual, também o clima pós Cretáceo, após o término das manifestações magmáticas relacionadas a separação da Gondwana. Aproximadamente 66 My sem tectonismos significativos e com períodos glaciais de diferentes intensidades e durações faz com que a ação climática seja a chave de respostas de como as paisagens do país foram modeladas.

Uma das consequências diretas do clima e que está diretamente relacionada ao modelado do relevo é a rede de drenagem. A análise geomorfológica das principais bacias hidrográficas de uma região no contexto da morfodinâmica sulamericana também pode revelar pontos relevantes para a compreensão da evolução da paisagem de longo-termo.

Estruturas geológicas como a Bacia Bauru (BB), área de estudo da tese (Figura 0.1), são chaves para a compreensão da evolução da paisagem no interior do continente sulamericano, desde a separação da Gondwana até os dias atuais.

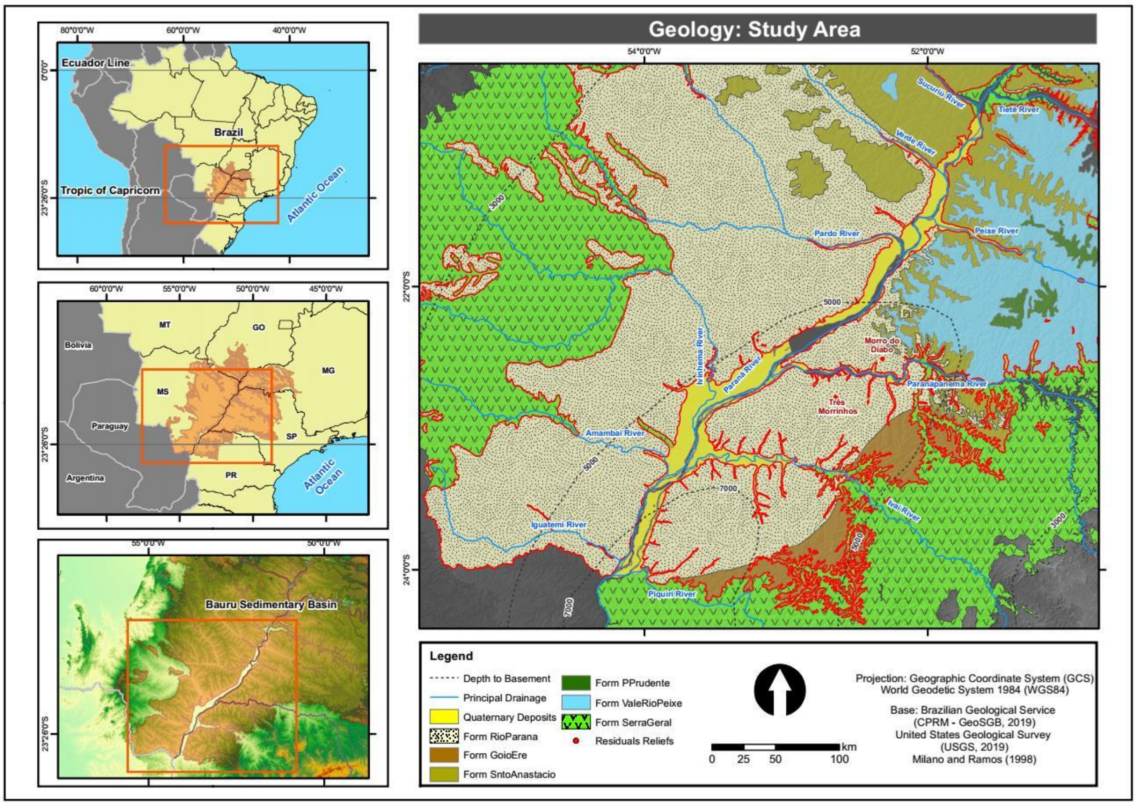

Figura 0.1: Área de estudo da tese, com a caracterização geológica simplificada.

Com uma área total de aproximadamente 370.000 km² (Fernandes et al., 2007), a BB apresenta lineamentos relacionados ao Transbrasiliano (Almeida et al,

2000) onde são encontrados grandes cursos hídricos como por exemplo o rio Paraná, e lineamentos perpendiculares posteriores (Milani e Ramos, 1998), associados a importantes drenagens no contexto regional como os rios Paranapanema, Ivaí, Piriquí, Ivinheima, entre outros.

A porção sul da BB apresenta uma especificidade geológica relevante para o entendimento da evolução do relevo sulamericano. O Grupo Caiuá, últimos depósitos da sequência estratigráfica da BB, composto pelas formações Santo Anastácio, Goio Erê e Rio Paraná, é constituído de rochas sedimentares formadas a partir da litificação de sedimentos do paleodeserto Caiuá (Fernandes, 1992). A localização do paleodeserto corresponde ao antigo depocentro da bacia, resposta isostática ao vulcanismo do cretáceo tardio (Milani e Ramos, 1998).

A evolução da paisagem, heranças de processos pretéritos que influenciaram, e continuam influenciando, na configuração atual da região, pode ser evidenciada em diversos elementos formadores das mesmas. Atualmente podemos encontrar, nas proximidades do antigo depocentro, o rio Paraná, correndo no lineamento Transbrasiliano (Almeida et al, 2000), em meio a uma litologia originada a partir do paleodeserto Caiuá. Porém como as últimas manifestações tectônicas foram há 66 My, os lineamentos tectônicos associados ao Transbrasiliano não condicionam a morfodinâmica recente da região.

Outras evidências de processos pretéritos, herdados de outras épocas geológicas que ainda influenciam a atual evolução da paisagem presentes na porção sul da BB, são algumas feições anômalas que foram identificadas pontualmente na região, e classificadas como relevos residuais compostos por arenitos silicificados (Fernandes et al., 2013) e algumas feições erosivas que, contrastando com erosões encontradas na região pós-ocupação do café em 1950, parecem remeter a condições climáticas distintas das atuais, possivelmente formadas durante a ação de paleoclimas, consideradas, portanto, como paleofeições[2] (Bigarella e Mazuchowski, 1985; Goulart e Santos, 2014).

As erosões contemporâneas na região sul da BB, na área de ocorrência do Gr. Caiuá, já chamavam a atenção dos pesquisadores desde os primeiros relatos de Maack (1968). Bigarella e Mazuchowski (1985) no livro guia do 3º Simpósio Nacional

---

[2] A explicação do conceito assim como a comprovação de que, de fato, são feições anteriores ao Holoceno foi feita ao longo da discussão dos resultados.

de Erosão realizado em Maringá-PR, abordam as características geológicas, pedológicas e climáticas, além da ocupação da região, que favoreceram a instalação, natural ou não, dos processos erosivos em meio a litologia dos arenitos do noroeste paranaense. Nota-se que não por acaso a realização de um evento nacional sobre erosão foi em uma área de ocorrência do atual Gr. Caiuá[3].

Um dos primeiros trabalhos a abordar a morfogenética da região de abrangência dessa litologia foi o de Justus (1985), publicado no ano do 3º Simpósio Nacional de Erosão. Para o referido autor, a geomorfologia atual da área é resultado de oscilações tectono-eustáticas do Terciário e glácio-eustáticas do Quaternário. Sendo que as oscilações paleoclimáticas quaternárias corresponderiam aos ciclos de dissecação e horizontalização do relevo na região.

A partir de 2012 o Laboratório de Biogeografia e Solos (LABS) da UFPR iniciou suas pesquisas na Região Noroeste do Paraná, tendo como principal enfoque a distribuição dos solos e sua relação com o relevo e a drenagem. As observações iniciais mostraram que ao norte do rio Ivaí predominam os Latossolos, associados a um relevo de colinas amplas e rede de drenagem pouco entalhada, enquanto que ao sul do rio Ivaí, com predomínio do relevo de colinas médias, onde os Argissolos ganham expressão, a rede de drenagem encontra-se mais densa e entalhada.

Essas observações somadas aos estudos desenvolvidos por Nakashima (1999), que caracterizaram morfologicamente e mediram essas formas relevo, indicam a ocorrência de diferentes graus de dissecação do mesmo na região, contudo, constatou-se que os trabalhos que visaram identificar e caracterizar os processos pedogenéticos, realizados em escala de topossequência, se mostraram insuficientes para uma melhor compreensão da relação solos e relevo em escala regional.

Assim, outras metodologias foram utilizadas para auxiliar nessa interpretação. Os primeiros resultados alcançados mostraram que às taxas de denudação onde predominam os Argissolos, são superiores quando comparadas ao norte do rio Ivaí, onde predominam os Latossolos, confirmando a hipótese inicial de que as vertentes

---

[3] Na época da publicação, ano de 1985, a classificação da unidade litoestratigráfica hoje conhecida como Grupo Caiuá era Formação Caiuá, tendo subido um nível categórico após o trabalho de Fernandes (1992) que elevou à Grupo Caiuá após o subdividir em três formações distintas conforme características estratigráficas e texturais: Formação Rio Paraná, Formação Goio Erê; e Formação Santo Anastácio.

ao sul se encontram em rearranjo morfológico, o que acelera os processos pedogenéticos de transformação vertical e lateral nas vertentes (do Couto, 2015).

Esses resultados permitiram a formulação de novas hipóteses, na expansão das pesquisas na região, como por exemplo o trabalho de Fumiya (2017), que identificou e mapeou a ocorrência de feições morfológicas, morretes, sustentados por ferricretes. Os resultados apontaram a origem desses materiais como provenientes da alteração do arenito, sendo possível identificar diferentes fases de precipitação de ferro até sua completa formação. O estudo da gênese desses ferricretes possibilitou a identificação de diferentes fases de ferruginização ocorridas pela acumulação absoluta do ferro em vales fluviais da região de estudo, criando encrustamentos de ferro nesses locais mais resistentes à erosão em relação aos materiais ao seu redor, resultando na inversão de relevo enquanto o processo de denudação da paisagem progredia (Fumiya, 2017).

A manutenção dessas feições morfológicas ao sul do rio Ivaí é um exemplo de que a maior taxa de denudação nessa área expôs esses corpos ferruginosos mais resistentes isolados por erosão diferencial, enquanto que ao norte, com menor taxa de denudação, essas feições sequer afloram.

Seguindo no mesmo raciocínio, a presença ou ausência de outras paleofeições apontadas por Bigarella e Mazuchowski (1985) e Goulart e Santos (2014), denominadas como paleovoçorocas[4], também revelariam a ação distinta da taxa de denudação nas margens do rio Ivaí. Ao norte do Ivaí a constatação da presença dessas feições, individualizadas, demonstraria a ação de processos já ocorridos ao sul, onde a taxa de denudação mais elevada possibilitou um maior recuo dos divisores de água e ao mesmo tempo uma coalescência das paleovoçorocas, não permitindo a sua identificação conforme ocorre ao norte do rio. O modelo teórico elaborado e separado em três fases, permite acompanhar a evolução desses processos descritos acima (Figura 0.2).

---

[4] A explicação do conceito assim como a comprovação de que, de fato, são voçorocas pleistocênicas foi feita ao longo da discussão dos resultados.

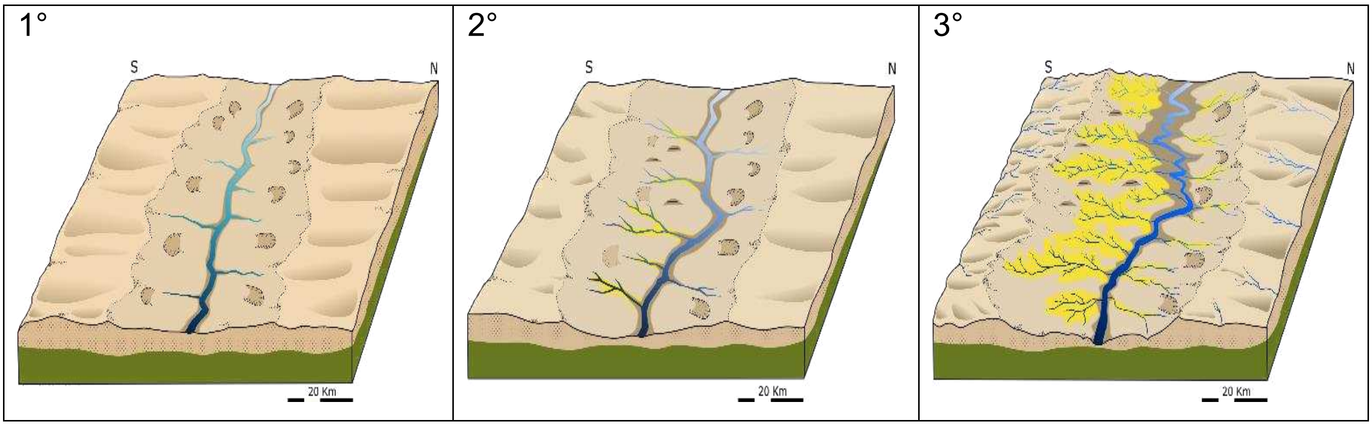

Figura 0.2: Modelo teórico de evolução do relevo na bacia do Rio Ivaí, Noroeste do Paraná: Basalto (Formação Serra Geral) em verde, Arenito (Grupo Caiuá) em bege e Argissolos em amarelo, com destaque para as paleovoçorocas nas fases 1 e 2 ao Norte e ao Sul, e na fase 3 apenas ao Norte, e para os morrotes, presentes a partir da exumação das superfícies sustentadas por ferricretes no tempo 2 e 3 apenas ao Sul. (Adaptado de Fumiya, 2017).

Assim, a existência dessas pesquisas pretéritas que se complementam e que lançam hipóteses até o momento ainda não comprovadas, justificam a continuidade dos estudos na região.

Prosseguindo com a ideia de compreender a evolução da paisagem da região Sul da Bacia Bauru, levantamentos de dados com metodologias baseadas na mensuração de taxas de denudação de grandes bacias, suplementares à análise já feita (do Couto et al., 2018) podem revelar como a morfodinâmica se deu a longo termo e em uma escala regional.

Diante desse contexto geomorfológico apresentado e do atual estado de desenvolvimento das pesquisas na região, as hipóteses aqui investigadas são as seguintes:

- A tendência observada por do Couto (2014) e do Couto et al. (2018) do sul da bacia do Ivaí ter taxas de denudação mais elevadas que o norte, pode ser extrapolada para as demais bacias que compõem o Gr. Caiuá;
- As paleovoçorocas interferem diretamente nas bacias em que estão presentes, fazendo com que a taxa de denudação dessas bacias, possivelmente muito elevadas, fique fora de um padrão regional.

Para tanto, a tese apresenta uma estrutura composta de itens denominados de gerais: introdução, metodologia, considerações e referências; e três capítulos de resultados compostos no formato de artigos. Assim, as partes gerais contribuem com assuntos mais abrangentes, genéricos, que se amarram com as aplicações feitas nos artigos dos resultados, mas que no corpo de um artigo, que é mais direto e aplicado na Geomorfologia, deixariam o texto carregado de informações, o que prejudicaria o foco da discussão. Visto que as partes gerais complementam o entendimento dos artigos, mas não necessariamente os compõem, essas foram escritas em português. Já os artigos dos resultados foram escritos em inglês, pois como já explicitado, pretende-se facilitar o procedimento de publicar a pesquisa em periódicos de visibilidade e relevância no contexto da Geomorfologia. As referências foram organizadas ao final de cada um dos respectivos artigos, sendo que as referências dos itens gerais encontra-se ao final da tese, no item denominado de referências gerais.

O primeiro capítulo dos resultados (item 3.1) analisou trabalhos de evolução de longo-termo do relevo já realizados no país, especificamente aqueles que se utilizaram do ^{10}Be para cálculos de taxas de denudação. O segundo capítulo dos resultados (item 3.2) trouxe uma descrição detalhada da região Sul da BB, com aplicações de índices morfométricos e extração de informações quantitativas da topografia digital que auxiliaram na interpretação da evolução da paisagem. O terceiro capítulo dos resultados (item 3.3) tratou da mensuração e posterior discussão das taxas de denudação de bacias hidrográficas da área de estudo, permitindo inferências sobre a morfodinâmica de longo termo do Sul da BB, além de um começo da compreensão da gênese e da evolução das paleofeições na dinâmica regional.

A abordagem da tese é, portanto, multiescalar espacial e temporalmente: afora o item 3.1, que aborda o estado da arte das pesquisas que se utilizam da mesma metodologia no país, os itens 3.2 e 3.3 abrangem uma escala temporal mais ampla, englobando os processos ocorridos desde o Mioceno até os dias de hoje. As escalas espaciais são também distintas, já que o item 3.2 analisa os processos regionais, do sul da BB, por meio do uso da morfometria e o item 3.3 foca na explicação da evolução geomorfológica das bacias hidrográficas situadas a sudoeste da BB, onde se concentram as pesquisas desenvolvidas pelo laboratório.

1.1 OBJETIVOS

1.1.1 OBJETIVO GERAL

A tese aqui apresentada tem o objetivo geral de compreender a evolução geomorfológica de longo-termo da porção sul da Bacia Sedimentar Bauru.

1.1.2 OBJETIVOS ESPECÍFICOS

- Realizar um levantamento detalhado dos trabalhos com ^{10}Be já realizados no país e sistematizar os resultados do estado da arte da referida metodologia;

- Identificar relevos residuais na região através de processos automatizados e associá-los a evolução regional;

- Aplicar índices morfométricos que relacionam os ajustes da rede de drenagem à evolução da paisagem;

- Correlacionar processos passados, antigos ciclos de erosões, através da análise em escala regional e local, caracterizando assim as *low reliefs surfaces*;

- Calcular a taxa de denudação, através da mensuração da abundância de ^{10}Be[5], em sedimentos fluviais extraídos de bacias hidrográficas representativas do Grupo Caiuá;

- Determinar a idade aproximada do início do processo de denudação das bacias mensuradas com nuclídeos cosmogênicos.

[5] O ^{26}Al e o ^{10}Be atmosférico também já foram mensurados juntamente com o ^{10}Be in situ. Porém como o prazo para a sistematização dos dados e redação da tese estava curto e as mensurações ainda estavam por terminar, optou-se por trabalhar apenas com o ^{10}Be in situ. Para as futuras publicações, espera-se integrar os demais isótopos cosmogênicos na análise.

2 METODOLOGIA GERAL

Os procedimentos metodológicos utilizados para alcançar os objetivos propostos acima foram divididos em dois subitens, para uma melhor organização das técnicas utilizadas em cada etapa do trabalho: Ferramentas Morfométricas e Ferramentas Isotópicas. É válido ressaltar que os três capítulos de discussão dos resultados se utilizaram das ferramentas abordadas a seguir. Como os resultados estão em formato de artigo e, consequentemente não há espaço para um detalhamento em cada um deles, optou-se por fazer essa descrição no item metodologia geral.

2.1 FERRAMENTAS MORFOMÉTRICAS

Nos últimos anos, o desenvolvimento tecnológico nas geociências permitiu um avanço sem precedentes no número de ferramentas e de índices utilizados para as análises geomorfológicas. Esse desenvolvimento possibilitou os geomorfólogos a extrair mais dados da superfície terrestre e de melhor qualidade, o que consequentemente impulsionou a comunidade científica a apresentar questões mais complexas sobre a evolução do modelado terrestre (Viles, 2016).

A morfometria ou geomorfometria, ciência que analisa quantitativamente a superfície terrestre, conjuntamente com os dados digitais, possibilitaram a criação de representações matemáticas que permitiram conjecturas para essas novas questões que vem surgindo com o aumento da complexidade das análises geomorfológicas. Sendo assim, a geomorfometria foi capaz de ampliar as escalas espaciais e temporais de análise da geomorfologia (Sofia, 2020).

Porém, como todo processo evolutivo na ciência, o desenvolvimento da geomorfometria acabou por apresentar novos desafios para os cientistas que se dedicaram ao incremento dessas técnicas e métodos inovadores, na quantificação dos processos geomorfológicos (Viles, 2016).

Em contraponto ao relevante trabalho de geomorfólogos clássicos de descrição de formas e de compreensão dos processos geomorfológicos mais latentes, atualmente a geomorfologia busca se embasar em técnicas capazes de revelar interações espaço-temporais multidimensionais novas entre formas e processos (Sofia, 2020).

O desenvolvimento das ferramentas morfométricas e o surgimento da geomorfometria só foram possíveis devido à quebra de alguns paradigmas dentro da comunidade geomorfológica, tornando a evolução tecnológica mais rápida e de fácil acesso para diversos cientistas em todo o globo. Algumas dessas mudanças foram possíveis pois a maioria das ferramentas morfométricas se utilizam de scripts e códigos para extração de dados quantitativos da topografia digital. Esse fato fez com que alguns cientistas comprometidos com o desenvolvimento científico partilhassem scripts (usualmente difundidos pelo GitHub) e dados (*open data*), além do desenvolvimento de softwares livres (Schwanghart e Scherler, 2014), fazendo com que as ferramentas morfométricas fossem facilmente reproduzidas (Sofia, 2020).

A fim de gerar dados quantitativos que representem a morfologia e os processos responsáveis pelas formas da superfície terrestre, alguns desses índices morfométricos foram aplicados ao longo dos 3 capítulos dessa tese. São eles: índice de Concentração de Rugosidade; índice χ; índice K_{sn}; a Integral Hipsométrica; além dos perfis topográficos longitudinais de rios e perfis swath.

O Índice de Concentração da Rugosidade (ICR), ou *Topographic Ruggedness Index* (TRI, sigla inglês), foi aprimorado por Riley et al. (1999). O ICR calcula a diferença de elevação entre um pixel central e os 8 pixels adjacentes a esse, utilizando como input um arquivo *raster*, um Modelo de Elevação Digital (DEM, sigla inglês). Em seguida, cada valor de diferença dos pixels vizinhos é elevado ao quadrado, para que permaneçam apenas valores positivos. Então é retirada a raiz quadrada da média desses valores para se derivar o valor do ICR do pixel central (Riley et al., 1999).

O índice χ é um proxy, desenvolvido por Willet et al. (2014), que utiliza a elevação da drenagem para o cálculo do *steady-state* dos interflúvios. Em outras palavras, o índice χ vai demonstrar as forças dos processos erosivos na busca de um reajuste dos divisores de água de diferentes bacias hidrográficas. Utilizando-se de um arquivo *raster*, DEM, como input, é feita a extração da rede de drenagem segundo os critérios estipulados pelo usuário, e para cada trecho dos rios é estipulado um valor de χ. Os valores do índice são plotados em *shape file*, estrutura vetorial em linha, e representam um modelo matemático que considera *steady-state* quando os valores se assemelham em ambos lados do divisor e em desequilíbrio quando os valores são diferentes. Essa distinção nos valores pode indicar uma migração dos divisores de drenagem, mudança geométrica, e/ou pirataria fluvial, mudança topológica, até que o *steady-state* seja novamente atingido (Willet et al., 2014).

Desenvolvido por Wobus et al. (2006), o K_{sn} ou *Steepness Index* é geralmente utilizado para associar a presença de *knickpoints* ao longo de perfis longitudinais de rios, associando essa mudança brusca na inclinação do canal com limites de áreas de atividade tectônica recentes. Assim como o índice χ, o K_{sn} é também plotado na rede de drenagem, onde cada trecho dos rios expressa a relação entre declividade do canal e área de contribuição da bacia a montante. O cálculo é feito a partir de um input de um arquivo *raster*, que será utilizado para fazer a extração da rede de drenagem e posteriormente para os cálculos dos valores de K_{sn}.

A Integral Hipsométrica ou *Hypsometric Integral* (HI, sigla inglês) é outro índice frequentemente utilizado nas análises quantitativas do relevo. A HI foi desenvolvida por Strahler (1952), para estabelecer uma relação entre as áreas mais elevadas de uma bacia e sua área. Essa relação é expressa em uma curva hipsométrica porcentual em que baixos valores, abaixo de 60%, representam bacias maduras, sem atividades tectônicas recentes e em relativo equilíbrio, já porcentagens acima de 60% representam bacias jovens, onde há influência de tectonismo recente e que consequentemente apresenta processos ativos, na busca de um equilíbrio interno, segundo o mesmo autor.

Perfis topográficos são representações gráficas de seções transversais do relevo (Hergarten et al., 2014), ainda amplamente utilizados em análises geomorfológicas. Segundo Hack (1973), os perfis longitudinais da principal drenagem da bacia tendem a ser ajustados de acordo com a intensidade dos processos denudacionais e deposicionais da mesma, de modo que, caso não exista processos tectônicos, o sistema entrará em equilíbrio com o passar do tempo. Assim, apesar da relativa simplicidade da técnica, a análise de perfis longitudinais da drenagem representa uma ferramenta relevante na interpretação da evolução do relevo, revelando desde características estruturais/litológicas até influências paleoclimáticas, como possíveis oscilações do nível de base regional e/ou global (Bishop et al., 2005; Santos et al., 2019).

O perfil swath segue o mesmo princípio dos perfis topográficos. Porém essa ferramenta é constituída de uma janela móvel, com área estipulada pelo usuário, para a complementação das mínimas e máximas encontradas perpendicularmente a cada nó, criando vários perfis laterais (Telbisz et al., 2013). Visto que um perfil topográfico amostra apenas uma linha de nós preestabelecidos pelo usuário, a mesma pode apresentar uma aleatoriedade na escolha de onde passará a linha base. O perfil swath reduz essa aleatoriedade ao expandir a amostragem do relevo perpendicularmente a linha base (Hergarten et al., 2014).

2.2 FERRAMENTAS ISOTÓPICAS

2.2.1 ISÓTOPOS COSMOGÊNICOS

Estudos que propõem modelos evolutivos da paisagem possuem uma grande variedade de metodologias para alcançar os diversos objetivos propostos. Para citar algumas dessas ferramentas pode-se mencionar os trabalhos com isótopos de determinados elementos químicos.

Segundo Gosse e Phillips (2001), isótopos são espécies atômicas do mesmo elemento químico e consequentemente mesmo número de prótons, conhecido como número atômico. Esses isótopos podem ser classificados como estáveis, quando suas combinações de nêutrons e prótons não variam, ou como instáveis ou radioativos quando apresentam massa atômica distintas (Martinelli et al., 2009).

O Berilo (Be), elemento de número atômico 4, possui 12 isótopos descritos (Dunai, 2010). Porém, apenas 3 desses são comumente mensurados: o isótopo estável ^{9}Be e os instáveis ^{7}Be e ^{10}Be. Estes últimos, radioativos, são denominados também de radioisótopos ou radionuclídeos devido ao fato de o átomo apresentar excesso de energia nuclear, tornando-o instável.

Como o ^{7}Be possui uma meia vida muito curta, apenas 53 dias, o isótopo mais frequentemente utilizado na ciência é o ^{10}Be, que possui meia vida de $1.387 \pm 0.012 \times 10^{6}$ anos (Korschinek et al., 2009; Chmeleff et al., 2010). Ambos são produzidos na interação de raios cósmicos com a atmosfera, os chamados meteóricos, e nos primeiros metros de profundidade da superfície terrestre, esses denominados de *in situ* (Lal, 1988).

Na alta atmosfera, partículas cósmicas de alta energia, principalmente prótons, colidem com átomos e iniciam cascatas de reações nucleares que são responsáveis pela produção de partículas cósmicas secundárias (Gosse e Phillips, 2001; Dunai, 2010). Com o decaimento em cascata na atmosfera, os nêutrons secundários atingem outros átomos alvo e produzem nuclídeos cosmogênicos meteóricos, como ^{7}Be, ^{10}Be, ^{14}C e ^{36}Cl (Dunai, 2010; von Blanckenburg e Willenbring, 2014). Durante este processo, nêutrons de alta energia e múons subatômicos instáveis eventualmente alcançam a superfície da Terra e penetram os poucos metros superiores de rocha exposta ou solo, onde produzem nuclídeos cosmogênicos[6] *in situ*, que podem ser estáveis (^{3}He e ^{21}Ne) ou radioativos (^{10}Be, ^{14}C , ^{26}Al, ^{36}Cl e ^{53}Mn).

Durante este bombardeio cósmico contínuo, a superfície da Terra continua evoluindo sob ações climáticas e forças tectônicas. O acúmulo cosmogênico registra a história de denudação da superfície enquanto o material é verticalmente misturado através dos metros superiores de regolito e, assim, integra os processos erosivos e de intemperismo associados à denudação e ao rebaixamento da superfície (Gosse e Phillips, 2001; Dunai, 2010)

A abundância e a resistência à degradação física e química tornam o Quartzo (SiO_2) um mineral ideal para ser isolado nos sedimentos amostrados e posteriormente mensuradas as concentrações de ^{10}Be *in situ* (Lal, 1991). A preparação das amostras conta com procedimentos químicos de dissolução em ácidos e de separação por densidade a fim de remover carbonatos e outros minerais, obtendo apenas o quartzo puro ao fim dos procedimentos.

A razão entre o isótopo estável, ^{9}Be, e o radioativo, ^{10}Be, interno aos sedimentos varia. Entretanto, presume-se que o quartzo purificado não contém o isótopo estável ^{9}Be, visto que esse é pouco frequente na natureza (Granger et al., 2013). Essa diferença na quantidade dos isótopos tornou a mensuração do ^{10}Be por espectrômetros de massa viável, sendo uma técnica frequentemente utilizada nas ciências da terra atualmente (Dunai, 2010).

A quantidade de ^{10}Be contido em uma rocha ou nos sedimentos de uma bacia indicam a exposição dos mesmos à radiação cósmica, o que torna possível o cálculo da taxa de denudação a partir de medidas de concentração desse isótopo radioativo. A relação entre a acumulação do ^{10}Be e a taxa de denudação é inversamente proporcional, visto que em situações de relativo equilíbrio, em que o processo erosivo é baixo, os quartzos que compõem o afloramento rochoso ou os sedimentos superficiais de uma bacia estão inertes, acumulando ^{10}Be. Já quando o processo erosivo se intensifica, os quartzos responsáveis pela absorção do ^{10}Be estão sendo transportados pelo processo erosivo e acabam por concentrar menos ^{10}Be.

A interpretação da taxa de erosão possui algumas premissas relevantes: (1) como não é possível medir a acumulação dos isótopos em diferentes épocas, o que

[6] Nuclídeo produzido pela interação de radiação cósmica secundária com átomos alvo expostos em materiais da superfície terrestre (Gosse e Phillips, 2001).

permitiria atribuir ciclos de maior e/ou menor intensidade erosiva, assume-se que a erosão é constante ao longo do tempo de integração do relógio isotópico; (2) se admitida a premissa 1, a amostra não poderia ter sido soterrada esporadicamente por algum processo geomorfológico por um período significativo de tempo antes da coleta (Lal, 1991).

Considerando o tempo de exposição como infinito, pode-se deduzir um modelo de concentração de ^{10}Be (at. g^{-1}) em função do tempo (t) de exposição aos raios cósmicos (Figura 0.3). O estado de equilíbrio entre a produção e perdas por decaimento radioativo e erosão é atingido anteriormente em altas taxas de erosão (curva de 1000 m/My), e mais lentamente em taxas mais lentas (curva de 1 m/My).

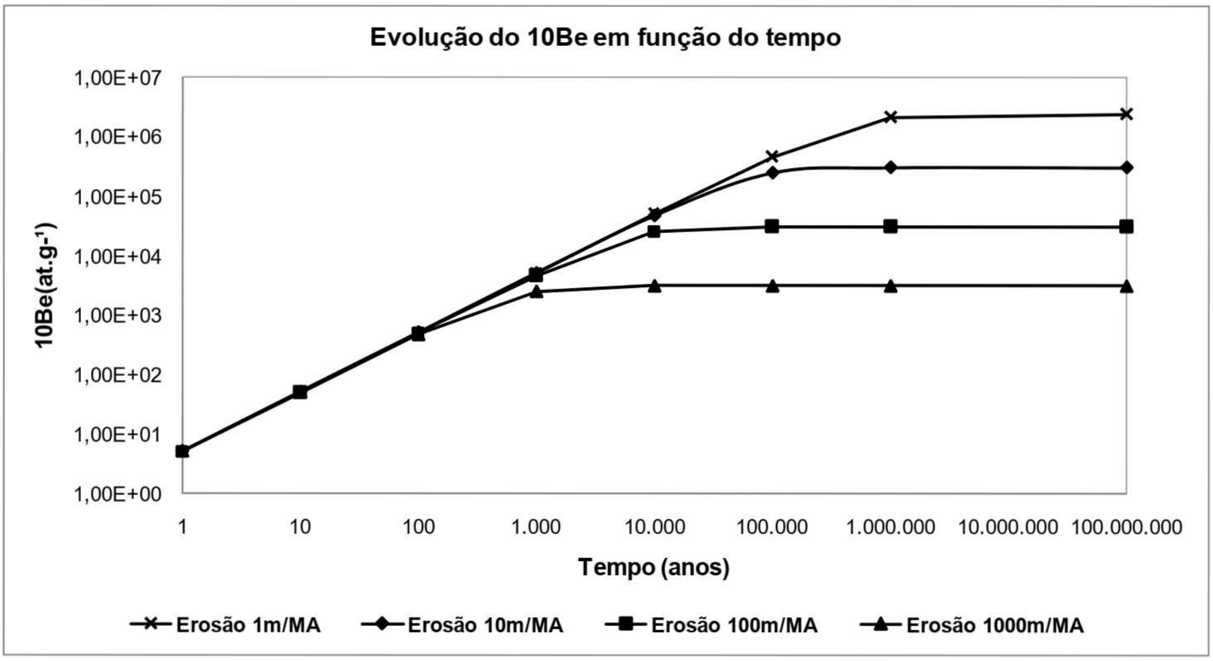

Figura 0.3: Curvas mostrando diferentes estados de equilíbrio do ^{10}Be, modelo de concentração do isótopo radioativo em função do tempo (Siame et al., 2000).

Utilizando-se das asserções do modelo de concentração do ^{10}Be em função do tempo, Brown et al. (1995) e Granger et al. (1996) aplicaram a mensuração do referido isótopo em bacias hidrográficas e inferiram que quanto maior a retenção de sedimentos em uma bacia, maior a acumulação do ^{10}Be e consequentemente quanto mais sedimentos retirados de uma bacia, menor a acumulação do isótopo. Uma vez que os rios carregam e misturam os sedimentos derivados das encostas cobertas pelo solo, eles são integradores espaciais naturais desses processos (Brown et al., 1995; Granger et al., 1996; von Blanckenburg, 2005; Granger e Schaller, 2014). Durante as últimas duas décadas, os isótopos cosmogênicos de ^{10}Be produzidos *in situ* foram amplamente utilizados em ambientes ricos em quartzo para quantificar a denudação da rocha e a dinâmica de paisagens em escalas de tempo de 10^3-10^6 anos e em um amplo espectro de configurações em todo o mundo (Granger et al., 2013).

Desde então, nota-se um aumento das pesquisas que utilizam a bacia hidrográfica como recorte espacial para realizar medições nas taxas de denudação (von Blanckenburg, 2005; Siame et al., 2011, 2015; Derrieux et al., 2014; Granger e Schaller, 2014; Regard et al., 2016; Wolff et al., 2018; Portenga et al., 2019), integrando esforços para a compreensão da evolução da paisagem nos últimos 1.5 My, o que permite avanços constantes na interpretação das morfodinâmicas da paisagem do Quaternário.

2.2.2 MENSURAÇÃO DAS AMOSTRAS E CÁLCULO DA TAXA DE DENUDAÇÃO

Para a mensuração do ^{10}Be produzidos *in situ*, a preparação das amostras para medições utilizando a espectrometria de massa com acelerador de partículas seguem procedimentos químicos adaptados de Brown et al. (1991) e Merchel e Herpers (1999). De acordo com os procedimentos indicados por Braucher (1998) e Siame et al. (2000), seguiu-se 4 etapas de trabalho: (i) preparação física, (ii) preparação química, (iii) quantificação do ^{10}Be, e (iv) cálculo da taxa de denudação (Braucher, 1998).

Após a coleta dos sedimentos aluviais, os mesmos foram secados em estufa (40°C) e em seguida peneirados, a fim de que fosse selecionada apenas a fração entre 1 e 0,25mm. Esses sedimentos já secos e selecionados segundo seus tamanhos foram acondicionados para posterior purificação do quartzo, que já faz parte da preparação química.

O tratamento químico teve por finalidade separar apenas o quartzo dos demais minerais que compunham as amostras. Desta forma, foram adicionados, em etapas distintas, ácido clorídrico (HCl) e ácido fluorsilícico (H_2SiF_6) para cada amostra. As amostras com os ácidos foram acondicionadas em frascos Nalgéne de 250ml e passaram 24h em mesas agitadoras (Braucher, 1998).

Esse processo deve ser repetido algumas vezes para atingir o nível de purificação necessário para a mensuração do ^{10}Be. No caso das amostras aqui trabalhadas, todas extraídas em litologias onde predominam arenitos, a purificação foi mais facilmente alcançada com poucas repetições devido a quantidade e proporção de quartzo presente nas amostras.

Para a eliminação do ^{10}Be atmosférico, assegurando que a mensuração é relativa apenas ao ^{10}Be *in situ*, foi adicionado ácido fluorídrico (HF). Após a repetição do processo até que o ^{10}Be atmosférico fosse totalmente eliminado, as amostras foram secas em estufa (90°C). Foram separados 20g de quartzo purificado para cada amostra e o restante, quando houve material excedente, foi colocado em reserva.

Na próxima etapa, foi adicionada uma solução de Phenakita contendo ^{9}Be nas amostras de quartzo purificado, visto que o isótopo estável de Be é utilizado para a quantificação da acumulação do ^{10}Be (Braucher, 1998). Sabendo-se a quantidade de ^{9}Be adicionada, pode-se comparar com a produção do isótopo radioativo. Com a solução de Phenakita já adicionada, foi feita a dissolução total do quartzo, novamente com HF, porém com um volume maior de ácido nessa etapa e com um tempo maior de movimento na mesa agitadora, 48h. A solução com o quartzo completamente dissolvido é então colocada em béqueres em uma placa aquecida a 200° para que o ácido evapore. O material residual é recuperado com a adição de poucos ml de HCl.

A fim de eliminar outros elementos traço presentes no quartzo purificado, como por exemplo o Boro (B), as amostras são passadas em tubos com resinas distintas, DOWEX 1*8 (SERVA 100-200 mesh) e DOWEX 50W*8 (SERVA 100-200 mesh). Os primeiros resíduos a precipitar foram descartados e em seguida é colocado um béquer para recuperar o ^{26}Al, o ^{10}Be e o ^{9}Be. A solução obtida após as colunas foi então seca novamente e recuperada com ácido nítrico (HNO_3) para ser centrifugada. O material sobrenadante foi descartado e o precipitado foi colocado em recipientes de porcelana, cadinho, para serem secados em estufa a 800°C (Braucher, 1998).

Após a secagem os cadinhos foram levados para o espectrômetro de massa, onde foi misturado a prata em pó e colocado dentro de catódos para posterior medição no acelerador de partículas por espectrometria de massa da concentração dos isótopos. A estrutura utilizada para as preparações físicas e químicas e para a mensuração dos isótopos foram as instalações do *Laboratoire Nacional de Nucléides Cosmogéniques* (L2NC), do *Centre Européen de Recherche et d'Enseignement en Géosciences de l'Environnement* (CEREGE), da *Aix-Marseille Université* localizados na região da Provença, Sul da França.

Nesta tese, as incertezas analíticas relatadas incluem incertezas nas estatísticas de contagem do acelerador de partículas, variações das razões isotópicas dos padrões durante a execução e incertezas externas ao ASTER-CEREGE (Arnold et al., 2010).

Com as medições dos isótopos realizadas, foram feitos os cálculos da exposição à radiação cósmica dos sedimentos e consequentemente da taxa de denudação de cada bacia. Esse cálculo considerou as variáveis que podem interferir na acumulação dos nuclídeos, como: a altitude (interferência atmosférica), latitude (interferência do campo magnético) e sombreamento topográfico (interferência direta da superfície terrestre). As idades de exposição das concentrações de ^{10}Be foram calculadas usando a taxa de produção de alta latitude ao nível do mar de 4.01 ±0.33 at/g/My (Borchers et al., 2016) e meia vida de 1.387 ±0.012 x10^6 My (Korschinek et al., 2009; Chmeleff et al., 2010).

Para todos os nuclídeos cosmogênicos, as concentrações isotópicas foram calculadas usando as funções de escala de Stone (2000) independentes do tempo para nêutrons de alta energia, com um comprimento de atenuação de 160 g/cm^2, e as de Braucher et al. (2011) para os múons. Uma densidade de rocha de 2.5 g/cm^3 foi assumida para todas as amostras. A interferência da topografia, *topographic shielding*, foi estimada no campo, como geralmente inferior a 0,01%.

Para determinar as taxas de denudação a partir das concentrações cosmogênicas de ^{10}Be produzidas in situ, foi necessário somar os termos exponenciais associados às partículas cósmicas secundárias que são nêutrons, múons lentos e rápidos (Braucher et al., 2011):

$$\begin{aligned} C(x,\epsilon,\mathrm{t}) \quad = \quad & \frac{P_{sp}.exp^{-\frac{x.\rho}{\Lambda_{sp}}}.(1-exp^{-t(\frac{\epsilon.\rho}{\Lambda_{sp}}+\lambda)})}{\frac{\epsilon.\rho}{\Lambda_{sp}}+\lambda} \\ & +\frac{P_{\mu s}.exp^{-\frac{x.\rho}{\Lambda_{\mu s}}}.(1-exp^{-t(\frac{\epsilon.\rho}{\Lambda_{\mu s}}+\lambda)})}{\frac{\epsilon.\rho}{\Lambda_{\mu s}}+\lambda} \\ & +\frac{P_{\mu f}.exp^{-\frac{x.\rho}{\Lambda_{\mu f}}}.(1-exp^{-t(\frac{\epsilon.\rho}{\Lambda_{\mu f}}+\lambda)})}{\frac{\epsilon.\rho}{\Lambda_{\mu f}}+\lambda} \end{aligned}$$

Onde $C\ (x,\epsilon,t)$ é a concentração de nuclídeo em função da profundidade x (cm), taxa de denudação ϵ (g/cm^2/ano), tempo de exposição t (ano), λ o decaimento radioativo do isótopo cosmogênico considerado (ano^{-1}). P_{sp} é a taxa de produção de espalhamento média da bacia, dimensionada para a variabilidade altitudinal e latitudinal (Stone, 2000), enquanto $P_{\mu s}$ e $P_{\mu f}$ são as taxas de produção média de múon lentas e rápidas da bacia dimensionadas apenas para a variabilidade de altitude

(Braucher et al., 2011). Os comprimentos de atenuação de nêutrons (Λ_n), múons lentos ($\Lambda_{\mu s}$) e múons rápidos ($\Lambda_{\mu s}$) adotados neste trabalho são 160, 1500 e 4320 g/cm^2, respectivamente (Braucher et al., 2011).

As taxas de denudação na escala da bacia podem ser determinadas resolvendo a equação (1), usando a estatística χ^2 que permite minimizar as diferenças entre as concentrações medidas (C_i^m) e teóricas (C_{th}), dentro das incertezas associadas às concentrações medidas (σ_i):

$$\chi^2 = \sum_{i=1}^{n} \frac{(C_i^m - C_{th})^2}{\sigma_i^2}$$

No *steady-state* cosmogênico, as abundâncias de ^{10}Be no mineral de quartzo fluvial registram taxas de denudação médias integradas no tempo que representam produtos de denudação combinados de todos os processos que ocorrem em uma determinada bacia hidrográfica (Bierman e Steig, 1996; Granger et al., 1996). Esta integração ocorre ao longo do tempo necessário para remover um comprimento de atenuação de nêutrons (por exemplo, ≈60 cm; Lal, 1991), que é normalmente da ordem de 10^4-10^5 anos no Brasil. O cálculo da média da bacia hidrográfica assume que o sedimento fluvial é representativo para a dinâmica erosiva em toda a bacia hidrográfica (Brown et al., 1995; Bierman e Steig, 1996; Granger et al., 1996) e que as amostras não sofreram soterramento de longo prazo.

Assim, chegou-se aos resultados, quantificados, da taxa de denudação para cada bacia. Esses resultados foram normatizados e foram aplicadas medidas de tendência central e de dispersão para a descrição dos mesmos. Outra técnica estatística comumente utilizada em trabalhos de nuclídeos cosmogênicos na Geomorfologia, a regressão linear, foi feita para a compreensão do grau de correlação entre a taxa de denudação e os parâmetros que controlam a mesma na paisagem.

3 RESULTADOS

3.1 UNDERSTANDING DENUDATION RATES FROM *IN SITU* ^{10}BE COSMOGENIC NUCLIDES ANALYSIS IN BRAZIL

3.1.1 INTRODUCTION

In the past several decades, the terms erosion and denudation have played an important role in the approaches of the natural sciences by their generic meaning of lowering of terrestrial surfaces (Dixon and Thorn, 2005; Gabrovsek, 2009; Portenga and Bierman, 2011; Harel et al., 2016). However, erosion and denudation should not be considered synonymous. Denudation presupposes a complex process, started and controlled by a variety of mechanisms and conditions, such as chemical and physical erosion, as well as glacial, tectonic, and climatic actions current and past (Mair et al., 2019). Thus, the commonly used rates of denudation refer to processes that occur in large areas and in temporal scales that refer to the geological time scale. This explains the association between mass units by area per time, usually expressed in m/My or mm/ky.

Another difference in the concepts occurs in the processes' measurement. The denudation measures refer to the quantification of all material that has been completely removed from a given area, that is, the amount of sediment removed that cannot be relocated inside (Ritter, 1967). Thus, the measurement of denudation tends to generalize the loss of sediments within the study area but does not reveal the erosive processes magnitude. For example, if the study area is a watershed, a landscape element often used for geomorphological studies, small erosive processes, internal sediment loss, and little adjustments may occur, without necessarily transporting the material outside the watershed boundaries. Therefore, the concept of denudation encompasses erosive processes, but expands the approach possibilities, allowing scientists to seek more complex explanations about the evolution of current landscapes.

Denudation studies help understanding several branches directly related or not to Geomorphology, as in the understanding of the landscape form in areas of tectonic activities, consequences of climate change, nutrients transport from the continents to the oceans, but mainly in the loss of soil/sediments on various spatial and temporal scales of analysis (McLennan, 1993; Peulvast, et al., 2009).

These denudation studies are not particularly new and have been used for many years in the field of Geomorphology. In the last century, scientists from all over the planet have tried to measure soil losses by surveying denudation rates in different contexts. Estimates of soil loss for the globe vary according to the model and/or techniques used to generate the results.

A technique that has been commonly used in the world since the 1980s is the measurement of ^{10}Be accumulation, an isotope produced by cosmogenic radiation in the Earth's environment (Portenga and Bierman, 2011). In 1934, Gosse formulated the hypothesis that cosmic radiation could produce nuclides in the interaction with Earth's surface materials (Dunai, 2010). Since then, the evolution of theories and techniques of measuring the natural *in situ* production of cosmogenic isotopes has grown, with works such as: Davis and Schaeffer (1955) the firsts to identify the production of isotopes in rocks, the ^{36}Cl in this case; Srinivasan (1976) who, twenty years after the first work, published about the use of cosmogenic isotopes of Xe in South Africa; Yokoyama et al. (1977) who assisted in the discussion of the principles of measurements and estimates of isotope production rate.

However, despite the relatively recent use of cosmogenic nuclides on the earth's surface, they were already used as important tools in meteorite and lunar studies (Reedy et al.,1983; Wieler, 2002), as well as atmospheric and oceanic analysis (Lal et al., 1958; Lal and Peters, 1962; 1967). Only in 1986/87s *in situ* studies began to be done on terrestrial rocks, using the isotopes of ^{3}He, ^{21}Ne, ^{22}Ne, ^{10}Be, ^{26}Al and ^{36}Cl (Craig and Poreda, 1986; Klein et al., 1986; Kurz, 1986a; 1986b; Nishiizumi et al., 1986; 1987; Phillips et al., 1986; Marti and Craig, 1987).

Shortly after the dissemination of cosmogenic studies in the late 1980s, isotope measurement techniques began to use refinement tools, such as the *Accelerator Mass Spectrometry* (AMS). This allowed the AMS, previously dedicated only to nuclear physics laboratories, to be used to natural sciences, bringing relevant data for oceanography, quaternary geology, archeology, among other areas (Hellborg and Skog, 2008).

AMS is used to detect a very low concentration of natural isotope ratios (between 10^{-12} and 10^{-16}, generally) whether these nuclides, such as ^{9}Be, ^{27}Al, and ^{37}Cl or not stable such as ^{10}Be, ^{26}Al, and ^{36}Cl often used in the analysis of denudational processes (Hellborg and Skog, 2008).

In a simplified way, the technique commonly used to determine denudation rates consists of verifying the accumulation of *in situ* ^{10}Be*,* and in some studies the atmospheric also, in the sampled fluvial sediment, in outcrop, or rock samples. Thus, the researchers, using the AMS, can measure the exposure to cosmic rays particles of the sampled sediments and consequently it is possible to calculate the denudation rate for the sampled site. Thereafter is possible to calibrate it with the topographic (Codilean, 2006), and the atmospheric shield (Balco et al., 2008) equations to estimate the denudation rate of each sampled catchment or outcrop.

However, the denudation rate is only one of the products that can be generated by measuring the ^{10}Be build-up. Other answers that the methodology can give are exposure dates of a given geological surface, tectonic uplift rates, and even pedological dynamics.

In South America, research using ^{10}Be for geomorphological analysis has been widely adopted in the last twenty years, especially in landscapes with certain specificities that draw the attention of geomorphologists. Attention was focused on the regions of greater relief amplitude and sometimes with active tectonism, which consequently accelerates the erosive process, as in the Andes (Safran et al., 2005; Zech et al., 2007; 2009; Saillard et al., 2009; Kober et al., 2009; Abbühl et al., 2011; Bookhagen and Strecker, 2012; Carretier et al., 2012; Bekaddour et al., 2014; Siame et al., 2015; Pousse-Beltran et al., 2017; Starke et al., 2017; Pingel et al., 2019;), in the surroundings of Ushuaia (Kaplan et al., 2007), in the Guyana shield (Edmond et al., 1995) and Patagonia (Lee et al., 2013).

In Brazil, the first study was conducted in 1998 (Braucher, et al., 1998), more than two decades ago. However, after 40 years of development of this method in the world, and twenty-two years after the first study in Brazil, as far as we know, no previous synthesis work has yet been done that compiles the denudation rates already calculated for the whole country. No previous research compared the denudations rate spatially, in order to understand the denudational processes patterns in Brazil. This remains a lack in Brazilian geomorphology. The problem can be tackled by using a comparative analysis approach, that is relevant for the beginning of a debate on the evolution of the relief aspects in the country, integrating data to explain the evolution of such distinct landscapes over the Brazilian territory.

Thus, the overall goal of this work was to summarize (general, qualitative analyses) and compare analytically (measured, quantitative analyses) the *in situ* denudation rates made with ^{10}Be in Brazil until 2019.

3.1.2 MATERIALS AND METHODS

The *in situ* production ^{10}Be data compiled in this paper comes from the sampling points of the surveys conducted in the country until the end of 2019.

For the comparison of the values, it was necessary to spatialize the results of each paper, each sampling point. However, not all papers have the coordinates of the sampled sites, sometimes the spatial representation in the published paper occurs only with the watershed map location, being impossible to reproduce the sampling points, like in Braucher et al. (1998; 2004), Salgado et al. (2006; 2007; 2008), Varajão et al. (2009), Wittmann et al. (2011) and Vasconcelos et al. (2019). Consequently, the automatic extraction of the studied watersheds and the respective application of morphometric tools that would assist in the interpretation of the data was made impossible.

Therefore, we prefer to work in a comparative-analytical way, using the individualized data of the exact sampled points when the coordinates are available. For these data, we used the expression "measured point" with a sample number of 191, used for quantitative weightings.

When the location data were not made available by the authors, we chose to stipulate a point in the proximity of the studied area with the mean values of all basins studied, only for the visual representation purpose and comparison of the general results. For these qualitative data, we assign the label "general data" and a total sample number of 20 (when reviewed by publication) and 22 (when spatially analyzed, because 2 papers presented measurements at very distant points, but that appear in the same paper, making it impossible to systematize a single point). When systematizing the general data of works done using watersheds, the studies that used outcrops were subtracted, which according to the compilation indicated a sample number of 16.

The criteria used for this comparative analysis were chosen because they are landscape elements that could influence a higher or lower denudation rate, which would allow an integrated analysis of these numbers explaining the recent relief evolution process in the country. The following parameters were chosen for the analysis: Number of papers per year of publication; Number of first authors; Sampling technique and the total number of samples per study; Latitudinal position and climatic zones; Elevation of sampled points; Lithology; Structural provinces (Almeida et al., 1981); Relief macrostructures (Ross, 2016); Large Watersheds and distance from the base level; and the Magnitude of the denudation rates measured.

The sample number and the sampling strategy in each paper are other points relevant to the synthesis. Most of the data represent denudation rates measured in watersheds, few researchers used outcrops for their analysis, which considerably alters the sampling and consequently the calculations of natural isotope production. Usually, the published data originate from samples in the watersheds mouth, constituting an average of the denudation of each watershed, which allows generating an average denudation rate for the entire watershed area (Bierman and Portenga, 2018). Thus, the more samples, the more basins the researcher was able to measure, the closer the relief evolution model will be to reality.

When available, the geographical coordinates, latitude, and longitude, of each of the sampling points were used. Latitude is an important element for the cosmogenic nuclides natural production analysis, as the cosmic radiation flow decreases with the decrease in latitude (Dunai, 2010). Latitude still influences the climate zones analysis, considering statistics for the intertropical zone and the temperate zone.

The elevation of the sampling point is relevant because the isotope accumulation depends on the thickness of the atmosphere: the higher the sampling, the smaller the thickness of the atmosphere and consequently the greater the accumulation of ^{10}Be (Dunai, 2010). For comparative purposes, the denudation quantifications were divided into four hypsometric classes: from 0 to 100m, 100 to 500m, 500 to 1000m, and above 1000m.

Geological/geomorphological parameters such as lithology, structural provinces (Almeida et al., 1981); relief macrostructures (Ross, 2016) also composed the comparative results analysis, because the explanation for the denudation rates present in several papers came from geological/geomorphological characteristics of the sampled areas. As the slope average was not possible to extract in each catchment due to the lack of precise sample coordinates, the hypsometric range was assumed in each study as a parameter to be analyzed.

The drainage network influence on the relief sculpting process was analyzed by quantifying the results by the main watersheds. It was also analyzed the watershed drainage direction, if they flow directly into the Atlantic, or if they drain to other basins in the continent inland. This parameter is directly correlated with the baselevel to which these sampled basins respond, which is significant when analyzing the denudation rates.

Finally, a comparison was made between the magnitude of the denudation rates measured in the country with worldwide data, to understand how assertive the current synthesis is. And to understand whether the 20 works compiled are only the state of the art of works with *in situ* ^{10}Be in the country or whether they can be as a basis for a generalization of the evolution of relief in the country.

ArcGis 10.5 and QGis 3.10 software were used to produce a country overview map. A shapefile file was made from the coordinates provided by the authors of the previous researches, already in UTM coordinates, with the respective zones: 21, 22, 23, and 24 South. The elevation of each point was obtained by crossing the coordinates with a Digital Elevation Model, SRTM of 90m in this case.

To systematize the discussion of the general results, two tables were made that summarize all the studies, with the data of the respective parameters analyzed (quantitative and qualitative). These tables were organized to assist the reader during the discussion of the results, because for each parameter analyzed the respective researches will be cited, avoiding the repetition of the authors.

3.1.3 RESULTS AND DISCUSSION

Twenty published papers (n=20) using denudation rates with *in situ* ^{10}Be in Brazilian territory were identified. The studies, with the respective parameters analyzed, are compiled in Tables 1.1 (quantitative) and 1.2 (qualitative) and spatialized in Figure 1.1.

As shown in Figure 1.1 and Tables 1.1 and 1.2, the first published paper is from 1998, with three ^{10}Be measurements in the Brazil countryside, general points in Cuiabá/MT, Itaberaba/BA and Gentio do Ouro/BA. In the next decade, from 2000 to 2010, there were 5 other papers, and in the last 10 years the number of publications grows to 14, totaling 20 papers with ^{10}Be measurements, in watersheds and outcrops, until the end of 2019 (Figure 1.1 and Tables 1.1 and 1.2).

1º Author	Average DR (m/My)	Average ± (m/My)	Máx DR (m/My)	Mín DR (m/My)	Máx Latitude	Mín Latitude	Elevation point sample	Sampled Numbers
BRAUCHER et al. (1998) [A; D; H]	Gentio do Ouro 9,21; Itaberaba 9,14; Cuiabá 7,64	Gentio do Ouro 0,71; Itaberaba 0,68; Cuiabá 0,98	Gentio do Ouro 13,1; Itaberaba 19,2; Cuiabá 14,9	Gentio do Ouro 5,2; Itaberaba 0,8; Cuiabá 5,5	Gentio do Ouro 11°51'92"; Itaberaba 12°46'06"; Cuiabá 15°91'14"	Gentio do Ouro 11°51'92"; Itaberaba 12°46'06"; Cuiabá 15°91'14"	Gentio do Ouro 893m; Itaberaba 599m; Cuiabá179m	Gentio do Ouro 13; Itaberaba 15; Cuiabá 9
BRAUCHER et al. (2004) [A; D; H]	Quartz vein 22,34; Stone line 12,31	Quartz vein 4,44; Stone line 1,74	Quartz vein 29,3; Stone line 17,4	Quartz vein 18,7; Stone line 4,5	15°97'21"	15°97'21"	837m	Quartz vein 5; Stone line 13
SALGADO et al. (2006) [B; D; H]	Inconclusive preliminary results	Inconclusive preliminary results	Inconclusive preliminary results	Inconclusive preliminary results	20°18'01"	20°18'01"	866m	15
SALGADO et al. (2007) [C; D; H]	Watersheds 10,52; Colúvios 4,89	Watersheds 2,80; Colúvios 0,84	Watersheds 14,91; Colúvios 14,45	Watersheds 4,31; Colúvios 0,16	20°15'08"	20°15'08"	811m	Watersheds 4; Colúvios 8
SALGADO et al. (2008) [B; D; H]	5,82	1,49	12,92	0,29	20°12'22"	20°12'22"	1039m	8
VARAJÃO et al. (2009) [B; E; H]	5,25	1,18	14,44	0,29	20°15'08"	20°15'08"	811m	18 (7 Unpublished and 11 already published)
WITTMANN et al. (2011) [B; D; H]	5,44	0,78	7,00	3,10	01°72'52"	01°72'52"	0m	45
CHEREM et al. (2012) [B; D; G]	12,98	0,09	23,07	5,21	20°57'20	20°43'04	Máx: 1054m; Min: 385m	19
BARRETO et al. (2013) [B; D; G]	4,22	0,12	6,30	1,80	19°30'13"	18°00'19"	Máx: 1320m; Min: 597m	28
REZENDE et al. (2013) [B; D; G]	14,53	0,49	26,50	7,55	22°18'52"	22°13'02"	Máx:1585m; Min:1031m	9
SALGADO et al. (2014) [B; D; G]	18,57	1,12	47,70	8,10	25°22'56"	25°15'25"	Máx: 875m; Min: 13m	10
NASCIMENTO PUPIM et al. (2015) [A; D; G]	10,00	Not reported	28,30	0,57	16°14'33"	15°41'18"	Máx: 453m; Min: 136m	10
GONZALEZ et al. (2016) [B; D; G]	RJ: 36,29; SC: 27,43	RJ: 2,71; SC: 1,86	RJ: 90,00; SC: 55,00	RJ: 13,00; SC: 19,00	27°19'48"	21°15'00"	Máx: 785m; Min: 32m	14
SALGADO et al. (2016) [B; E; G]	19,82	1,18	48,80	6,30	22°19'09"	22°13'02"	Máx: 1585m; Min: 15m	30 (21 Unpublished and 9 already published)
MARENT et al. (2018) [B; F; G]	26,04	1,87	47,70	15,50	25°22'56"	25°15'25"	Máx: 875m; Min: 13m	5 (0 Unpublished and 5 already published)
doCOUTO et al. (2018) [B; D; G]	8,61	0,30	16,25	3,90	22°57'34"	23°50'05"	Máx: 459m; Min: 260m	14
SORDI et al. (2018) [B; D; G]	23,50	3,39	58,80	2,80	27°05'55"	26°15'52"	Máx: 1084m; Min: 499m	10
VARAJÃO et al. (2018) [B; D; G]	6,12	0,48	8,40	4,75	19°12'49"	19°01'35"	Máx: 713m; Min: 131m	10
SOUZA et al. (2019) [B; E; G]	15,37	1,26	53,30	5,20	23°23'27"	22°26'33	Máx: 1522m; Min: 33m	48 (18 Unpublished and 30 already published)
VASCONCELOS et al. (2019) [A; D; H]	0,14	0,03	0,18	0,11	19°18'41"	19°18'41"	886m	3

Table 1.1: Summarized quantitative data. Sampling techniques: [A] samples in Outcrops, [B] samples in watersheds, [C] samples in watersheds and Outcrops. New data: [D] unpublished rates, [E] data already published + unpublished rates, [F] Only rates already published. Point: [G] measured point, [H] general data.

1º Author	Litology	Drainage	Main Watersheds	Relief macrostructures (Ross, 2016)	Structural provinces (Almeida et al., 1981)
BRAUCHER et al. (1998) [A; D; H]	Quartz veins and stone lines	Continental	Parana, Paraguai, Prata Basins; Atlantic East and Southeast Basins; São Francisco Basin	Planaltos e Serras do Atlântico Leste-Sudeste and Depressão Cuiabana e do Alto Paraguai	Tocantins; São Francisco
BRAUCHER et al. (2004) [A; D; H]	Quartz veins and stone lines	Continental	São Francisco Basin	Planaltos e Serras de Goias - Minas	São Francisco
SALGADO et al. (2006) [B; D; H]	Marbles; schists, phyllites, granites, gneisses and migmatites; quartzites and itabirites	Continental	São Francisco Basin	Planaltos e Serras do Atlântico Leste-Sudeste	São Francisco
SALGADO et al. (2007) [C; D; H]	granite, gneiss and phyllite	Continental	São Francisco Basin	Planaltos e Serras do Atlântico Leste-Sudeste	São Francisco
SALGADO et al. (2008) [B; D; H]	Quartzites, Schistphyllites, granite and gneisses	Continental	São Francisco Basin	Planaltos e Serras do Atlântico Leste-Sudeste	São Francisco
VARAJÃO et al. (2009) [B; E; H]	granite and gneiss	Continental	São Francisco Basin	Planaltos e Serras do Atlântico Leste-Sudeste	São Francisco
WITTMANN et al. (2011) [B; D; H]	Actual river sediments	Continental	Amazon Basin	Planícies Fluviais Interiores	North Amazon
CHEREM et al. (2012) [B; D; G]	granite and gneiss	Continental	Atlantic East and Southeast Basins; São Francisco Basin	Planaltos e Serras do Atlântico Leste-Sudeste	São Francisco; Mantiqueira
BARRETO et al. (2013) [B; D; G]	Marbles and carbonates	Continental	Atlantic East, Southeast Basins, São Francisco Basin	Planaltos e Serras do Atlântico Leste-Sudeste	São Francisco
REZENDE et al. (2013) [B; D; G]	granite	Continental	Parana, Paraguai, Prata Basins; Atlantic East and Southeast Basins	Planaltos e Serras do Atlântico Leste-Sudeste	Tocantins
SALGADO et al. (2014) [B; D; G]	granite and gneiss	both (Continental and oceanic)	Uruguai and Atlantic Southeast basins	Planaltos e Serras do Atlântico Leste-Sudeste	Mantiqueira
NASCIMENTO PUPIM et al. (2015) [A; D; G]	clastic–laterite; quartzite; metasandstone; phyllite	Continental	Parana, Paraguai, Prata Basins	Depressão Cuiabana e do Alto Paraguai	Tocantins
GONZALEZ et al. (2016) [B; D; G]	Basalt, gneisses, granites, and migmatites	both (Continental and oceanic)	Uruguai and Atlantic Southeast basins Atlantic East and Southeast Basins	Planaltos e Serras do Atlântico Leste-Sudeste and Tabuleiros e Planícies costeiras do Atlântico	Mantiqueira; Paraná
SALGADO et al. (2016) [B; E; G]	gneisses, granites, and migmatites	both (Continental and oceanic)	Parana, Paraguai, Prata Basins; Atlantic East and Southeast Basins	Planaltos e Serras do Atlântico Leste-Sudeste	Tocantins; Mantiqueira
MARENT et al. (2018) [B; F; G]	granites, gneisses and migmatites;	Oceanic	Uruguai and Atlantic Southeast basins	Planaltos e Serras do Atlântico Leste-Sudeste and Tabuleiros e Planícies costeiras do Atlântico	Mantiqueira
do COUTO et al. (2018) [B; D; G]	Sandstone	Continental	Parana, Paraguai, Prata Basins	Planaltos e Chapadas da bacia do Paraná	Paraná
SORDI et al. (2018) [B; D; G]	Basalt	Continental	Parana, Paraguai, Prata Basins; Uruguai and Atlantic Southeast basins	Planaltos e Serras do Atlântico Leste-Sudeste and Depressão Periférica da borda leste da bacia do Paraná	Paraná
VARAJÃO et al. (2018) [B; D; G]	gneisses and granitoids	Continental	Atlantic East and Southeast Basins	Planaltos e Serras do Atlântico Leste-Sudeste	Mantiqueira
SOUZA et al. (2019) [B; E; G]	granite, gneiss	both (Continental and oceanic)	Parana, Paraguai, Prata Basins; Atlantic East and Southeast Basins	Planaltos e Serras do Atlântico Leste-Sudeste	Tocantins; Mantiqueira
VASCONCELOS et al. (2019) [A; D; H]	Arcóseos ferruginosos e/ou calcíferos, conglomerados petromíticos com matriz arcosiana, siltitos e arenitos	Continental	Parana, Paraguai, Prata Basins	Planaltos Residuais em Coberturas de Plataformas–Norte e Sul	Tocantins

Table 1. 2: Summarized qualitative data. Sampling techniques: [A] samples in Outcrops, [B] samples in watersheds, [C] samples in watersheds and Outcrops. New data: [D] unpublished rates, [E] data already published + unpublished rates, [F] Only rates already published. Point: [G] measured point, [H] general data.

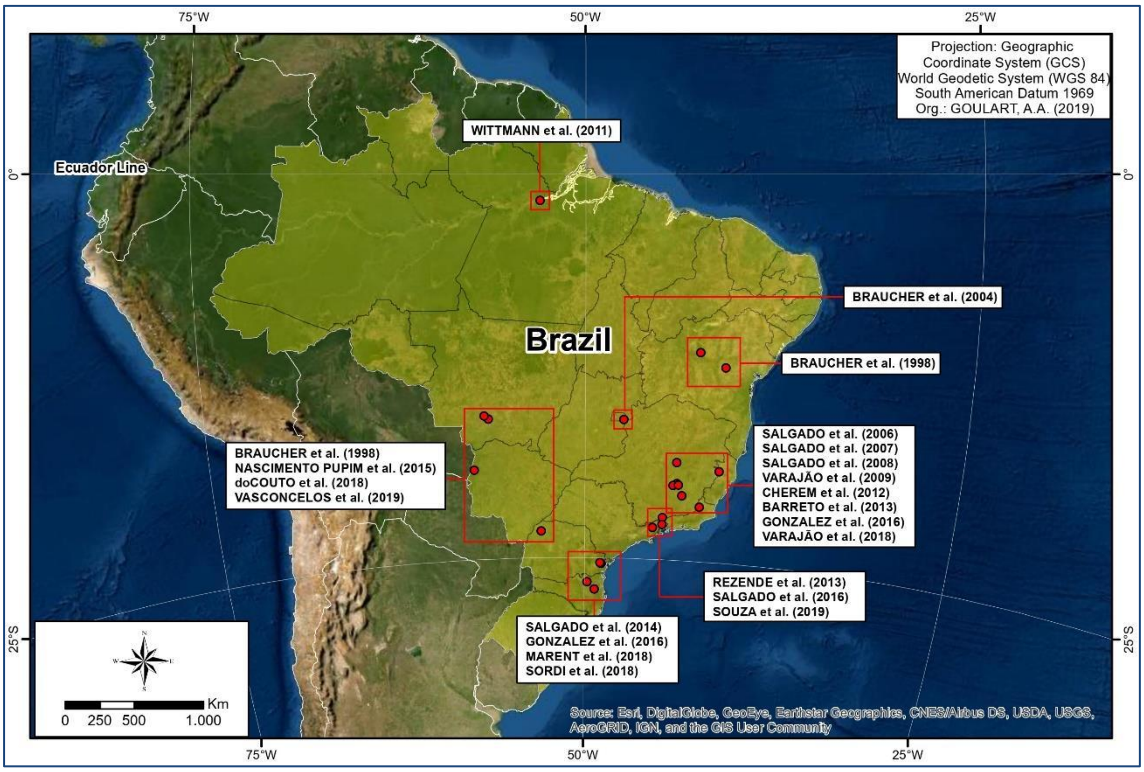

Figure 1.1: Geographical distribution of ^{10}Be researches done in the country.

A first finding that can already be made is that given the whole territorial extent of Brazil and all the heterogeneity of the landscapes that cover the country territory, only 20 studies would not be able to explain the morphodynamics evolution in all territory, regardless of spatialization, dispersion/concentration of studies.

Considering all papers in watershed and outcrops (n=20), 14 first different authors were found (Tables 1.1 and 1.2). These indicate a concentration of studies from certain research groups, which have some international agreements. That allows researchers based in Brazil to work together with research center teams that have their own AMSs. One of these cases mentioned is the international collaboration program between the *Coordenação de Aperfeiçoamento de Pessoal de Nível Superior* (CAPES) and the *Comité Français d'evaluation de la coopération universitaire avec le Brésil* (CoFECUB), which allowed 15 of the 20 studies raised to be done.

3.1.3.1 Sampling Technique and Total Numbers

There is a similarity in most methodologies applied. If all papers are considered (n=20), the survey shows that in 15 papers the measurement was made only in watersheds, in 4 papers is measured in outcrops and 1 study used both measurements, watersheds and colluvial deposits, to calculate regional denudation rate (Table 1.1). This can be explained by the fact that there are no recent and significant tectonic activities in Brazil, which gives the climate and drainage network the function of main relief modeling agents. In addition to the fact that watersheds analyses are more regionally representative, as they allow a generalization to a more comprehensive area when compared to outcrops samples or that result in specific analyses.

The number of watersheds samples in each study also had significant variation (Table 1.1), in total there were 271 samples of *in situ* ^{10}Be throughout the country. The publication that used fewer samples, 4 points in watersheds mouth, made by Salgado et al. (2007), which can be explained because the author also uses samples taken in colluvium for the denudation calculation in this publication. Souza et al. (2019) is the author of the study who used but did not necessarily collect, a greater number of samples in watersheds mouth for the measurement, totaling 48 sampling points (18 unpublished points and another 30 already published by Rezende et al., 2013; and Salgado et al., 2016), in the drainage dividers of Mantiqueira and Serra do Mar. The sampling range was stipulated in 44 samples, a variation that responds to the characteristics of the sampling strategy and the spatial scale of each study analysis.

The methodology of some studies seeks to complement the model of geomorphological evolution of the region, such as Souza et al. (2019), which uses the data already sampled and analyzed by Salgado et al. (2016) and Rezende et al. (2013) as a basis for incorporating new numbers and thus refining regional analysis. It is a methodological choice that complements the analysis with new measurements in an area that already had denudation data, thus improving the metrics for the local processes interpretation. However, this methodological strategy ends up concentrating denudation measures and studies in the same area, when there are other areas without measurements of denudation rates. The average sample per a study, in watersheds, made in the country (n=16) is approximately 17 samples per work, which corroborates the regional scale to which many researchers focus their analyses with the use of this methodology.

3.1.3.2 Latitudinal Position and Climatic Zone Analysis

Considering the general analyses papers (n=20) the measurement *in situ* closest to Ecuador was made by Wittmann et al. (2011) (general data) near latitude 1°75'55" South, in the Amazon River and some of its tributaries (Table 1.1). The highest latitude sample was made by Gonzalez et al. (2016) in the inland south country, near latitude 27°03'52" South (Table 1.1). Thus, totaling a latitudinal variation of 26°72'03", a value that covers a large part of the Brazilian territory. Since latitude influences the natural production of ^{10}Be, this factor becomes fundamental for understanding the numbers after measuring the ^{10}Be concentration.

The results association with climate revealed that the denudation was higher in the temperate zone, 22.2 ±2.3 [24.0] (5) [7] m/My, than in the tropical zone 11.1 ±2.0 [9.0] (17) m/My (Table 1.1). The low sample number eventually demonstrated an inversion of the expected trend. The tropical zone tends to accelerate the denudational process more than temperate climates. Perhaps a more refined correlation, using the rainfall erosivity of each studied area, could highlight significant correlations for the denudation rates explanation.

The simple linear regression between the sample measured point coordinates (n = 191) and latitude did not show a satisfactory correlation between denudation rate and latitude ($R^2 \cong 0.16$). Figure 1.2 shows that there is a tendency to increase the speed of the denudational processes further south but to assume this interpretation with samples concentrated in small areas would be a mistake.

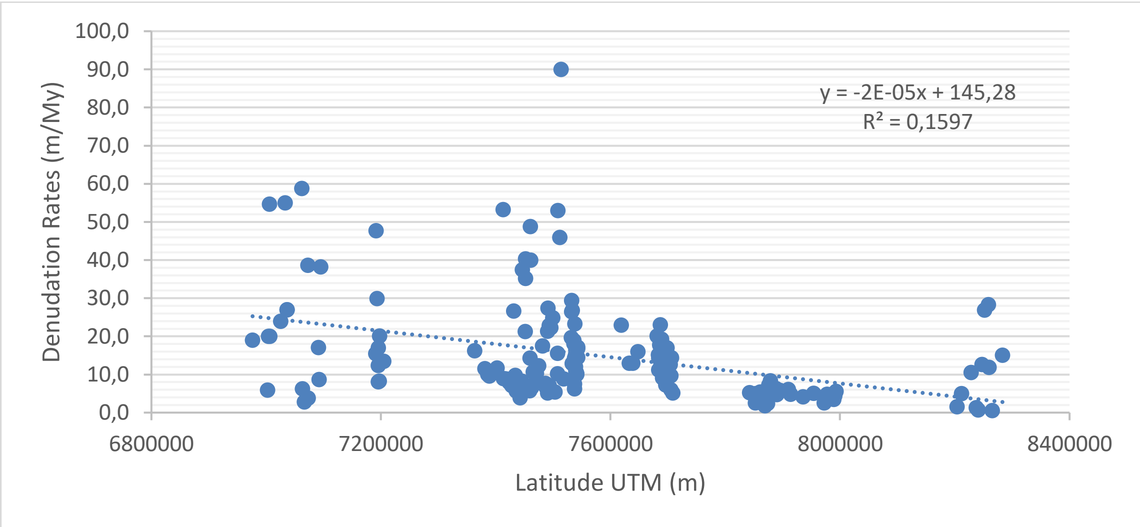

Figure 1.2: Regression plot of the relationship between denudation rates and latitude (UTM).

[7] The results description pattern was made as follows: AVERAGE ± UNCERTAINTY [MEDIAN] (NUMBER OF SAMPLES) m/My.

3.1.3.3 Hypsometric Analysis

Considering each sample measured point coordinates, when available by the authors (n=191), the highest point sampled is located near the Serra da Mantiqueira on the border of Rio de Janeiro, São Paulo, and Minas Gerais States, approximately 1585 m above sea level (Rezende et al., 2013; Salgado et al., 2016; Souza et al., 2019). On the other hand, the lowest sample concerning to sea level was made on the Paraná State coastal plain, at only 13m elevation (Gonzalez et al., 2016).

The altimetric results of all samples with measured point coordinates were 761.6 ±32.7 [784] (191) m. This is a weighting between samples in strands of ancient orogenetic structures such as Serra do Mar and Mantiqueira and samples at low elevations such as in the proximity of the Paraná River and the Brazilian coastal plain. The standard deviation of the hypsometric data was 451.3 m (191), remarkably high, but it can be explained by the heterogeneity of the values that constitute the population, with an altimetric range of 1572 m. The natural production of ^{10}Be is also influenced by the sample elevation because the atmosphere thickness interferes with the radiation input that is responsible for the isotope accumulation in quartz.

The denudation rates according to the hypsometric classes were: 34.5 ±2.8 [36.3] (20) m/My from 0 to 100m; 15.7 ±2.2 [11.6] (38) m/My from 100 to 500 m; 13.7 ±1.5 [13.3] (73) m/My from 500 to 1000 m; 12.0 ±0.9 [10.8] (60) m/My for samplings above 1000 m. Thus, a pattern was found, in which the highest denudation rates were measured in the hypsometric classes of lower value (Figure 1.3), which can be explained by the position of the samples made preferably in the watershed mouth. Therefore, the sampling point hypsometry does not necessarily mean that the entire watershed area is at an approximate elevation of the sampled point, on the contrary, the mouth is the lowest point of the watershed. The pattern found in this parameter analysis is expected, since many watersheds are found in large altimetric range areas, such as in the eastern Serra do Mar hillside.

Corroborating with the hypsometric classes, the linear regression analysis between sampled points elevation and denudation rates shows a trend towards a higher denudation speed the closer to sea level. However, the correlation is very weak ($R^2 \cong 0.08$), which does not indicate a pattern of erosive rate behavior. The trend observed in Figure 1.4 can be explained by the number of samplings in the coastal plain to measure the denudation rates of the eastern slope of the Serra do Mar.

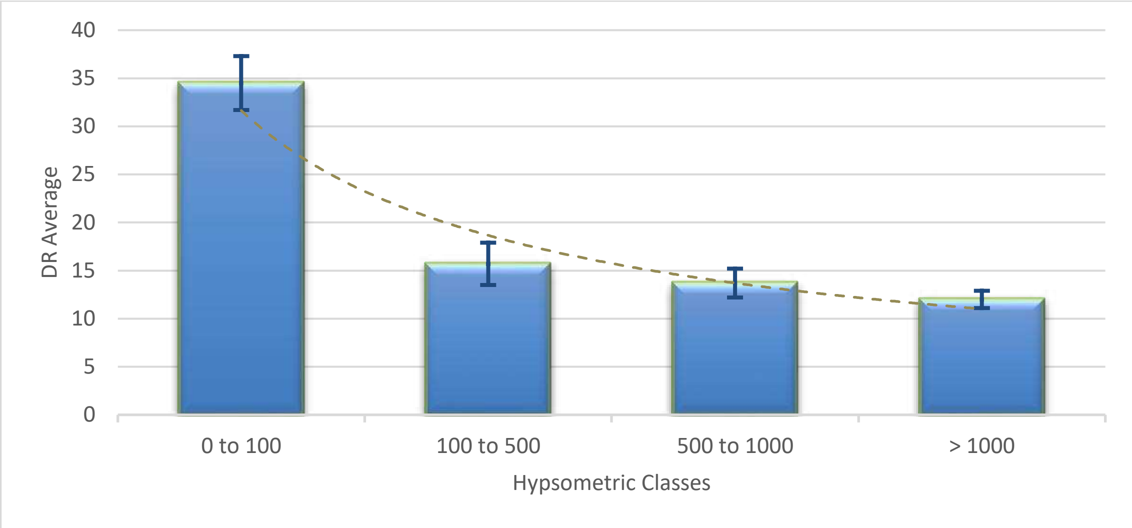

Figure 1.3: Denudation rates according to the hypsometric classes.

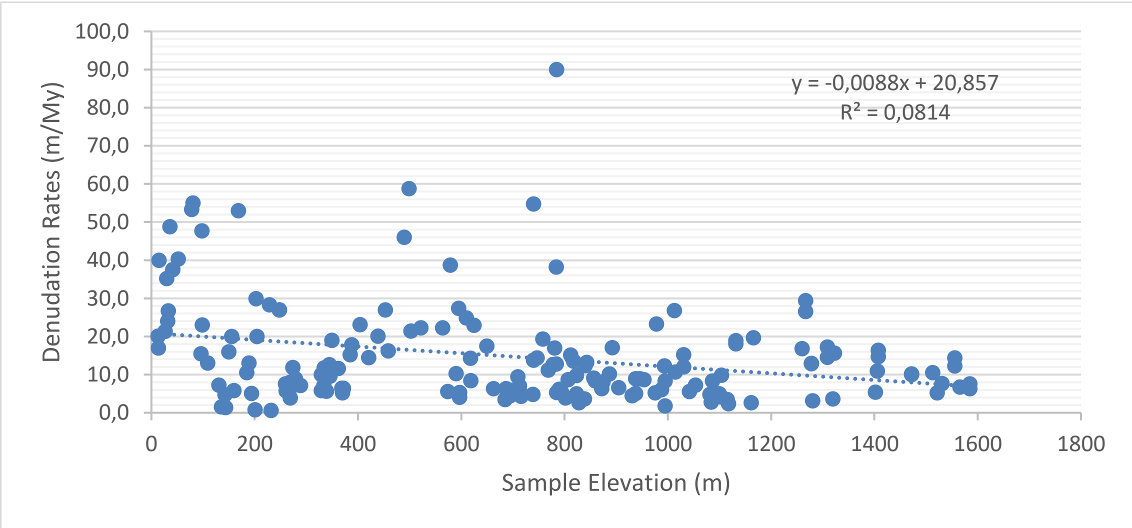

Figure 1.4: Regression plot of the relationship between the denudation rates and samples elevations.

3.1.3.4 Lithology Analysis

Another landscape element that varied considerably was the lithology in which the samplings were performed, as can be seen in Table 1.2. Generally analyzing (20), 11 papers work with granites, gneisses, and/or quartzites, 2 with a sampling of stone-lines and related sediments, 2 with basalt, 2 with sediments associated with conglomerates, laterites, 1 with sandstone, 1 with marbles and carbonates, and 1 with current alluvial sediments. This geological heterogeneity may prove to be a limiting factor for generalizations of relief evolution throughout the country. Detailed geology studies of each sampled watershed would be necessary to make precise inferences about the basement interference in the denudation rate value. Only the authors who found a correlation between the rock type and the ^{10}Be concentration in the sediments make this association and bring the data in their work discussion. In most cases, the geology approach is restricted only to a well-generalized characterization of the study area.

3.1.3.5 Structural Provinces

The research concentration in certain regions is also reflected in the analysis of the structural provinces (Almeida et al., 1981) (Table 1.2). In Figure 1.5, from general data (22), 8 studies can be observed in the province of São Francisco, 7 in the Mantiqueira, 4 in the Tocantins, 2 in the Paraná, and 1 in the North Amazon. We notice that three structural provinces – The South Amazon, Borborema, and Parnaíba – do not even have at least one paper in which denudation rates were measured for the interpretation of long-term landscape development. These provinces may eventually assist in the interpretation of studies already done in neighboring provinces and even throughout South America since these are part of the same geological evolution context, related to the rearrangements of the Transbrasiliano cycle (Almeida et al, 2000). This spatialization also evidences the lack of published in the North-Northeast Brazil regions, where fundamental structures are found for understanding continental morphodynamics.

In the measured point analysis (Table 1.1 and Figure 1.6) of the watershed sampled points (191) the São Francisco structural province was a result of 6.2 ±0.7 [5.0] (38) m/My; 20.6 ±1.7 [15.5] (81) m/My in Mantiqueira; 15.3 ±0.9 [14.7] (47) m/My in Tocantins; 15.4 ±3.1 [8.9] (25) m/My in Paraná. It was noticed that the São Francisco provinces tend to lower values and consequently slower denudation processes, while in the Tocantins province the average resembles the national average, and in Mantiqueira and Paraná the processes are faster.

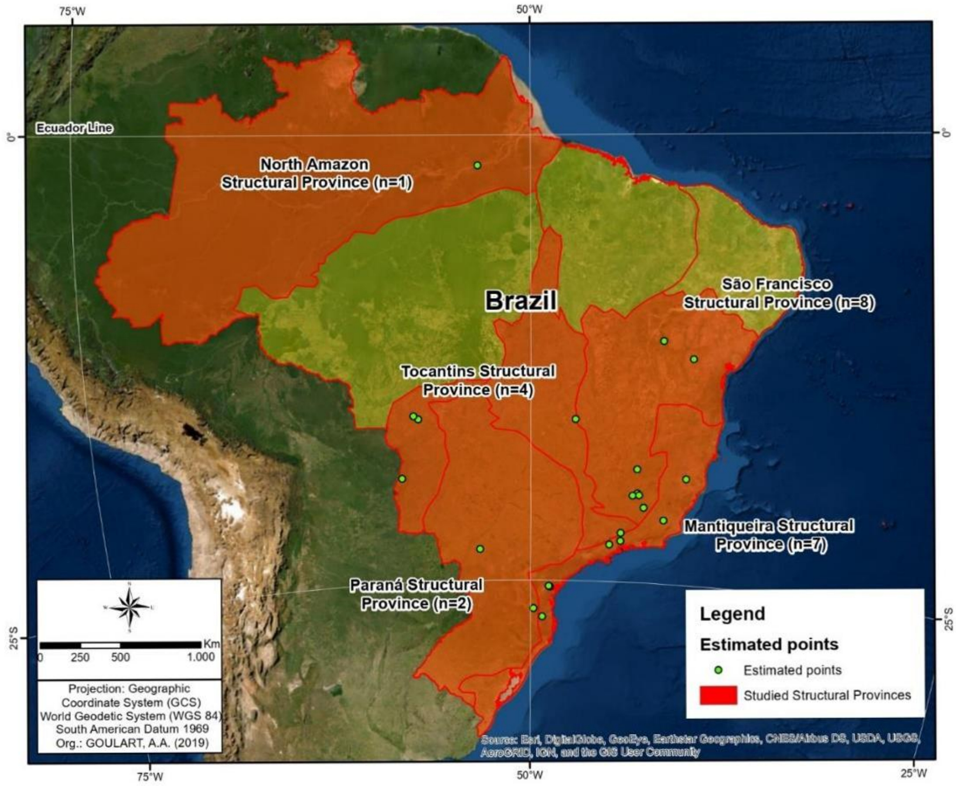

Figure 1.5: Distribution of ^{10}Be general data in Brazil according to the structural provinces (Almeida et al., 1981), showing which of the country provinces have already been worked on and the number of jobs in each one.

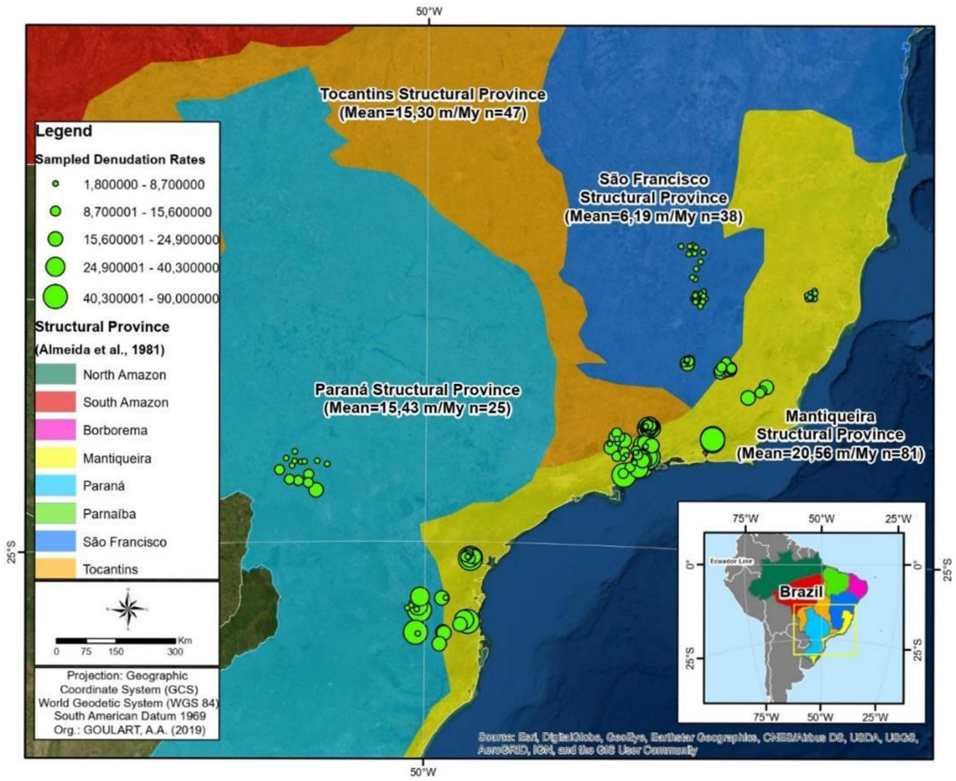

Figure 1.6: Distribution of the watersheds measured point sampled points with ^{10}Be in Brazil according to the country structural provinces (Almeida et al., 1981), showing the sampled number and the averages for each one.

3.1.3.6 Relief Macrostructures

Regarding the general analysis (22) of the relief macrostructures (Ross, 2016), 6 were surveyed with ^{10}Be in Brazil (Figure 1.7 and Table 1.1): Planaltos e Serras do Atlântico Leste-Sudeste (16); Depressão Cuiabana e do Alto Paraguai (2); Planaltos Residuais em Coberturas de Plataformas-Norte e sul Amazônicos (1); Planícies Fluviais Interiores (1); Planaltos e Serras de Goiás – Minas (1); and Planaltos e Chapadas da bacia do Paraná (1).

The Figure 1.8 shows the measured point values (191) of denudation made according to Table 1.2, by macrostructure. The numbers were as follows: 15.6 ±0.9 [12.7] (168) m/My in *Planaltos e Serras do Atlântico Leste-Sudeste*; 53.3 ±4.2 (1) m/My in *Tabuleiros e Planícies costeiras do Atlântico*; 26.1 ±8.5 [22.2] (8) m/My in *Depressão Periférica da borda leste da bacia do Paraná*; 8.6 ±0.8 [7.8] (14) m/My in *Planaltos e Chapadas da bacia do Paraná*. A values discrepancy was noticed when the sampling number is low, which makes it difficult to validate a specific evolution model to each macrostructure.

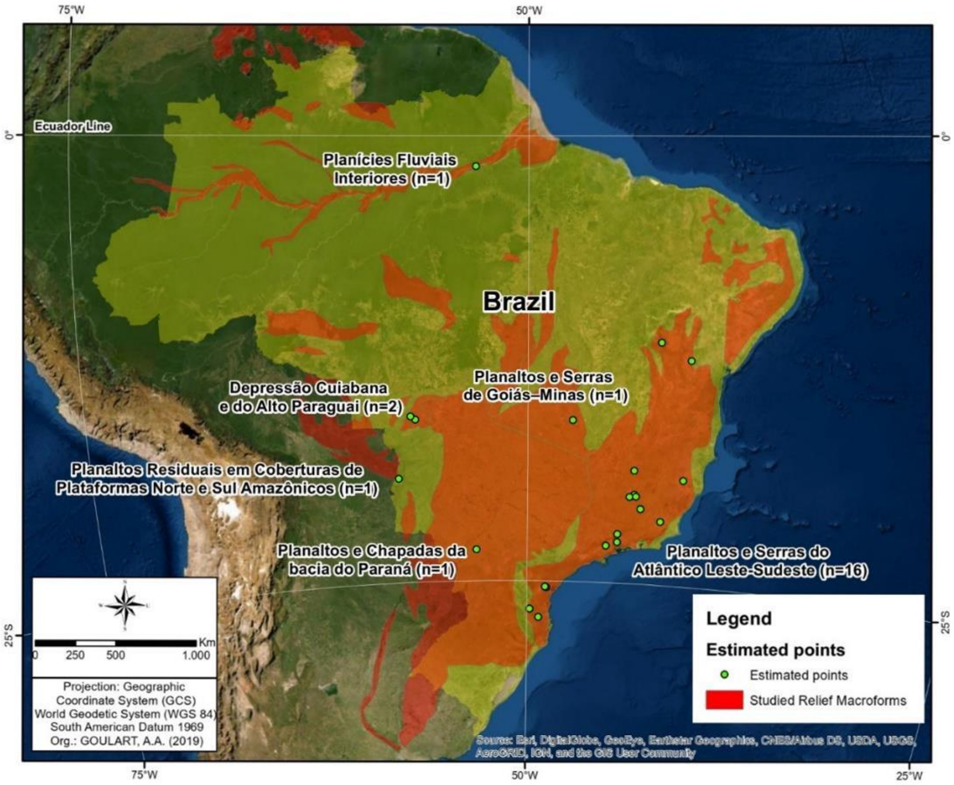

Figure 1.7: Distribution of the general data of ^{10}Be in Brazil according to the South America relief macrostructures (Ross, 2016), demonstrating which of the country macrostructures have already been worked and the number of works in each one.

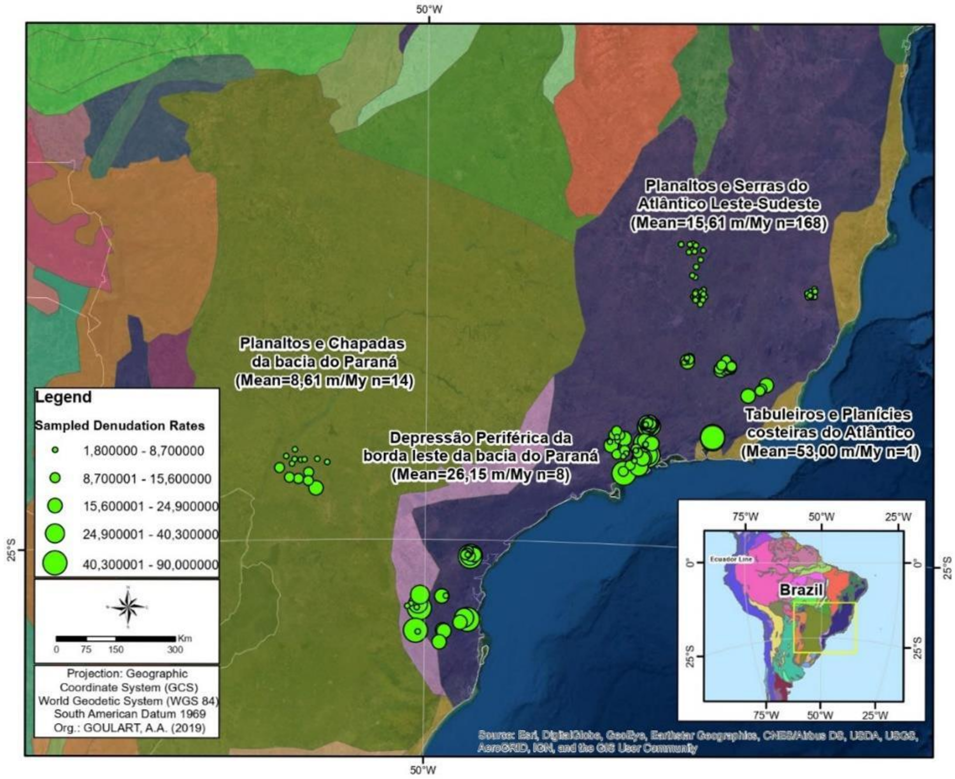

Figure 1.8: Distribution of the measured point sampled points of watersheds with ^{10}Be in Brazil according to the South American relief macrostructures (Ross, 2016), showing the sampled number and the average for each one.

3.1.3.7 Watersheds and Baselevel

The sampled watersheds baselevel, continental or oceanic levels also vary considerably in the publications analyzed (Table 1.2). Figure 1.9 shows the general analysis values (22), with 8 studies that measured the rates of watersheds that drain into the continent inland, 13 that measure the two sides of the Serra do Mar mountains, and only 1 paper was made outside this context, measuring the denudation rates of the Amazon basins.

The measured point analysis (191) in watersheds that drain into the inland yield an average of 9.2 ±0.7 [8.0] (61) m/My (Figure 1.10, Table 1.1). The watersheds, with coordinates, which drained directly to the Atlantic have twice the values of the continental ones, 18.8 ±1.3 [14.8] (130) m/My. These numbers reflect the considerations made in some of these studies, demonstrating that the eastern slope of the Serra do Mar mountains has a higher denudation speed than the western slope, which can be explained by the difference in each baselevel.

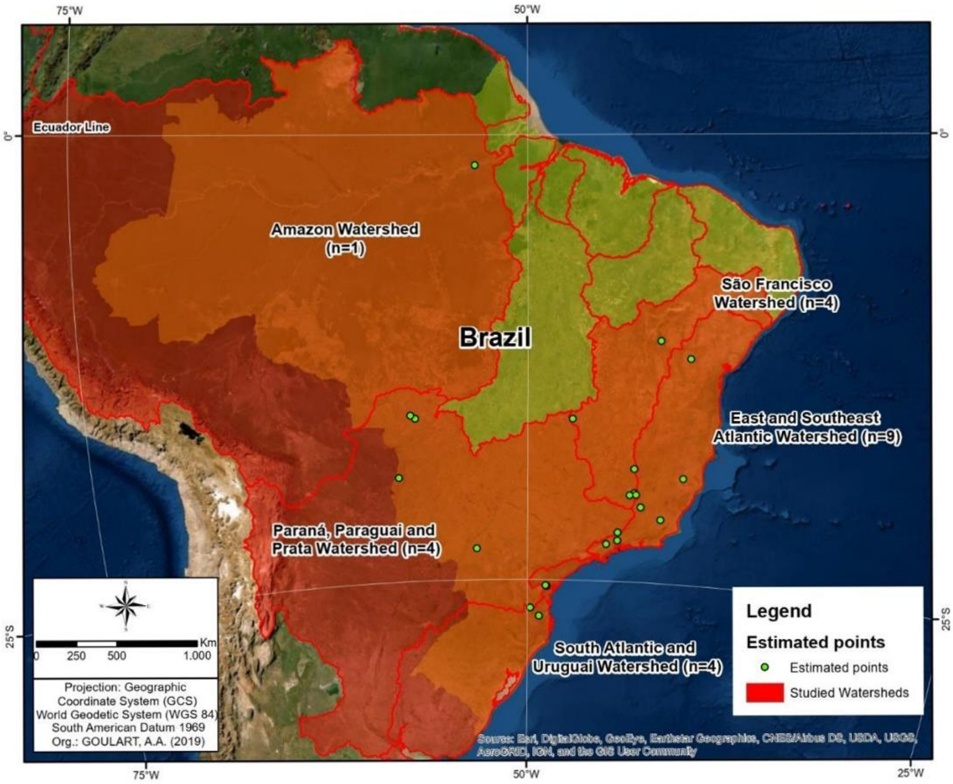

Figure 1.9: Distribution of the ^{10}Be papers general data in Brazil, showing which of the main country watersheds have already been worked and the number of works in each one.

Analyzing the watersheds specifically, the results of 4.1 ±0.3 [4.0] (16) m/My was calculated for the São Francisco watershed; 11.1 ±0.9 [10.2] (45) m/My was calculated for the Paraná/Prata watershed; 17.6 ±1.3 [13.4] (108) m/My was calculated for the East/Southeast Atlantic watershed; 24.6 ±3.5 [20.0] (22) m/My was calculated for the South Atlantic/Uruguay watershed; and 5.4 ±0.9 (1) m/My for the Amazon watershed.

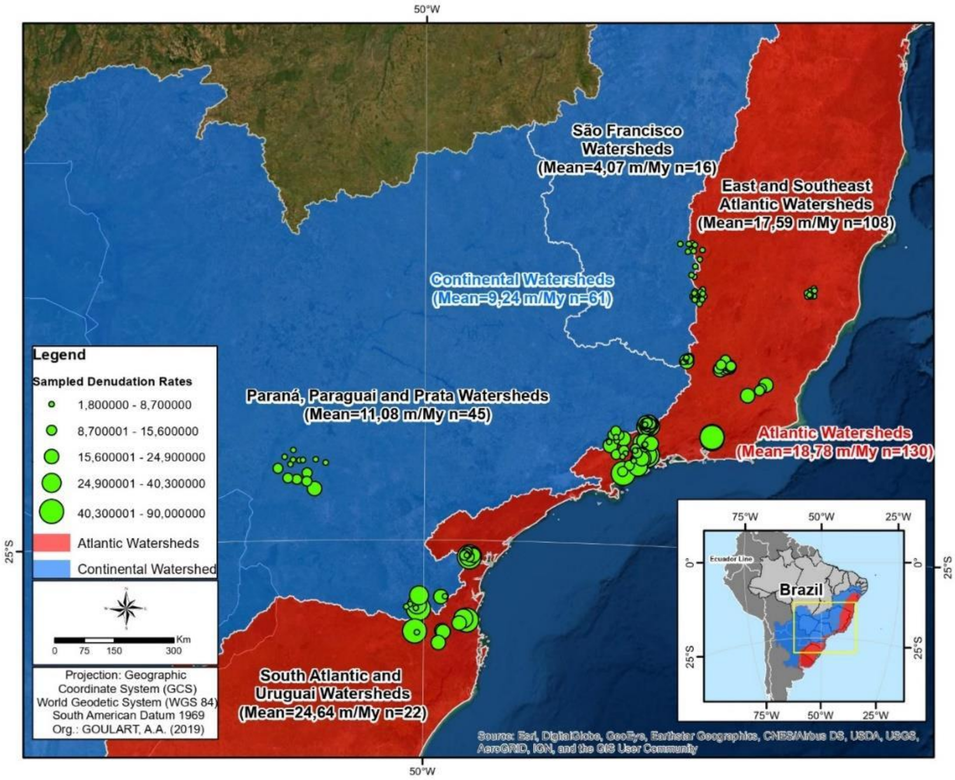

Figure 1.10: Distribution of the measured point sampled points of watersheds with ^{10}Be in Brazil according to the main country watersheds, showing the number of samples and the averages for the Atlantic and Continental Basins.

3.1.3.8 Denudation Rates Magnitude

The values and averages variations for each parameter analyzed already indicates that the magnitude of the denudational rates did not show a spatial pattern in Brazil. The spatial distribution of the studies (Figure 1.1), concentrated in some regions, reflects the distribution framework of public universities in Brazil. Because there is a concentration of universities in the same regions in which ^{10}Be studies accumulated could be observed, in southeast/south regions. For other country areas, such as the north and northeast, only 1 and 2 studies were found, respectively (Figure 1.1 and Table 1.2).

It was also noted, about the studies spatialization, that there is a tendency of the authors to concentrate their research on close points or even in points already studied, in an attempt to better assimilate the relief evolution model for these specific areas. Or even studies that reuse denudation rates already published, to refine the data (Table 1.1), but that ended up (re)concentrating data spatially.

The range between the basin with the highest and lowest denudation rate measured in Brazil is high, 89.7 m/My, with total values ranging from 0.29 to 90.0 m/My (Table 1.1). According to Salgado et al. (2006; 2008), the lowest value of denudation was conditioned by the watershed lithology, composed of rocks more resistant to the erosive process, corresponding to Itabirites and quartzites occurrence areas. The highest value was explained by Gonzalez et al. (2016) by the watershed slope, located on the escarpment of Serra do Mar mountains.

For the whole of Brazil, the result was 15.0 ±2.4 [13.8] (16) m/My. The lack of pattern of the numbers that constitute the population studied suggests that there are local elements that condition the denudation processes speed, specific to each region and that was reported in each paper, causing the rates to vary greatly.

According to the mean calculated for Brazil, the country denudation is far below the world averages reported in the scientific literature. To exemplify global denudation averages, the values of 67 m/My calculated by Wilkinson (2005), 47 m/My (Harrison, 1994), 64 m/My (Walling, 1987), 54 m/My (Portenga and Biergman, 2011) and 41 m/My (Summerfield and Hulton, 1994).

According to Portenga and Bierman (2011), the factors that have a better correlation (high R^2) are the climate, the tectonism, and the lithology. However, the sample concentration in certain country regions does not allow climate correlations for the whole of Brazil. When this association was tested, it was noticed that the means values of samples located in the subtropical zone were higher, but the low sample number of studies published in the temperate zone makes this result doubtful.

Another factor indicated by Portenga and Biergman (2011) that can explain denudation rate patterns and is used in some papers discussion is the lithology. The highest denudation rates are in watersheds above gneisses and granite lithologies that constitute the Serra do Mar. However, for the denudation rate, this resistant lithology should represent a speed attenuation factor, not a catalyst for the process. As an example of publications in this lithology, we can mention the work of Salgado et al. (2016) that reports an average of 4.8 m/My above the national average.

Another example of the lithology influence that comes out of the expected pattern in the country's numbers comparison is the paper of Couto et al. (2018). Even on a very friable lithology, sandstone, the denudation rates are low when compared to the national average, 6.4 m/My below the Brazilian average.

So, another factor should condition the country's denuding pattern: the slope. According to Nascimento Pupim et al. (2015), rates are moderately correlated ($R^2 \cong 0.47$) to the slope of the watershed. This pattern can be observed in the correlation of the highest denudation rates with the smaller hypsometric classes, which correspond to samples made in the coastal plain, of watersheds that drain from the Serra do Mar to the Atlantic; and with the baselevel in the Atlantic Ocean.

This suggests that the current possibility of a standard denudation rate is linked to regional portions within Brazilian territory, as on both sides of the Serra do Mar and in the Minas Gerais State. However, it is not yet feasible how denudation is acting in the whole country.

Finally, it should be emphasized that the local and particular factors that cause the denudation rates vary so much are the result of the landscape evolution process among the last million years. Therefore, the search for an evolution pattern that explains the denudation throughout the country can not only consider the current picture but must take into account the landscape evolution and the dynamics characteristics of each of its elements over geological time.

3.1.4 FINAL CONSIDERATIONS

As we have argued, there is no direct correlation that explains one pattern of the country's denudation rates. None of the criteria analyzed has a greater influence on the denudation rates determination, even some explaining the measurements performed punctually.

This lack of pattern can be explained by the landscape characteristics, in which in some studies one of the factors will be predominant over the others for the rates explanation. Generally, these factors are punctual and should be characterized in each case, such as slope (mean) and lithology (predominant, considering relevant specificities).

It should be considered that landscape evolution analyses should be made considering landscape-forming aspects over geological time, which demands that each author seek explanations for local patterns, but at the same time makes it impossible to determine how relief evolves throughout the country.

Although the most accepted synthesis, it suffers from some limitations due to the unavailability of sampling point coordinates in some studies, becoming these works analysis more superficial in the country context.

The spatial concentration of studies and the republication of already published data also prevent the determination of a denudation pattern in the country. For a better understanding of morphodynamic processes in Brazil, it would be opportune to calculate the rates through ^{10}Be measurements in areas not yet measured or with few samples, but which are relevant in the national geomorphology context.

It is important to note, that with the data compiled until the end of 2019 it was not possible to propose a relief evolution model. At this stage of understanding the denudation rates in Brazil, we believe that regionally, for some well-sampled and well-explained areas these patterns can be visualized, but not yet for the whole country. However, the comparative analysis of the data compiled is the first step to understand the state-of-the-art of these studies and begin the discussion about the possibility of studies in areas still little studied, understanding the evolution and interaction of other elements that form the current landscape.

3.1.5 REFERENCES

ABBÜHL, L.; NORTON, K.; JANSEN, J.; SCHLUNEGGER, F.; ALDAHAN, A.; POSSNERT, G. Erosion rates and mechanisms of knickzone retreat inferred from Be-10 measured across strong climate gradients on the northern and central Andes Western Escarpment. **Earth Surface Processes and Landforms**, 36, 1464–1473. 2011.

ALMEIDA, F. F. M. de; BRITO NEVES, B. B. de; CARNEIRO, C. D.R. The origin and evolution of the South American platform. ***Earth-Science Reviews***[S.l.], v. 50, n. 1-2, p. 77-111, 2000.

ALMEIDA, F. M. M. Brazilian structural provinces: an introduction; **Earth Science Review**, n. 17, p. 1-29. 1981.

BALCO, G., STONE, J.O., LIFTON, N.A., DUNAI, T.J. A complete and easily accessible means of calculating surface exposure ages or erosion rates from ^{10}Be and ^{26}Al measurements. **Quaternary Geochronology** 3, 174–195. 2008.

BARRETO, H.N.; VARAJÃO, C.A.C.; BRAUCHER, R.; BOURLÈS, D.L.; SALGADO, A.A.R.; VARAJÃO, A.F.D.C. Denudation rates of the Southern Espinhaço Range, Minas Gerais, Brazil, determined by in situ-produced cosmogenic beryllium-10. **Geomorphology**, Volume 191, Pages 1-13, 2013.

BEKADDOUR, T.; SCHLUNEGGER, F.; VOGEL, H.; DELUNEL, R.; NORTON, K.P.; AKÇAR, N.; KUBIK, P. Paleo erosion rates and climate shifts recorded by Quaternary cut-and-fill sequences in the Pisco valley, central Peru. **Earth and Planetary Science Letters**. Volume 390. p. 103-115. 2014.

BIERMAN, P. R.; PORTENGA, E. Beryllium Isotopes. In: White, W.M. (Ed.) **Encyclopedia of Geochemistry**. Springer International Publishing. 2018.

BOOKHAGEN, B.; STRECKER, M. Spatiotemporal trends in erosion rates across a pronounced rainfall gradient: Examples from the southern Central Andes. **Earth and Planetary Science Letters**. p. 97–110. 2012.

BRAUCHER, R. Stone-line formation processes documented by in situ-produced ^{10}Be distribution, Jardim River basin, DF, Brazil. **Earth and Planetary Science Letters**. 222. p.645-651. 2004.

BRAUCHER, R.; BOURLÈS, D.L.; COLIN, F.; BROWN, E.T.; BOULANGÉ, B. Brazilian laterite dynamics using in-situ produced ^{10}Be, **Earth and Planetary Science Letters**, 163. 197–205. 1998.

CARRETIER, S.; REGARD, V.; VASSALLO, R.; AGUILAR, G.; MARTINOD, J.; RIQUELME, R.; PEPIN, E.; CHARRIER, R.; HÉRAIL, G.; FARIAS, M.; GUYOT, J.; VARGAS EASTON, G.; LAGANE, C. Slope and climate variability control of erosion in the Andes of Central Chile. **Geology**. 41. 195-198. 2013.

CHAMPAGNAC, J.D.; VALLA, P.; HERMAN, F. Late-Cenozoic relief evolution under evolving climate: A review of quantitative arguments. **Tectonophysics**, Volume 614, p.44-65. 2014.

CHEREM, L.F.; VARAJAO, C.; BRAUCHER, R. BOURLÈS, D.; SALGADO, A.; VARAJÃO, A. Long-term evolution of denudational escarpments in southeastern Brazil. **Geomorphology**. 2012.

CODILEAN, A.T. Calculation of the cosmogenic nuclide production topographic shielding scaling factor for large areas using DEMs. **Earth Surface Processes and Landforms** 31 (6), 785–794. 2006.

CRAIG, H.; POREDA, R. J. Cosmogenic 3He in terrestrial rocks: the summit lavas of Maui, **Proc. Natl. Acad. Sci**. 83 1970–1974. 1986.

DAVIS, R.; SCHAEFFER, O. A. Chlorine-36 in nature, **ann. Ny acad. Sci**. 62 105–122. 1955.

DIXON, J.; THORN, C. Chemical weathering and landscape development in midlatitude alpine environments. **Geomorphology**. 67, 127–145. 2005.

do COUTO, E.V.; SANTOS, L.J.C.; SORDI, M.V.; BOURLÈS, D.; BRAUCHER, R.; SALGADO, A.A.R.; LÉANNI, L.; FERREIRA, J.H.D.; ASTER TEAM. Changes of the base levels in the Ivaí and Paraná Rivers confluence zone (Southern Brazil): Denudational reflexes in the evolution of the upstream drainage network. **Zeitschrift für Geomorphologie**. Volume 62 Issue 1 , p.23-40. 2018.

DUNAI, T. **Cosmogenic Nuclides**: Principles, Concepts and Applications in the Earth Surface Sciences. 1-187. 2010.

EDMOND, J.M.; PALMER, M.R.; MEASURES, C.I.; GRANT, B.; STALLARD, R.F. The fluvial geochemistry and denudation rate of the Guayana Shield in Venezuela, Colombia, and Brazil, **Geochimica et Cosmochimica Acta**, Volume 59, Issue 16, p.3301-3325. 1995.

GABROVŠEK, F. On concepts and methods for the estimation of dissolutional denudation rates in karst areas. **Geomorphology**, Volume 106, Issues 1–2, p. 9-14. 2009.

GODARD, V.; DOSSETO, A.; FLEURY, J.; BELLIER, O.; SIAME, L. Transient landscape dynamics across the Southeastern Australian Escarpment. **Earth and Planetary Science Letters**. Volume 506. P. 397-406. 2019.

GONZALEZ, V.S.; BIERMAN, P.R.; FERNANDES, N.F.; ROOD, D.H. Long-term background denudation rates of southern and southeastern Brazilian watersheds estimated with cosmogenic ^{10}Be. **Geomorphology**, Volume 268, Pages 54-63. 2016.

HAREL, M.A.; MUDD, S.M.; ATTAL, M. Global analysis of the stream power law parameters based on worldwide 10Be denudation rates. **Geomorphology**, *268*, pp.184-196. 2016.

HARRISON, C.G.A. Rates of continental erosion and mountain building. **Geologische Rundschau**. 83, 431–447. 1994.

HELLBORG, R.; SKOG, G. Accelerator mass spectrometry. **Mass spectrometry reviews**. 27. 398-427. 2008.

KAPLAN, M.R.; CORONATO, A.; HULTON, N.R.J.; RABASSA, J.O.; KUBIK, P.W.; FREEMAN, S.P.H.T. Cosmogenic nuclide measurements in southernmost South America and implications for landscape change, **Geomorphology**, Volume 87, Issue 4, p.284-301. 2007.

KLEIN, J.; GIEGENGACK, R.; MIDDLETON, R.; SHARMA, P.; UNDERWOOD, J. R.; WEEKS, W.A. Revealing histories of exposure using in-situ produced 26Al and ^{10}Be in Libyan desert glass, **Radiocarbon** 28 547–555. 1986.

KOBER, F.; IVY-OCHS, F.; ZEILINGER, G.; SCHLUNEGGER, F.; KUBIK, P.W.; BAUR, H.; WIELER R. Complex multiple cosmogenic nuclide concentration and histories in the arid Rio Lluta catchment, northern Chile. **Earth Surface Processes and Landforms**, 34, 398–412. 2009.

KURZ, M. D. Cosmogenic helium in terrestrial igneous rock, **Nature** 320 435–439. 1986a.

KURZ, M. D. In situ production of terrestrial cosmogenic helium and some applications to geochronology, **Geochim. Cosmochim. Acta** 50 2855–2862. 1986b.

LAL, D. Investigations of Nuclear Interactions Produced by Cosmic Rays, **PhD Thesis**, Bombay University. 1958.

LAL, D.; PETERS, B. Cosmic ray produced isotopes and their application to problems in geophysics. In: J. G. Wilson and S. A. Wouthuysen, (Eds), **Progress in Elementary Particle and Cosmic Ray Physics 6**, Amsterdam: North Holland Publishing Company, pp. 77–243. 1962.

LAL, D.; PETERS, B., Cosmic ray produced radioactivity on Earth. In: S. Flugg, (Ed), **Handbook of Physics** 46/2, Berlin: Springer, pp. 551–612. 1967.

LEE, B.; HAN, Y.; HUH, Y.; LUNDSTROM, C.; SIAME, L.; LEE, J.; PARK, B. Chemical and physical weathering in south Patagonian rivers: A combined Sr–U–Be isotope approach, **Geochimica et Cosmochimica Acta**, Volume 101, p.173-190. 2013.

MAIR, D.; LECHMANN, A.; YESILYURT, S.; TIKHOMIROV, D.; DELUNEL, R.; VOCKENHUBER, C.; AKÇAR, N.; SCHLUNEGGER, F. Fast long-term denudation rate of steep alpine headwalls inferred from cosmogenic 36Cl depth profiles. **Nature Sci Rep** 9, 11023. 2019.

MARENT, B.R. **Mensuração dos processos desnudacionais a longo-termo (^{10}Be) na Serra do Mar no estado do Paraná: implicações para a evolução do relevo**. Dissertação (Mestrado em Geografia. Universidade Federal de Minas Gerais). Belo Horizonte, 107f. 2011.

MARENT, B.R.; SALGADO, A.; SANTOS, L.J.C.; PAULA, E.V.; BARRETO, H.; VARAJÃO, C. Importância da denudação diferencial nos granitoides da serra do Mar para a evolução do relevo da região da baía de Antonina – PR, Brasil. **Geosul**, Florianópolis, v. 33, n. 67, p. 200-213, maio 2018.

MARTI, K.; CRAIG, H. Cosmic-ray-produced neon and helium in the summit lavas of Maui, **Nature** 325 335–337. 1987.

MCLENNAN, S. Weathering and Global Denudation. **The Journal of Geology**, *101*(2), 295-303. 1993.

NISHIIZUMI, K.; KLEIN, J.; MIDDLETON, R.; CRAIG, H. In situ produced ^{10}Be and 26Al in olivine from Maui, **EOS** 68 1268. 1987.

NISHIIZUMI, K.; LAL, D.; KLEIN, J.; MIDDLETON, R.; ARNOLD, J. R. Production of ^{10}Be and 26Al by cosmic rays in terrestrial quartz in situ and implications for erosion rates, **Nature** 319 134–135. 1986.

PEULVAST, J.P.; BÉTARD, F.; LAGEAT, Y. Long-term landscape evolution and denudation rates in shield and platform areas: a morphostratigraphic approach. **Géomorphologie: relief, processus, environnement** 15 (2), 95-108. 2009.

PHILLIPS, F.M.; LEAVY, B.D.; JANNIK, N.O.; ELMORE, D.; KUBIK, P.W. The accumulation of cosmogenic chlorine-36 in rocks: a method for surface exposure dating. **Science** 231 41–43. 1986.

PINGEL, H.; SCHILDGEN, T.; STRECKER, M.; WITTMANN, H. Pliocene–Pleistocene orographic control on denudation in northwest Argentina. **Geology**. 2019.

PORTENGA, E.; BIERMAN, P. Understanding Earth's eroding surface with ^{10}Be. **GSA Today**. 21. P. 4-10. 2011.

PORTENGA, E.W.; Bierman, P.R. Understanding Earth's eroding surface with 10Be. **GSA today**, *21*(8), pp.4-10. 2011.

POUSSE-BELTRAN, L.; VASSALLO, R.; AUDEMARD, F.; JOUANNE, F.; CARCAILLET, J.; PATHIER, E.; VOLAT, M. Pleistocene slip rates on the Boconó Fault along the North Andean Block plate boundary, Venezuela. **Tectonics**. 2017.

PUPIM, F.; BIERMAN, P.; ASSINE, M.; ROOD, D.; SILVA, A.; MERINO, E. Erosion rates and landscape evolution of the lowlands of the Upper Paraguay river basin (Brazil) from cosmogenic ^{10}Be. **Geomorphology**. 2015.

REEDY, R.C.; ARNOLD, J.R.; LAL, D. Cosmic-ray record in solar system matter, **Science** 219 127–134. 1983.

REZENDE, É.; SALGADO, A.A.; SILVA, J.; BOURLÈS, D.; BRAUCHER, R.; LEANNI, L. Fatores controladores da evolução do relevo no flanco NNW do Rift Continental do Sudeste do Brasil: uma análise baseada na mensuração dos processos denudacionais de longo-termo. **Revista Brasileira de Geomorfologia**. 2013.

RITTER, D.F. Rates of Denudation, **Journal of Geological Education**, 15:4, 154-159. 1967.

ROSS, J.L.S. O relevo brasileiro no contexto da América do Sul. **RGB - Revista Brasileira de Geografia**, Rio de Janeiro, v. 61, p. 21-58, 2016.

SAFRAN, E.; BIERMAN, P.R.; AALTO, R.; DUNNE, T.G.; WHIPPLE, K.X.; CAFFEE, M.W. Erosion Rates Driven by Channel Network Incision in the Bolivian Andes. **Earth Surface Processes and Landforms**. 2005.

SAILLARD, M.; HALL, S.R.; AUDIN, L.; FARBER, D.L.; HÉRAIL, G.; MARTINOD, J.; REGARD, V.; FINKEL, R.C.; BONDOUX, F. Non-steady long-term uplift rates and Pleistocene marine terrace development along the Andean margin of Chile (31°S) inferred from ^{10}Be dating. **Earth and Planetary Science Letters**. Volume 277, Issues 1–2, 2009. p.50-63.

SALGADO A. A. R., BRAUCHER R., COLIN F., NALINI JUNIOR H. A., VARAJÃO A. F. D. C., VARAJÃO C. A. C. Denudation rates of the Quadrilátero Ferrífero (MinasGerais, Brazil): Preliminary results from measurements of solute fluxes in rivers and in situ-produced cosmogenic ^{10}Be. ***J. Geochem. Explor***., 88: 313-317. 2006.

SALGADO AAR, BRAUCHER R, VARAJÃO CAC, COLIN F, VARAJÃO AFDC, NALINI JÚNIOR AH. Relief evolution of the Quadrilátero Ferrífero (Minas Gerais, Brazil) by means of (^{10}Be) cosmogenic nuclei. **Zeitschrift für Geomorphologie** 52: 317–323. 2008.

SALGADO, A.A.R. **Estudo da evolução do relevo do Quadrilátero Ferrífero, MG–Brasil, através da quantificação dos processos erosivos e denudacionais**. 125 f. Tese (Doutorado em Evolução Crustal e Recursos Naturais) - Universidade Federal de Ouro Preto, Ouro Preto, 2006.

SALGADO, A.A.R., REZENDE, E.A., BOURLÈS, D., BRAUCHER, R., DA SILVA, J.R., GARCIA, R.A. Relief evolution of the continental rift of Southeast Brazil revealed by in situproduced ^{10}Be concentrations in river-borne sediments. **J. South America Earth Science**. 67: 89–99. 2016.

SALGADO, A.A.R.; VARAJÃO, C.A.C.; COLIN, F.; BRAUCHER, R., VARAJÃO, A.F.D.C.; NALINI JUNIOR, H.A. Study of the erosion rates in the upper Maracujá Basin (Quadrilátero Ferrífero/MG, Brazil) by the in situ produced cosmogenic ^{10}Be method. **Earth Surface Processes and Landforms**, v. 32, p. 905-911, 2007.

SALGADO, A.R.; MARENT, B.R.; CHEREM, L.F.S.; BOURLES, D.; SANTOS, L.J.C.; BRAUCHER, R.; BARRETO, H.N. Denudation and retreat of the Serra do Mar escarpment in southern Brazil derived from in situ-produced ^{10}Be concentration in river sediment. **Earth Surf. Process Landf**. 39, 311 e 319. 2014.

SIAME, L.; SÉBRIER, M.; BELLIER, O.; BOURLÈS, D.; COSTA, C.; AHUMADA, E.; GARDINI, C.; CISNEROS, H. Active basement uplift of Sierra Pie de Palo (Northwestern Argentina): Rates and inception from ^{10}Be cosmogenic nuclide concentrations: Active basement uplift. **Tectonics**. 34. 2015.

SORDI, M.C.; SALGADO, A.A.R.; SIAME, L.; BOURLÈS, D.; PAISANI, J.C.; LÉANNI, L.; BRAUCHER, R.; COUTO, E.V.; ASTER Team. Implications of drainage rearrangement for passive margin escarpment evolution in southern Brazil. **Geomorphology** 306, 155–169. 2018.

SOUZA, D.; STUART, F.; RODES, A.; PUPIM, F.; HACKSPACHER, P. Controls on the erosion of the continental margin of southeast Brazil from cosmogenic ^{10}Be in river sediments. **Geomorphology**. 330. 2019.

SRINIVASAN, B. Barites: anomalous xenon from spallation and neutron induced reactions. **Earth Planet. Sci. Lett**. 31 129–141. 1976.

STARKE, J.; EHLERS, T.; SCHALLER, M. Plate tectonic and climatic controls on the spatial distribution of denudation rates in northern Chile (18°S to 23°S) determined from cosmogenic nuclides. **Journal of Geophysical Research: Earth Surface**. 2017.
SUMMERFIELD, M.A.; HULTON, N.J. Natural controls of fluvial denudation rates in major world drainage basins: **Journal of Geophysical Research**, v. 99, p. 13,871–13,883. 1994.
VARAJAO, C.; ALKMIM, F.; BRAUCHER, R.; ENDO, I.; CHEREM, L.F.; SALGADO, A.; VARAJÃO, A. Denudation rates in the Pancas Bornhardt Province (SE Brazil), inferred from in situ produced cosmogenic ^{10}Be. **Zeitschrift für Geomorphologie**. 62. 2018.
VARAJÃO, C.A.C; SALGADO, A.A.R.; VARAJÃO, A.F.D.C.; BRAUCHER, R.; COLIN, F.; NALINI JUNIOR, H.A. Estudo da evolução da paisagem do quadrilátero ferrífero (Minas Gerais, Brasil) por meio da mensuração das taxas de erosão (^{10}Be) e da pedogênese. **Rev. Bras. Ciênc. Solo**, Viçosa, v. 33, n. 5, p. 1409-1425, 2009.
VASCONCELOS, P.; FARLEY, K.; STONE, J.; PIACENTINI, T.; FIFIELD, L. Stranded landscapes in the humid tropics: Earth's oldest land surfaces. **Earth and Planetary Science Letters**. 519. 152-164. 2019.
WALLING, D.E. Rainfall, runoff, and soil erosion of the land: a global review, In: Gregory, K.J. (ed.), **Energetics of the Physical Environment**, Chichester, England: J. Wiley and Sons, Ltd., pp. 89–117. 1987.
WIELER, R. Cosmic-ray-produced noble gases in meteorites, **Reviews in Mineralogy and Geochemistry** 47 125–170. 2002.
WILKINSON, B.H. Humans as geologic agents: a deep-time perspective. **Geology**. 33(3):161-4. 2005.
WITTMANN, H.; BLANCKENBURG, F.; BOURGOIN, L.; GUYOT, J.; KUBICK, P.W. Recycling of Amazon floodplain sediment quantified by cosmogenic Al-26 and Be-10. **Geology**. 39. 467-470. 2011.
YOKOYAMA, Y.; REYSS, J.-L.; GUICHARD, F. Production of radionuclides by cosmic rays at mountain altitudes. **Earth Planet. Sci. Lett**. 36 44–50. 1977.
ZECH, R., SMITH, J., KAPLAN, M. Chronologies of the LGM and its Termination in the Andes based on Surface Exposure Dating. In: F. Vimeux, F. Sylvestre, M. Khodri (Eds.), **Past climate variability in South America and surrounding regions**. From the Last Glacial Maximum to the Holocene. Springer, pp. 61-87. 2009.
ZECH, R.; KULL, CH.; KUBIK, P.W.; VEIT, H. LGM and Late Glacial glacier advances in the Cordillera Real and Cochabamba (Bolivia) deduced from ^{10}Be surface exposure dating. **Climate of the Past Discussions**, European Geosciences Union (EGU), 3 (3), pp.839-869. 2007.

3.2 MORPHOMETRIC TOOLS AND INDEXES APPLIED TO LONG TERM LANDSCAPE EVOLUTION ANALYSES OF THE SOUTHERN BAURU SEDIMENTARY BASIN.

3.2.1 INTRODUCTION

During the last 20 years, with the hardware development capable of processing greater data volume, some tools have been elaborated to generate morphometric indexes and graphical representations that help to interpret how the processes responsible for morphodynamics acted overtime to produce the current landscape.

These geomorphic indexes derived from *Digital Elevation Models* (DEMs) allowed geomorphologists to broaden their approaches in different landscapes along the globe. As an example of this diversity, we can mention the application of these tools to investigate Mediterranean Calanques features (Buccolini et al., 2012), sand dunes (Almeida et al., 2019), sediments production, and transport in Himalaya (Swarnkar et al., 2020), active tectonics settings (Pavano et al., 2019; Matos et al., 2016), landslide susceptibility occurrence (Othman et al., 2018), volcanic cones (Grosse et al., 2012), karst lithology zones (Donnaloia et al., 2019) and even on coral reef terraces (Nexer et al., 2015).

Some of the most used morphometric tools/indexes are: slope, hillside orientation, and curvature, escarpment front sinuosity, knickpoints concentration, K_{sn} index, watershed curvature and hypsometric integral, roughness index, watershed (a)symmetry, sediment transport capacity, planimetric ratio, Chi index (χ), drainage longitudinal profile, swath profile, residual reliefs, drainage incision gradient, knickpoints presence and distribution, first-order channel capture area, fork rate, and drainage network channels average junction angle (Shtober-Zisu et al., 2008; Richardson et al, 2016; Zhang et al., 2020).

These tools allowed scientists to combine digital processing data with field sampling and laboratory tests, increasing the time scale covered and the complexity of the interactions between the processes responsible for the landscape morphodynamics. These analyses allowed the researchers to conjecture more accurately about relief transformations during the late Cenozoic, which led to the definition of the terminology "long-term relief evolution" (Granger et al., 1996; Brocard et al., 2003; Inkpen et al., 2010; Gonzalez et al., 2016a; 2016b; Scuderi, 2017; Sembroni and Molin, 2018; Van Binh et al., 2019).

However, many studies focus on landscape dynamics considered periods of stability, which are relative, in a given period for the characterization of one or another main geomorphological process. But landscapes stack up evidence of several processes over time and in a regional context, these processes can coexist, with long periods of stability and other fast orogenesis episodes in the same region.

Landscape analysis assumes stable periods that can be integrated with morphodynamic adjustments. It is understood that the current relief is the result of long-term evolution integrating responses to past processes that may still influence current morphodynamics. Thus, studies that link 2 or more processes in a different time scale emerge in an attempt to complete the current dynamics, like glacial, paleoclimatic processes, (Schlunegger et al., 2002; Lane et al., 2017; Godard et al., 2019), or even tectonism and current erosive processes (Dorsey and Roering, 2006; Willenbring et al., 2013; Giletycz et al., 2015; Jaiswara et al., 2019; Geurts et al., 2020; Liu et al., 2020). In brief, distinct processes which predominate in the landscape in different periods could still be responsible for current erosive processes in the modern landscape.

The Bauru Basin is one of the most relevant areas for understanding the influence of past processes on South American morphodynamics. This sedimentary basin has characteristics inherited from Cretaceous tectonics, and its southern part constitutes an old center of sediment deposits. Consequently, it is an interesting area for the proxies application to generate paleoecological information that helps to understand the entire South American continent morphodynamics after Gondwana (Almeida et al., 2000; Brito Neves et al., 2002; Tedesco et al., 2019; Resende et al., 2020).

The paleoclimates that formed the sedimentary basin associated with the current occupation, without planning, and the deforestation after the 1950s accelerated erosive processes in the south of the sedimentary basin, creating large active erosive features (do Couto et al., 2018). An ideal geological-geomorphological context for the morphometric tools application to investigate the long-term morphodynamics registered regionally in the landscape.

Therefore, the subject of this chapter is to apply morphometric indexes to understand how morphodynamics occurred in long-term, during the upper Cenozoic, in the Bauru Sedimentary Basin Southern part.

3.2.2 MATERIALS AND METHODS

3.2.2.1 Regional Settings

One of the main South American Paleozoic Basins, the Bauru Basin has approximately 330,000 km² (Battezelli, 2005), covering a large portion of the Brazilian territory (Figure 2.1).

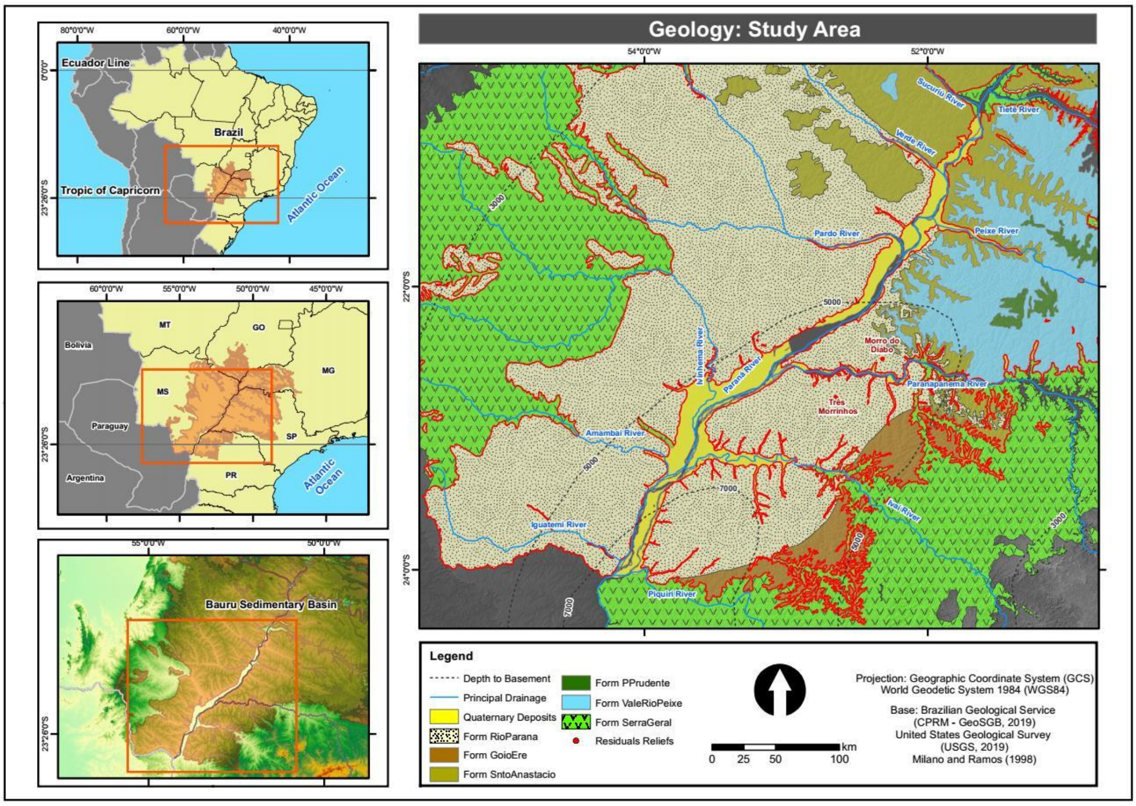

Figure 2.1: Southern Bauru Basin simplified geological map.

According to Battezelli (2003), the Bauru Basin is a geotectonic entity that originated in the upper Cretaceous through subsidence related to the Precambrian basement lineaments reactivation, forming mainly on sandstones and basalts, the Caiuá Group and the Serra Geral Formation respectively (Fernandes, 1992).

The Bauru Basin has its depocenter in the vicinity of the Paraná River. Its center is associated with isostatic compensation of the Serra Geral basalt flow and tertiary restructure, such as the uplifting of Serra do Mar and Alto Paranaíba craton (Battezelli, 2005).

According to Fernandes (2004), the tectonic reactivation of side areas to the Basin provided conditions for the emergence of the alluvial fan at the edges of the basin, contributing to the ordination of some of the geological formations identified in the area today, e.g.: Presidente Prudente Fm., São José do Rio Preto Fm.

To the South, in its most inner region, the basin accumulated 300m of sediment in a single sequence, forming a wide and shallow interior basin of endorheic character. This southernmost part was no longer under the humidity influence of the edges and river flows, but rather of the wind deposits (Fernandes, 2004).

More specifically, the Caiuá Group is a geological unit formed in the interval between 133 My, the last manifestations of magmatism date that originated the Serra Geral Formation, and 85 My, start estimative of the lithification process, such as the sandstones (Fernandes, 2004). The sediments that make up the current sandstone homonymous to the Caiuá Group, formed a large paleodesert (sandsea) located in the central portion of the basin, with its depocenter in the Paraná river Neighborhoods (Bigarella and Mazuchowski, 1985; Fernandes and Coimbra, 1994). The Caiuá paleodesert gave rise to a landscape with specific geomorphological characteristics that often appear in the scientific literature as a flat landscape, monotonous, uniform relief, without substantial elevation changes (Santos et al., 2006).

Near the southern limit of the basin, the region morphodynamics understanding can be fundamental to comprehend the evolution of the landscape from the sedimentary basin center during the last 65 My, when its edges were defined like as we know them today.

3.2.2.2 Morphometric Tools

The study area covers the southern portion of the Bauru Sedimentary Basin (from approximately 21°S to 24°S). For the longitudinal boundaries, we considered the basin Central/East area, the former deposition center that originated the Paraná River Formation (Gr. Caiuá), located among the Serra Geral Formation (Gr. São Bento) basalt flows (55°W and 52°W).

For the roughness and relief patterns identification, a decision tree has been processed to automate the classification process according to parameters pre-established. We chose to use the slope and subsequently the roughness index in the tree nodes, thus generating three classes: Low (flattest terrains), Intermediate (poorly dissected terrains), and High (moderate dissected terrains) roughness.

The drainage network adjustment analysis and consequently watersheds limits displacement was made using the χ index (Willet et al., 2014). The base level used for the calculation was stipulated at 200m elevation, which allowed covering the entire drainage network in the southern sedimentary basin.

At the regional scale, the relief correlation analysis was made with swath profiles. With It was possible to investigate some formation patterns. This allowed inferences on low relief surfaces, thus demonstrating relatively flat surfaces, which correspond to different erosion cycles.

As a result, a raster file was made with possible low relief surfaces in good agreement with the scientific literature dealing with possible paleosurfaces or ancient surface levels before the Holocene. The raster with the low relief surfaces was also made from the decision tree, using a first slope node: class below ten degrees; and a second of hypsometry separated into three classes with elevation adjusted for the regional context: South American Surface (King, 1965), Regional Pediments and Local Pediplans (Bigarella et al., 1965).

The study spatial scale is regional, however, it should be emphasized the importance of anomalous/relictual patterns and local particularities indicated by the topographic analysis, which, if understood in the regional context, can help south basin evolution discussion.

3.2.3 RESULTS AND DISCUSSION

3.2.3.1 Roughness Index

The index demonstrated great efficiency in identifying relief feature patterns in the study area. Regionally, it is a markedly flat zone due to the lithological formation from the Caiuá paleodesert. The Bauru Basin southern region had a predominance of the intermediate class, with poorly dissected terrains standing out at first (Figure 2.2).

The high roughness class is concentrated on the sedimentary basin edges (basalt transition), besides being punctually distributed in the Caiuá Group domains (Figure 2.2). The concentration of moderate dissected terrains, even if punctually throughout the Caiuá Group, deserves special attention in understanding the landscape evolution.

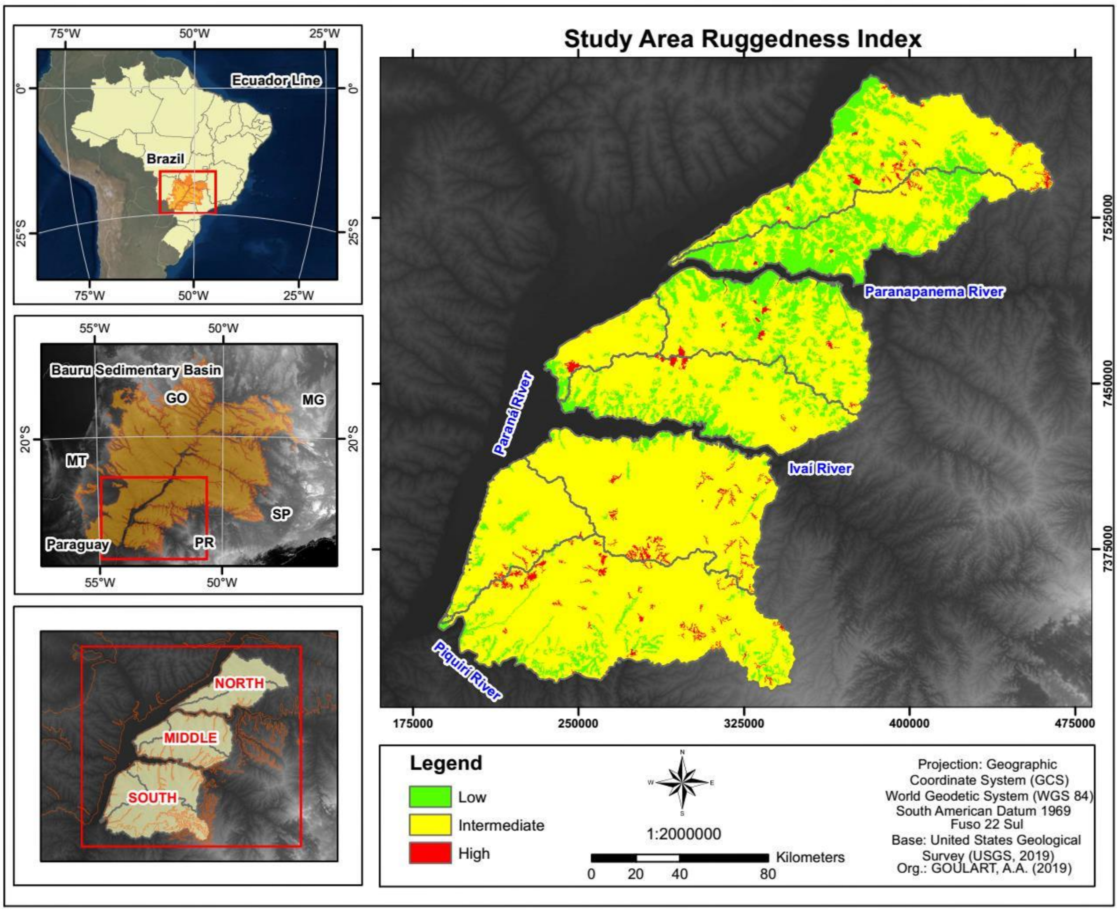

Figure 2.2: Study area roughness index.

The total roughness classes for the Paraná River eastern bank area presented low values for the lower classes (16%) and high (2%), with the majority pixels identified as the intermediate class (82%).

The roughness comparative analysis also indicates a difference in North-Middle-South values. The paleodesert portion that is further north corresponded to 32% of pixels identified as low roughness class, and only 2% of pixels are in the highest class (Table 2.1). These numbers indicate that despite the intermediate class predominance, 66%, there were still significant values for the flattest terrain occurrence. Also, the method was able to identify the Morro do Diabo (moderate dissected terrains), a feature that had its distinct morphological evolution compared to the surrounding landscape, here classified as an anomalous/relictual relief feature.

NORTH (watersheds)	Low	Intermediate	High	Σ
Paraná	1125493	3657047	110484	4893024
Paranapanema	1667635	2039825	23440	3730900
Total	2793128	5696872	133924	8623924
%	32.39	66.06	1.55	100

Table 2.1: Roughness classes distribution in the study area northern portion.

Towards the South, in the middle zone, a smaller proportion of roughness lower class pixels was identified (Table 2.2), 20%, compared to the 32% identified in the North for the same class. For the higher roughness class, just 1% was identified, although the difference is not so great when compared to the North, less than 1%. It is observed that there is a flattest terrains values distinction between the Paranapanema and Ivaí watersheds, the first had most of the low roughness class pixels, similar to the values found in the north portion.

The high roughness class in the middle zone also covers a relictual relief, the Três Morrinhos or Morro dos três irmãos (Figure 2.3), a geomorphological formation similar to Morro do Diabo (Figure 2.2). In addition to the residual relief already identified, the greater roughness pixels have a specific location in the areas near the regional interfluves, which separate the Paranapanema and Ivaí watersheds.

MIDDLE (watersheds)	Low	Intermediate	High	Σ
Ivaí	721703	3488240	36807	4246750
Paraná	136828	1036399	25417	1198644
Paranapanema	1150925	3168471	49412	4368808
Total	2009456	7693110	111636	9814202
%	20.47	78.39	1.14	100

Table 2.2: Roughness classes distribution in the middle study area portion.

Figure 2.3: Relictual relief named as Três Morrinhos identify in the high roughness class.

The Southern portion presented the lowest values proportionally (Table 2.3), for the flattest terrains class, 5%, and the highest values of the moderate dissected terrains class, 2%. Even without presenting any relictual structure known in the region as the residual reliefs supported by silicified sandstones, the portion still presented higher roughness values proportionally. It is noted that the greater roughness pixels concentration, 93% of moderate dissected terrains, are in the interfluves neighborhood, but there are also some features identified as anomalous in the middle slope, in the main rivers' watersheds dividers (Figure 2.2).

SOUTH (watersheds)	Low	Intermediate	High	Σ
Ivaí	145101	5425044	154248	5724393
Paraná	121659	2232845	29157	2383661
Piquirí	526973	6922424	204024	7653421
Totais	793733	14580313	387429	15761475
%	5.04	92.51	2.46	100

Table 2.3: roughness classes Distribution in the south study area portion.

Generally, the roughness low class values, flattest terrains, decrease as the southernmost portions are analyzed. The opposite happens in the high roughness values, moderately dissected terrains, that increase in the southernmost portion. Demonstrating that to the south there is more dissected and to the north flattest reliefs.

The areas identified as moderate dissected terrains, a total of 1.9% of all study area, could be associated with the most relevant processes that shaped the landscape.

These pixels may represent an anomalous relief occurrence pattern, possible residual reliefs, which reveal the landscape morphodynamics characteristic.

A geomorphological pattern identified by the moderate dissected terrains class is the presence of the residual relief supported by silicified sandstones of the K-T surface level, correlated to the South American surface (King, 1956), as the Morro dos Três Irmãos and Morro do Diabo (Figure 2.2 and 2.3). Such geomorphological anomalies are *inselbergs*, a result of previous surface degradation, but which remained due to structural characteristics, silicified by silica hydrothermal fluids, presenting a 130 meters gap in relation to regional surfaces (Fernandes et al., 2012). Unlike the other areas identified as the roughness high class, these features are the only positive relief areas found in the index application. It is remarkable these features correlate with the landscape characteristics, since it is the endogenetic Mesozoic process's results, but it resisted the denudational processes due to the erosive differential imposed by the inside silica cementation.

The last features classified pattern with the roughness high class that deserve attention because they fit into anomalous/relictual features are the presence of possible Paleo features (Figure 2.2). Corroborating with Bigarella and Mazuchowski (1985) about the Paleoclimates relevance to explain the region morphodynamics, Justus (1985) suggests that the current area topography is the result of Quaternary glaciation oscillations, and also Tertiary tectonic activities. Therefore, for the authors, added to the specific tectonic actions that hardly interfere in the current landscape evolution, quaternary paleoclimatic oscillations correspond to the erosional cycles and some flatness relief in the region evidenced by Bigarella and Mazuchowski (1985).

More recently, the last finding that confirms these areas are Paleo features was made by Goulart and Santos (2014). The features overlapping, in a Digital Elevation Model with the first region aerial photographs, made in 1953, made it possible to note that these erosive features presence even before the region anthropic occupation process and the replacement of the original forest by local agricultural activities. According to the authors, three large paleo features groupings were identified in the study area.

Considering that lithology is the same, Gr. Caiuá, and analyzing the roughness numbers can be conjectured that the relictual/anomalous features idealized by Bigarella and Mazuchowski (1985) and found punctually by Goulart and Santos (2014), have already occurred in the South. However, due to the higher denudation rate (do

Couto, 2014), there was the paleofeatures coalescence and the relief dissection in a more advanced stage when compared to the northern portions.

Therefore, the current relief is the sum result of the past action and current morphogenetic processes, denoting the landscape morphodynamics, with vertical dissecting periods (chemical weathering and pedogenesis predominance) interspersed by lateral degradation periods (physical weathering and morphogenes predominance) (Bigarella and Mazuchowski, 1985; Justus, 1985). These processes allowed the extensive erosion surfaces evolution punctuated by smaller geomorphological features, but relevant to the regional relief evolution understanding such as anomalous/relictual features identified by the roughness index.

3.2.3.2 Drainage Network Adjustment Index (X)

The whole Bauru Basin χ (Chi) index values range from 0.2 to 14.30, indicating drainage network sections greater and lesser aggressiveness (Willet et al., 2014). However, to have a drainage network adjustment prediction, the neighboring basins' values must be contrasting, with one being more aggressive and generally taking area and even capturing drainages from the higher value basins in the surroundings (Willet et al., 2014).

This does not occur in the study area, when comparing χ values for both sides of the main regional divide it is possible to notice that the values are close (Figure 2.4), with corresponding values in the basins adjacent to the divisor. As expected, the highest χ values are found on the basin edges, in the transition with the Serra Geral Formation basalts, and the lowest values are found in the largest rivers neighborhood, closer to the base level and consequently with greater erosive potential.

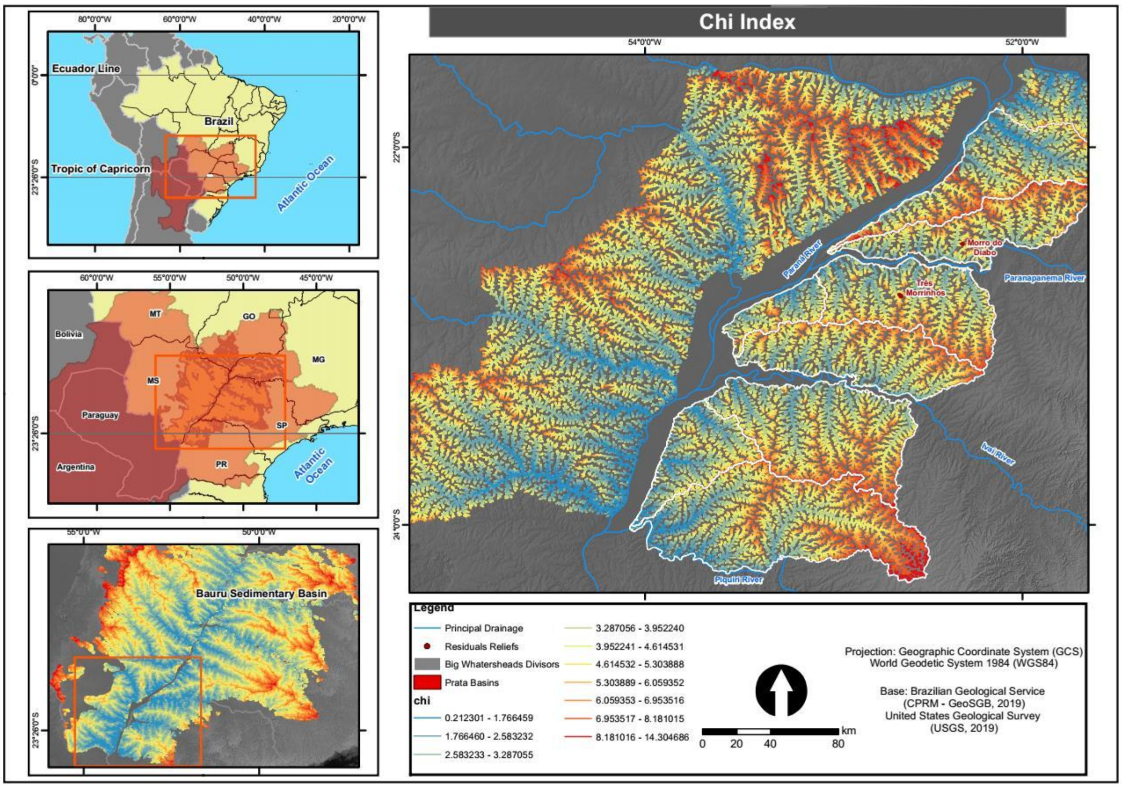

Figure 2.4: Study area χ index.

The χ map shows relative stability when comparing the values closest to the watershed in the northern regions. It was noted that the values are equivalent in the different region watersheds, which is consistent with a relative equilibrium state, steady state. This fact can be explained by the study area is very close to the basin center, which despite the watersheds of different divisor sides flows to the same main river, the Paraná river, with a very close base level, a difference of approximately 50 m from the Paranapanema delta to the Ivaí delta.

On a local scale, the correspondence of the value is even clearer, as in one of the study area main interfluves, between drainages that flow to Paranapanema and Ivaí rivers (Figure 2.5). Even when comparing areas of moderate dissected terrains near the divider (highlighted area in Figure 2.5), identified in the roughness index, the χ does not show an interfluve rearrangement process.

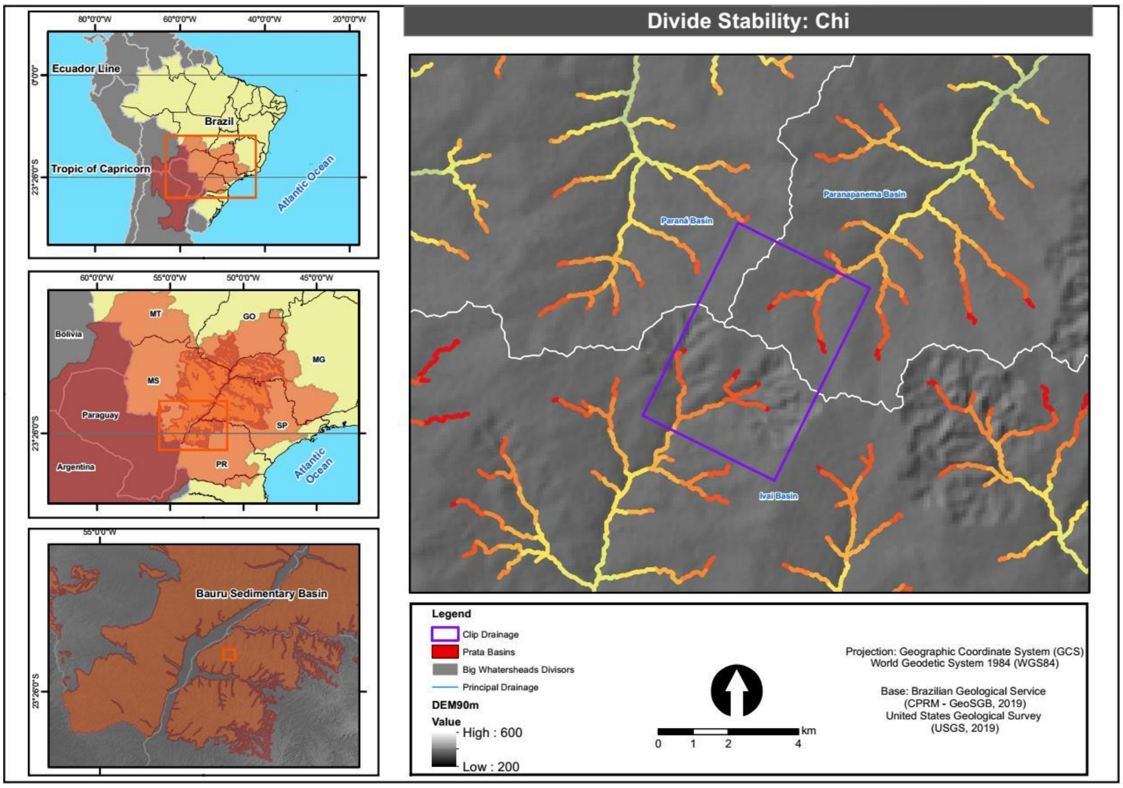

Figure 2.5: χ index local scale analysis, at the divider limit of the three watersheds (Paraná, Paranapanema and Ivaí).

However, the assertion that there is a steady state in the large watersheds analyzed in the area, can bring a relevant answer. The landscape evolution is the processes accumulation that have acted at different times, but which may be recorded in some specific features, or in more regional morphologies that do not seem to respond to the current morphodynamics.

However, these anomalous/relict features are still part of the dynamic, not necessarily as something atypical, but which is in balance and constant evolution, harmoniously with the landscape around it. In other words, the roughness that makes these features anomalous/relictual exists and is striking, but the χ will not show this difference if the drainage network geometry is not very contrasting with that of the watershed on the other interfluve side. Other morphometric indexes proposed, such as Forte and Whipple (2018), for the watershed stability analysis, may generate different and interesting results if tested in areas with clear morphological differences such as anomalous features and their encounter with neighboring watersheds.

3.2.3.3 Low Relief Surfaces

The regional Low Relief surfaces show relatively flattened and correlated hypsometric levels on both Paraná River banks (Figure 2.6).

The late Cretaceous basalt spills and the isostatic compensation of this material volume deposited on the Bauru basin surface added to the later erosive process created the relief range that can be noted when analyzing the landscape morphodynamics. Thus, each low relief surface should be understood here as an allusion to a relatively flat surface, formed by erosive cycles, mainly commanded by paleoclimatic pulses.

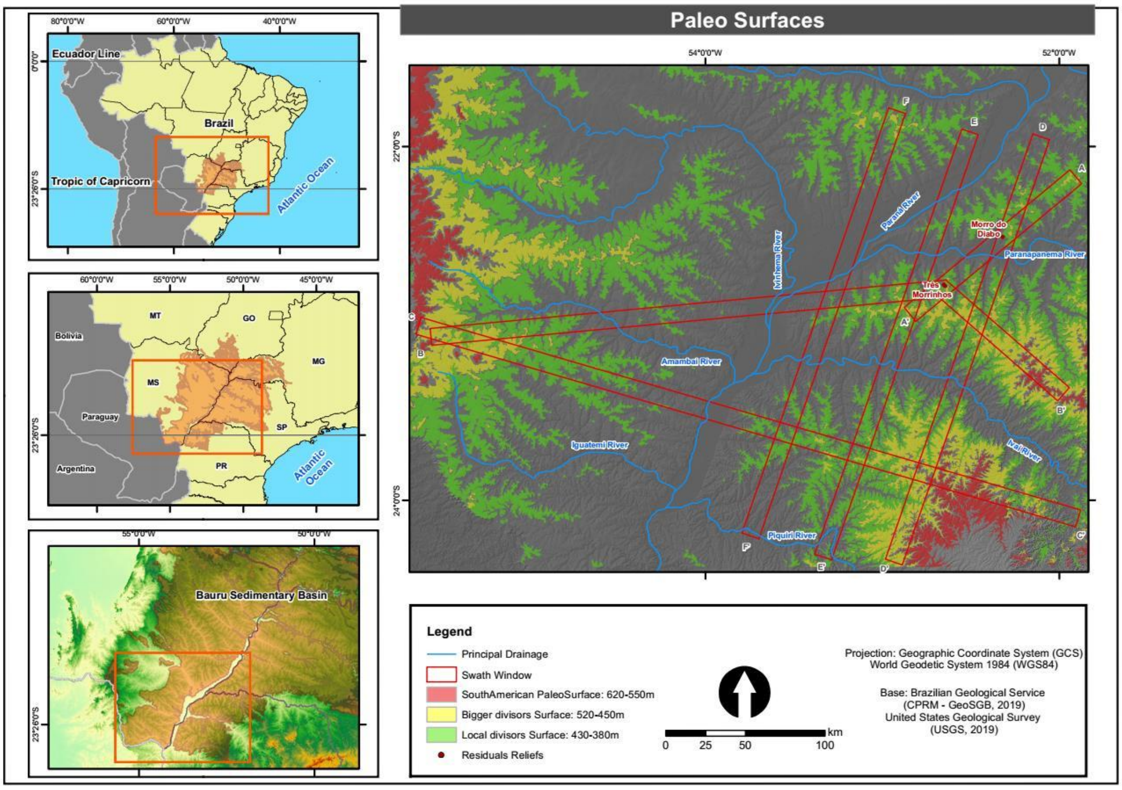

Figure 2.6: Bauru basin south low relief surfaces, with the respective swath profiles windows.

There is a first level, correlated to the modeling processes dating from the first erosive cycle, identified by the decision tree corresponding to the **South American Surface** (King, 1956), also called K-T flat surface (Fernandes et al., 2012) (Figure 2.6). At this surface, from 620 to 550m above sea level, the Serra Geral end of magmatism was associated, approximately 65My, extending its erosive cycle from the Paleocene to the Eocene. The South American surface was linked to the Paraná riverbed formation that currently runs through the sedimentary basin center, conditioned by the

South American surface edges and by Transbrasiliano geological lineaments (Almeida et al, 2000).

In accordance with the border's elevation, but close to the basin center, there are still the residual reliefs supported by silicified sandstones (Fernandes et al., 2012). The Morro dos Três Irmãos and Morro do Diabo was identified in the roughness index as anomalous/relictual reliefs, being classified by the decision tree as remnants of the South American surface, because these residual reliefs are at the K-T surface level, in contrast to the areas of flattest and poorly dissected terrains in their immediate surroundings.

When describing the flat low relief generated from the South American surface, Bigarella and Mazuchowski (1985) focus on the evidence of pedimentation and pediplanation processes that can be found in the region and that consequently mark the landscape, forming other flat surfaces after the South American erosive cycle.

This intermediate surface, 520 to 450m elevations, corresponds to **regional water dividers**, separating some regionally relevant watersheds such as Paranapanema, Ivaí, Piquirí, Ivinhema, Amabaí among others that drain directly to the Paraná River, in the Bauru Basin center. The regional hypsometric correspondence and the topographic position in the landscape allowed an association of this low relief surface with the pediments identified in the area by Bigarella et al. (1965). This second erosive pulse may still have a significant presence of features in the field, called velhas erosion cycle (King, 1956), was the 34My, throughout all the Oligocene and Miocene.

The last *low relief* surface identified is that represented by the **local drainage dividers**, responsible for subdividing regional basins. This surface extends from 430 to 380 m elevations along the study area, with the beginning of its erosive cycle in 5.3 My (Bigarella and Mozuchowski, 1985), lasting all the Plio-Pleistocene, ceasing during the Holocene. The geological period in which there were great changes in the modeling of the earth's surface because it was the last great glacial period. This erosive cycle became known as Paraguaçu erosive cycle (King, 1956). Bigarella and Mozuchowski (1985) reiterate that the current relief with morphological flat steps is the result of successive reshaping that occurred during the Cenozoic, more specifically during the Plio-Pleistocene. The pediplans designated by Bigarella et al. (1965) it were identified on this surface.

Variations in humid (interglacial) and semi-arid (glacial periods) climates, with small climatic fluctuation (Bigarella et al., 1961), suggest that erosive processes were intense during the transition from the most recent episodes of prolonged drought (Bigarella and Mazuchowski, 1985). This paleoenvironmental picture may have generated significant changes in the region geomorphology during this period, originating, in the Pleistocene, point incisions in a predominantly ancient flat relief.

According to these authors, some Paraná River east areas have a slope gathering, with all the visual characteristics of a gully, in different evolution stages, but currently stable, compatible with a possible formation in Pleistocene paleoclimates. They came to conjecture about these features being possible paleo erosive features, already calling them Paleo gullies.

This statement reinforces the idea of the anomalous/relict features occurrence in the region, that were identified in the moderate dissected terrains class in the roughness index results. However, the differentiation between the active/current erosions that formed due to disordered occupation (Maack, 1968) and other anthropic interferences and the previous forms of gullies is practically impossible, if only radar images, aerial photographs, or satellite images are used.

Some areas not classified by the decision tree are in central basin areas, where current morphodynamic processes are developing, shaping the most recent surface, the current terraces.

The terraces of the Paraná River extend from 350 to 250 m approximately in the southern area of the Basin. These constitute large colluvial and alluvial deposits already in the Holocene, 0.01 My (Souza Filho et al., 1997). The terraces were not identified, as they would not bring information about the landscape morphodynamics, since they are still in formation and their erosive cycle has not yet ceased but is forming and conditioning the entire southern study area landscape.

3.2.3.4 Swath Profiles

Using swath profiles, it was possible to verify some morphological aspects that characterize punctually or regionally the landscape evolution (Figures 2.6 and 2.7).

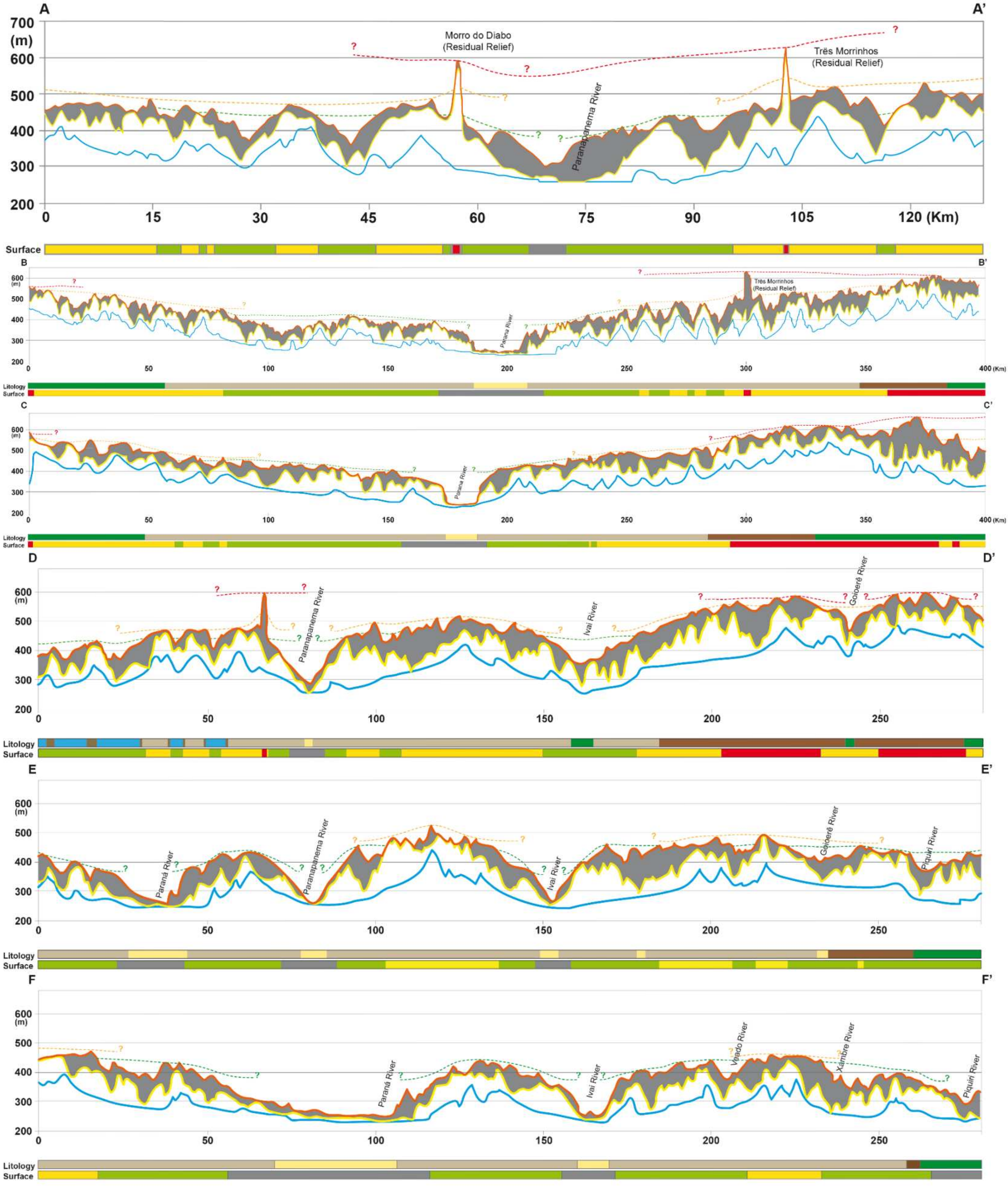

Figure 2.7: Swath profiles, with associated lithology representations as shown in Figure 2.1 and the low relief surfaces as shown in Figure 2.6.

The swath profile **A-A'** (Figures 2.6 and 2.7) was made to show the correlated residual reliefs hypsometry supported by silicified sandstones at the South American surface level described by King (1956), as well as the other subsequent surfaces. The two inselbergs longitudinal position visualized in this profile resembles (Morro do Diabo 52°33'W and Morro dos Três Irmãos 52°64'W) and the alignment of both is parallel to the Paraná River that drains the central basin. Its topographic positions and genesis, which is originated from the same process, allow us to suggest that possibly these residual reliefs are remaining from the South American surface in the southern basin center, an altimetric level closer to the Caiuá paleodesert ancient level.

The regional water dividers surface can be observed at pediment levels around the South American surface and at the residual relief edges with a relative continuity of about 500m of elevation in this profile. Another interesting point that can be observed in profile A-A' is that the northern portion relief of the Paranapanema River is flat than the south, which is consistent with the roughness results for both portions. The geophysical relief analysis shows the recent Paranapanema River incision and some other areas closer to the Três Morrinhos that are also identified in the roughness as moderate dissected terrains, anomalous/relictual features that may have been formed in erosive pulses under the paleoclimates action, such as during the Paraguaçu erosive cycle (King, 1956), which refers again to the Paleo gullies idea showed by Bigarella and Mazuchowski (1985).

The second swath profile, the **B-B'** (Figures 2.6 and 2.7), crosses the south of the Basin, from one edge to another, following the regional interfluves, which divide the Amambaí and Iguatemí rivers in the Paraná river west bank and Paranapanema and Ivaí in the east bank. The profile analysis reveals the structure influence on the relief range, with the South American surface at the edges, where the predominant lithology comes from the basalt transition, and in the residual relief, with the representation of the residual relief Três Irmãos. The regional pediments surface and the local Pediplans appear on levels on both sides of the basin, with more separate levels on the West Bank. Such step surfaces can mean different evolutionary stages of landscape morphodynamics.

The **C-C'** profile (Figures 2.6 and 2.7), also positioned transversely to the Basin, reveals that the Southern Caiuá portion has the same pattern of hypsometric distribution dimensions when compared to the Northern portion of the Group. In the transition of the Caiuá Group with the Serra Geral Formation are the areas identified as South American Surface remnants, but with the residual relief absence in this study area portion.

The longitudinal analysis of the Basin's southern eastern margin can be seen in the next three swath profiles. In the easternmost profile, **D-D'** (Figures 2.6 and 2.7) we can notice the same hypsometric correlation, but in the Northeast-Southwest direction. It is possible to notice the correlation expressed between Morro do Diabo and the divider in the southernmost portion, with altimetry close to 600m elevation. The main drainages also refer to erosive cycles, such as the Goio-Erê River that notches the remnants of the South American surface and is currently on the regional pediments level; the Ivaí River, which currently drains at the local Pediplans level, but which notches the regional pediments surface; and the Paranapanema River, which has its bed related to current processes, with its drainage commanding the regional base level.

It can be observed that the Caiuá Group is smaller at the edge of the basin on its eastern margin compared to the western margin, maintaining approximately 600m on both edges. Thus, it is expected that morphodynamics will be faster in the South, with a bigger range and greater geophysical relief, than in the North.

The last two North-South profiles, E-E' and F-F' (Figures 2.6 and 2.7), show the Regional Pediments and Local Pediplans correlation. The lithology no longer interferes in the distribution of the levels observed from the old erosion cycles, but rather the distance to the Paraná River, the general study area base level. In the **E-E'** profile, it was noted that the Regional Pediments surface appears specifically in the regional drainage dividers, which separate the Paranapanema, Ivaí, and Piquiri rivers. In the **F-F'** profile, the Local Pediplans position in the regional rivers tributaries dividers, already in the Paraná River vicinity, was clear.

3.2.3.5 Low Relief Surfaces Approximate Age of the Denudation Process Beginning

Considering that the South American surface has an average age of 49.5 My, it was formed after the Cretaceous, between the Paleocene and Eocene, and that it had average elevation levels of 600m (Figure 2.7), the denudation rate up to reaching the regional base level, 250m on the Paraná River (350m range), would be 7.1 m/My.

For the water dividers' regional surface, an age of 19.6My was considered, an average of the geological times of the Oligocene and Miocene, and an average elevation of 520m, which results in a range of 270m to be incised up to the base level of the river Paraná. Thus, resulting in a rate above the South American surface, with denudation of 13.7 m/My.

An even higher denudation rate was calculated for the local surface drainage dividers, considering the average age of 2.6My, between Pliocene and Pleistocene, with a range of 180m between the altimetric levels of 430m and 250m of the regional base level of the Paraná River. Resulting in a rate of 69.2 m/My.

There was an increase in the speed of denudation rates over the analyzed period, which corroborates with the scientific literature. Calculations made by Goulart (in press, item 3.3) based on denudation rates with measurements of *in situ* ^{10}Be in the study area, indicated that the regional basins started their denudational process still in the Miocene. As for the average of denudation, in these basins, the aforementioned author measured results of 12.2 ±2.0 m/My, number according to the 13.7 m/My found in the estimation of the denudation speed of the regional water dividers surface.

For the local surface drainage dividers, the denudation rate of 69.2 m/My, corresponds to some basins on a local scale measured by Goulart (in press, item 3.3). According to the author, some basins that deviate from the regional pattern, considered as possible paleo features were formed under paleoclimatic action during the Pleistocene glaciation, when denudational processes allowed the acceleration of denudation rates. These, according to Goulart (in press, item 3.3) reached 60.2 ± 7.0 and 77.4 ± 6.5, numbers similar to the one calculated for the local surface drainage dividers, of 69.2 m/My.

3.2.4 FINAL CONSIDERATIONS

The morphometric tools allowed a relief long-term evolution analysis, revealing the analyzed landscape morphodynamics. Combining the geological/ geomorphological Bauru Basin South characteristics with the indexes and tools applied in the study, it was possible to conjecture about the speed of the relief-modeling processes, as well as some anomalous/relictual patterns that are evidenced throughout the study area.

The roughness index allowed the identification of features and points that should be better evaluated in the morphodynamics interpretation, such as inselbergs or the possible erosive paleofeatures present punctually in the area. This index also helped to explain the process's speed, since the areas further to the north present flattest reliefs in contrast to the areas further south.

This idea is reaffirmed on the low relief surfaces, identifying the erosive cycles and their remaining and correlated levels in the basin. Swath profiles exemplify this hypsometric correlation and the erosive pulses of each cycle.

For the χ index, the results showed a steady state of illusory character, since the other indexes show that there is an ongoing morphodynamic process that tends to readjust some areas indicated in the roughness index as moderate dissected terrains, close to regional dividers. Thus, for this index, the results are still unsatisfactory and require correlation with other interfluves adjustment indexes using drainage as a parameter for comparative analysis.

In general, the regionally flattened landscape that the morphometric tools indicated, either by the lithological constitution from a paleodesert, or by the constant processes and cycles of relief horizontalization, hides some interesting processes/features for the regional morphodynamic interpretation.

However, more research with isotopic analyses is needed to create a relief evolution model for the Southern region of the Basin. The indexes and other results generated here are current tools and extremely relevant for the morphodynamics interpretation. Such results can be even more robust if associated with isotopic data sampled in watersheds in the study area.

3.2.5 REFERENCES

ALMEIDA L.R. DE; GONZÁLEZ, M.; MEDINA, R. Morphometric characterization of foredunes along the coast of northern Spain. ***Geomorphology***. Volume 338. P. 68-78. 2019.

ALMEIDA, F. F. M. de; BRITO NEVES, B. B. de; CARNEIRO, C. D.R. The origin and evolution of the South American platform. ***Earth-Science Reviews***[S.l.], v. 50, n. 1-2, p. 77-111, 2000.

BATEZELLI, A. **Análise da Sedimentação Cretácea no Triângulo Mineiro e sua Correlação com Áreas Adjacentes**. 183 f. Tese (Doutorado em Geologia), Instituto de Geociências e Ciências Exatas, UNESP, Rio Claro, 2003.

BATEZELLI, A., GOMES, N.S., PERINOTTO, J.A.J. Petrográfica e evolução diagenética dos arenitos da porção norte e nordeste da bacia Bauru (Cretáceo Superior). **Revista Brasileira de Geociências**, v. 35, n.3, p.311-322, 2005.

BIGARELLA J.J., MARQUES FILHO, P.; AB'SÁBER A.N. Ocorrências de pedimentos remanescentes nas fraldas da serra do Iqueririm (Garuva-SC). **Bol. Paran. Geografia**, (4 e 5), p.71-85. 1961.

BIGARELLA, J. J.; MOUSINHO, M. R.; SILVA, J. X. Pediplanos, pedimentos e seus depósitos correlativos no Brasil. **Bolm parana. Geogr**., v. 16/17, p. 117-151, 1965.

BIGARELLA, J.J. e MAZUCHOWSKI, J.Z. **Simpósio nacional de controle de erosão.** Anais. Maringá, 1985.

BRITO NEVES, B. B. Main Stages of the Development of the Sedimentary Basins of South America and their Relationship with the Tectonics of Supercontinents. **Gondwana Research**, 5(1), 175–196. 2002.

BROCARD, G.Y.; VAN DER BEEK, P.A.; BOURLÈS, D.L.; SIAME, L.L.; MUGNIER, J-L. Long-term fluvial incision rates and postglacial river relaxation time in the French Western Alps from 10Be dating of alluvial terraces with assessment of inheritance, soil development and wind ablation effects. ***Earth Planet***. Sc. Lett., 209, 197-214. 2003.

BUCCOLINI, M.; COCO, L.; CAPPADONIA, C.; ROTIGLIANO, E. Relationships between a new slope morphometric index and calanchi erosion in northern Sicily, Italy. ***Geomorphology***, p. 41-48. 2012.

do COUTO, E.V.; SANTOS, L.J.C.; SORDI, M.V.; BOURLÈS, D.; BRAUCHER, R.; SALGADO, A.A.R.; LÉANNI, L.; FERREIRA, J.H.D.; ASTER TEAM. Changes of the base levels in the Ivaí and Paraná Rivers confluence zone (Southern Brazil): Denudational reflexes in the evolution of the upstream drainage network. **Zeitschrift für Geomorphologie**. Volume 62 Issue 1 , p.23-40. 2018.

DONNALOIA, M.; GIACHETTA, E.; CAPOLONGO, D.; PENNETTA, L. Evolution of fluviokarst canyons in response to the Quaternary tectonic uplift of the Apulia Carbonate Platform (southern Italy): Insights from morphometric analysis of drainage basins. ***Geomorphology***. Volume 336. P. 18-30. 2019.

DORSEY, R.J.; ROERING, J.J. Quaternary landscape evolution in the San Jacinto fault zone, Peninsular Ranges of Southern California: Transient response to strike-slip initiation, ***Geomorphology***, 73(1–2), 16–32. 2006.

FERNANDES L.A.; COIMBRA A.M. O Grupo Caiuá (Ks): revisão estratigráfica e contexto deposicional. **Rev. Bras. Geociências**, 24(3):164-176, 1994.

FERNANDES, L.A. **A cobertura cretácea suprabasáltica no Paraná e Pontal do Paranapanema (SP)**: os grupos Bauru e Caiuá. São Paulo. 129p. (Dissertação de Mestrado, IGc/USP). 1992.

FERNANDES, L.A. Mapa litoestratigráfico da parte Oriental da Bacia Bauru. **Boletim Paranaense de Geociências**, n.55, p. 53-66, 2004.

FERNANDES, L.A.; COUTO, E.V.; SANTOS, L.J.C. Três Morrinhos, Terra Rica, PR Arenitos silicificados de dunas do Deserto Caiuá testemunham nível de superfície de aplainamento K-T. In: WINGE, M. et al (edit./org.). **Sítios geológicos e paleontológicos do Brasil**, vol. III. Brasília. Serviço Geológico do Brasil – CPRM, v. III, p. 69-87.2013.

FORTE, A.M., WHIPPLE K.X., Criteria and Tools for Determining Drainage Divide Stability, **Earth and Planetary Science Letters**, v. 493, p.102-117. 2018

FUMIYA, M.H.; SANTOS, L.J.C.; MANGUEIRA, C.G.; COUTO, E.V. Emprego do índice de concentração da rugosidade para a identificação de feições morfológicas associadas as crostas ferruginosas no Noroeste do Paraná. **Revista Brasileira de Geomorfologia**, v. 17, nº 3 2016

GEURTS, A.H.; WHITTAKER, A.C.; GAWTHORPE, R.L.; COWIE, P.A. Transient landscape and stratigraphic responses to drainage integration in the actively extending central Italian Apennines. ***Geomorphology***. Volume 353. 2020.

GILETYCZ, S.; LOGET, N.; CHANG, C.P.; MOUTHEREAU, F. Transient fluvial landscape and preservation of low-relief terrains in an emerging orogen: Example from Hengchun Peninsula, Taiwan. ***Geomorphology***. Volume 231, p. 169-181. 2015.

GODARD, V.; DOSSETO, A.; FLEURY, J.; BELLIER, O.; SIAME, L. Transient landscape dynamics across the Southeastern Australian Escarpment. ***Earth and Planetary Science Letters***. Volume 506. P. 397-406. 2019.

GONZALEZ, V.S.; BIERMAN, P.R.; FERNANDES, N.F; HOOD, D.H. Long-term background denudation rates of southern and southeastern Brazilian watersheds estimated with cosmogenic 10Be. ***Geomorphology***. Volume 268 p.54–63. 2016b.

GONZALEZ, V.S.; BIERMAN, P.R.; NICHOLS, K.K.;. ROOD, D.H. Long-term erosion rates of Panamanian drainage basins determined using in situ 10Be. ***Geomorphology***. Volume 275. P. 1-15. 2016a.

GOULART, A.Á.; SANTOS, L.J.C. Evolução temporal e espacial das paleovoçorocas presentes no município de Loanda/PR. **Revista Geonorte**, Edição Especial, v. 10, p. 81-86, 2014.

GRANGER D.E.; KIRCHNER J.W.; FINKEL R. Spatially averaged long-term erosion rates measured from in situ-produced cosmogenic nuclides in alluvial sediments. ***Journal of Geology***. 104: p.249–257. 1996.

GROSSE, P.; VAN WYK DE VRIES, B.; EUILLADES P.A.; KERVYN, M.; PETRINOVIC, I. Systematic morphometric characterization of volcanic edifices using digital elevation models. ***Geomorphology*** 136:114–131. 2012.

INKPEN, R.J.; STEPHENSON, W.J.; KIRK, R.M.; HEMMINGSEN, M.A.; HEMMINGSEN, S.A. Analysis of relationships between micro-topography and short- and long-term erosion rates on shore platforms at Kaikoura Peninsula, South Island, New Zealand. ***Geomorphology***. Volume 121, Issues 3–4. P. 266-273. 2010.

JAISWARA, N.K.; KUMAR, K.S.; PANDEY, A.K.; PANDEY, P. Transient basin as indicator of tectonic expressions in bedrock landscape: Approach based on MATLAB geomorphic tool (Transient-profiler). ***Geomorphology***. 2019.

JUSTUS, J.O. **Subsídios para interpretação morfogenética através da utilização de imagens de radar**. 204 f. Dissertação (Mestrado em Geografia) – Universidade Federal da Bahia, Salvador. 1985.

KING, L. A geomorfologia do Brasil oriental. **Rev. Bras. Geogr.**, 18(2), 147-265. 1956.

LANE, S.N.; BAKKER, M.; GABBUD, C.; MICHELETTI, N.; JEAN-NOEL, S. Sediment export, transient landscape response and catchment-scale connectivity following rapid climate warming and Alpine glacier recession, ***Geomorphology***. 2016.

LIU, Z.; HAN, L.; BOULTON, S.J.; WU, T.; GUO, J. Quantifying the transient landscape response to active faulting using fluvial geomorphic analysis in the Qianhe Graben on the southwest margin of Ordos, China, ***Geomorphology***. 2019.

MAACK, R. **Geografia física do Estado do Paraná**. Rio de Janeiro: Livraria José Olympio, 442 p.1968.

MATOŠ, B.; PÉREZ-PEÑA, J.V.; TOMLJENOVIĆ, B. Landscape response to recent tectonic deformation in the SW Pannonian Basin: Evidences from DEM-based morphometric analysis of the Bilogora Mt. area, NE Croatia, ***Geomorphology***. 2016.

NAKASHIMA, P. **Sistemas pedológicos da região noroeste do Estado do Paraná: distribuição e subsídios para o controle da erosão**. São Paulo, Tese (Doutorado em Geografia Física) Faculdade de Filosofia, Letras e Ciências Humanas, Universidade de São Paulo, 1999.

NEXER, M.; AUTHEMAYOU, C.; SCHILDGEN, T.; HANTORO, W.S.; MOLLIEX, S.; DELCAILLAU, B.; PEDOJA, K.; HUSSON, L.; REGARD, V. Evaluation of morphometric proxies for uplift on sequences of coral reef terraces: A case study from Sumba Island (Indonesia). ***Geomorphology***, 241, p.145-159. 2015.

OTHMAN, A.A.; GLOAGUEN, R.; ANDREANI, L.; RAHNAMA, M. Improving landslide susceptibility mapping using morphometric features in the Mawat area, Kurdistan Region, NE Iraq: Comparison of different statistical models. ***Geomorphology***. 2018.

PAVANO, F.; ROMAGNOLI, G.; TORTORICI, G.; CATALANO, S. Morphometric evidences of recent tectonic deformation along the southeastern margin of the Hyblean Plateau (SE-Sicily, Italy). ***Geomorphology***. Volume 342. 2019.

RESENDE, R.S., TELLO SÁENZ, C.A., DANTAS, E.L., HACKSPACHER, P.C., CHAVEZ MACHACA, C.A., GLASMACHER, U.A., Thermochronology and exhumation history of the basement and sediments of the one border of the Paraná Basin, Brazil, **Journal of South American Earth Sciences**. 2020.

RICHARDSON, J.C.; HODGSON, D.M.; WILSON, A.; CARRIVICK, J.L.; LANG, A. Testing the applicability of morphometric characterisation in discordant catchments to ancient landscapes: A case study from southern Africa, ***Geomorphology***. 2016.

SANTOS, L. J. C.; OKA-FIORI, C.; CANALLI, N. E.; FIORI, A. P.; SILVEIRA, C. T.; SILVA, J. M. F.; ROSS, J. L. S. Mapeamento Geomorfológico do Estado do Paraná. **Revista Brasileira de Geomorfologia**, Ano 7, nº 2, p. 03-12, 2006.

SCHLUNEGGER, F.; DETZNER, K.; OLSSON, D. The evolution towards steady state erosion in a soil-mantled drainage basin: semi-quantitative data from a transient landscape in the Swiss Alps. ***Geomorphology***. Volume 43, Issues 1–2. Pages 55-76. 2002.

SCUDERI, L.A. Quantification of long-term erosion rates from root exposure/tree age relationships in an alpine meadow catchment. ***Geomorphology***. Volume 283. p. 114-121. 2017.

SEMBRONI, A.; MOLIN, P. Long-term drainage system evolution in the Wabe Shebele River basin (SE Ethiopia-SW Somalia). ***Geomorphology***. Volume 320, p. 45-63, 2018.

SHTOBER-ZISU, N.; GREENBAUM, N.; INBAR, M.; FLEXER, A. Morphometric and geomorphic approaches for assessment of tectonic activity, Dead Sea Rift (Israel). ***Geomorphology***, volume 102, p.93-104. 2008.

STEVAUX, JC., SOUZA-FILHO, EE. and JABUR, IC., A história quaternária do rio Paraná em seu alto curso. In VAZZOLER, AEAM., AGOSTINHO, AA. and HAHN, NS. (Eds.). **A Planície de inundação do Alto Rio Paraná: aspectos físicos, biológicos e socio-econômicos**. Maringá: Eduem. p. 47-72. 1997.

SWARNKAR, S.; SINHA, R.; TRIPATHI, S. Morphometric diversity of supply-limited and transport-limited river systems in the Himalayan foreland. ***Geomorphology***. Volume 348. 2020.

TEDESCO J.; CAGLIARI J.; CHEMALE JUNIOR F.; GIRELLI T.; LANA C. Provenance and paleogeography of the Southern Paraná Basin: Geochemistry and U-Pb zircon geochronology of the Carboniferous-Permian transition, **Sedimentary Geology.** 2019.

VAN BINH, D.; KANTOUSH, S.; SUMI, T. Changes to long-term discharge and sediment loads in the Vietnamese Mekong Delta caused by upstream dams, ***Geomorphology***. 2019.

WILLENBRING, J.K.; GASPARINI, N.M.; CROSBY, B.T.; BROCARD, G. What does a mean mean? The temporal evolution of detrital cosmogenic denudation rates in a transient landscape. ***Geology***. 2013.

WILLETT, S.D.; MCCOY, S.W.; PERRON, J.T.; GOREN, L.; CHEN, C.-Y. Dynamic reorganization of river basins. **Science**, 343. 2014.

ZHANG, Y.; HASSAN, M.A.; KING, L.; FU, X.; ISTANBULLUOGLU, E.; WANG, G. Morphometrics of China's Loess Plateau: The spatial legacy of tectonics, climate, and loess deposition history. ***Geomorphology***. 2020.

3.3 LONG-TERM EVOLUTION OF THE SOUTHEAST BAURU SEDIMENTARY BASIN, BRAZIL

3.3.1 INTRODUCTION

Geomorphic dynamics are the result of different processes, many of which come from the weathering of the rocks, combined producing sediments to be transported and deposited, and sculpting the Earth's surface over time. The general balance between mantle convection, tectonic movements as well as chemical and physical erosion is responsible for the terrestrial topography as we observe it today(Granger and Schaller, 2014).

Morphodynamics studies may focus on short-term transformations in the landscape, in which the transport and deposition of sediments quickly transform the landscape, such as the dynamics of coastal areas (Masselink et al., 2006; Zarzuelo et al., 2018), recurrent rearrangements in the river network (Cherem et al., 2013; Ielpi, 2017; 2018; Heckmann et al., 2017; Maselli et al., 2018; Wu et al., 2020) and the retreat of glaciers (Lim et al., 2019, Winkler et al., 2020). In contrast, long-term morphodynamics studies may reveal the cumulative influence of processes that have prevailed over geological time.

In Geomorphology, some of these studies usually examine the remaining relief features, formed under the past process's actions (generically characterized as relictual), which may provide explanations about the development of the relief over the Quaternary (Hughes, 2010). Paleoshorelines (Komatsu et al.,2001; Martinod et al., 2016; Evenstar et al., 2018), ancient river terraces (Gao et al., 2019; Su et al., 2019; Maddy et al., 2020; Yang et al., 2019; Arzhannikova et al., 2018) and paleochannels (Stevaux, 2000; Leigh, 2008; Kiss et al., 2014; de Morais et al., 2016;), as well as moraines (Hu et al., 2020) are examples of such geomorphic features that are often addressed in long-term geomorphic studies.

This long-term integration of processes, driven by the evolution of field data collection techniques experienced in recent years, allowed new approaches to tackle how the Quaternary morphodynamics occurred (Viles, 2016).

This scale diversity approach is not restricted to temporal scales, e.g., along the Quaternary, but also spatial ones (de Boer, 1992; Summerfield, 2005). Relief features in disagreement with current climatic and/or tectonic conditions appear from local to regional scales and these simultaneously allow the researcher to make hypotheses about the evolution of the landscape over geological time.

According to Wolman and Gerson (1978), the geomorphic analysis must assume that the occurrence of a feature registered in one point could or will, over time, occur in another point in the same region. This assumption allows the extrapolation of geomorphological forms and processes from one point to an entire region.

Regional scales are especially relevant for morphodynamics. Hierarchically, large areas tend to respond slowly to environmental changes (in the long term) compared to local scales[8] in which the processes tend to be responses to specific events (in the short term) (de Boer, 1992; Summerfield, 2005).

In Brazil, one of the regions in which remnants of past geomorphological processes are found in the Bauru Sedimentary Basin (Table 3.1). Located in the center of the South American continent, this basin is a sediment-receiving area during the last 133 My, from the Lower Cretaceous, combining evidence of South American morphodynamics (Almeida et al., 2000; Batezelli et al., 2005). Above the Cretaceous basalt, there are still signs of past processes, geomorphological features that attest to paleoclimatic activities, currently found at different spatial scales, local to regional.

	Inselbergs, hillocks	**Ruiniform surface features**	**Erosive Paleofeatures**
Morphology	Hills supported by siliceous sandstone of K-T surface level	Lateritic profiles associated of the South American Surface.	Large erosive features, similar to gullies, formed during the Pleistocene and stable today.
Timescale	66 My	35 My	2.6 My
Spatial Scale	Local - 1:10,000	Regional - 1:1,500,000	Local - 1:60,000
Location	Punctual character in several lithological units	Remnants of poorly preserved weathered surfaces at the edges of the Paraná Sedimentary Basin, second plateau and occasionally on the third plateau.	Punctual character in several lithological units, higher concentration in the vicinity of water dividers.
References	Fernandes et al., 1993; Fernandes et al., 2013; Fumiya et al., 2019.	King, 1956; Riffel et al., 2015; Fumiya et al., 2016.	Bigarella and Mazuchowski, 1985; do Couto, 2014; Goulart and Santos, 2014.

Table 3.1: Southern Bauru Basin relictual features.

There are some structures already described in the scientific literature as relictual features, anomalies that are outside the pattern of the flat relief found in the

[8] It is understood as local scales, scales of greater detail, larger scales. And as regional scales, scales of less detail, smaller scales.

region (Goulart, in press, item 3.2), in the south of the Bauru Basin. As examples, we can mention: (1) the occurrence of erosive paleofeatures, Pleistocene gullies or paleogullies [9] (Figure 3.1) formed under the action of glacial paleoclimates that are no longer active (Bigarella and Mazuchowski, 1985; do Couto et al., 2014; Goulart and Santos, 2014); and (2) the presence of inselbergs in the area (Figure 3.1), remnants of old levels of flat surfaces (Fernandes et al., 1993; 2013; Fumiya et al., 2019), denoting altimetric levels of pre-Holocene surfaces, recognized today as regional low relief (Goulart, in press, item 3.2). Also the regional examples of past processes that allow for broader spatial correlations, such as remnants of more frequent ruiniform surfaces at the edges of the basin (Riffel et al., 2015), but that also occur within the Caiuá Group punctually (Fumiya et al., 2016).

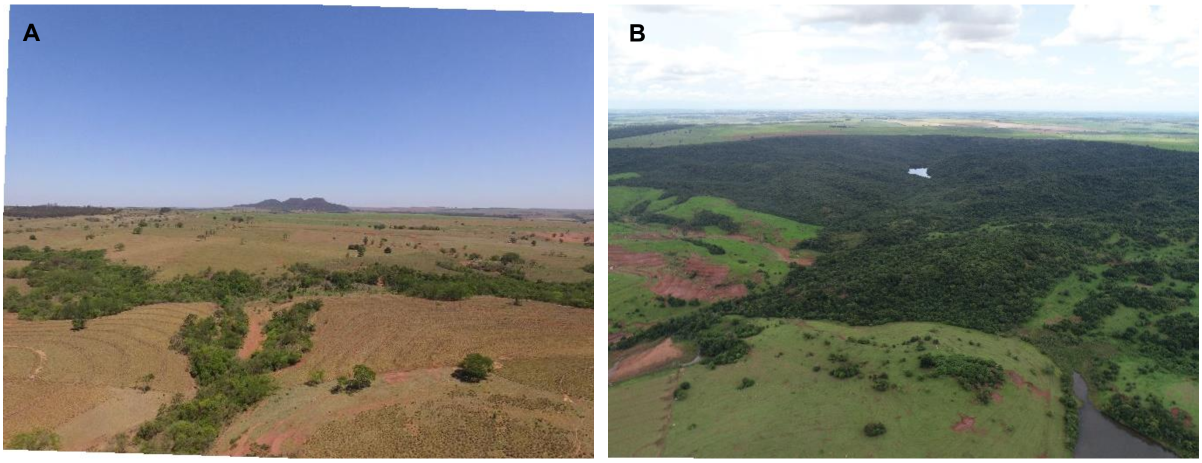

Figure 3.1: Relictual features in the study area. (A) Inselbergs named três morrinhos, (B) Paleogullie measured as PG5 along this chapter.

These geomorphological features that were formed before the Holocene may be fundamental for understanding the regional long-term evolution, revealing processes that occurred in different periods of geological times. These patterns of evolution that are outside the standard are often excluded from the analysis, whereas they constitute fundamental points for the interpretation of a balance in a wide time scale.

---

[9] In this chapter, we chose to use the term paleogullies, according to analogies with the concept of relictual paleosol (Queiroz Neto, 1974) and paleofeatures (Guerra e Guerra, 2008), which refer to those erosive features, of dense dissection and which present characteristics visuals identical to the active gullies frequently found throughout the southern Bauru Basin, but that their genesis is considered disharmonious within the current morphoclimatic system, denoting that they were formed and/or evolved under different conditions than the current ones.

One technique that allows explanations of long-term morphodynamics is denudation measurement. Denudation rates allow associations of the geomorphological processes magnitude, correlating them, for example, with (paleo) climatic actions, in the search for a regional evolution pattern (Wolman and Gerson, 1978).

The first denudation measurements in the southern part of the Bauru Basin were made by do Couto et al. (2018). Noting a difference in the soil distribution between the two banks of the Ivaí River (do Couto, 2014), the authors opted to investigate the denunciation rates using *in situ* ^{10}Be concentrations in small watersheds that constitute the tributaries of that river. The sampled basins revealed a small difference between the Ivaí River banks, with a higher rate in the denudational processes of the South bank (10.9 ±2.7 m/My), when compared to the North bank (6.4 ±1.30 m/My).

Knowing that the constituent landscape elements are the same on the South and North banks of the Ivaí River, do Couto et al. (2018) assigned this difference in the rate of the processes to changes in the regional base level caused by ancient tectonism and paleoclimates. However, is this small difference in the denudation rate described by do Couto et al. (2018) regionally representative? And what is the relictual features influence on regional morphodynamics? Are these gullies translucent/invisible to regional processes, not interfering with regional averages, or are some of these features directly controlling the rate of denudation at a regional scale?

Based on the results of do Couto et al. (2018), expanding the scales of analysis, spatially and temporally, and integrating relictual features in the landscape analysis, we sought to understand the long-term morphodynamics of the Southeast of the Bauru Basin, associating measurement and interpretation of the denudation rates estimated by cosmogenic nuclides, ^{10}Be, *in situ* produced.

3.3.2 REGIONAL SETTINGS

The study area, approximately 20.000 km², is located between the coordinates 22°50’ and 24°30’ South and 54°10’ and 52°10’ West, in the Bauru Sedimentary Basin southeast portion, in the vicinity of the old paleo desert center Caiuá (Fernandes, 1992; Battezelli, 2005).

The lithology that defines the study area is the Caiuá Group sandstone, constituted by two formations in the area: the Goio-erê Formation, which has sedimentological characteristics of desert edges, with deposits associated with river transport; and the Rio Paraná Formation, which has characteristics related to the paleodesert central areas of deposit, formed by ancient wind influence for sediment transport (Fernandes, 1994; 2004) (Figure 3.2).

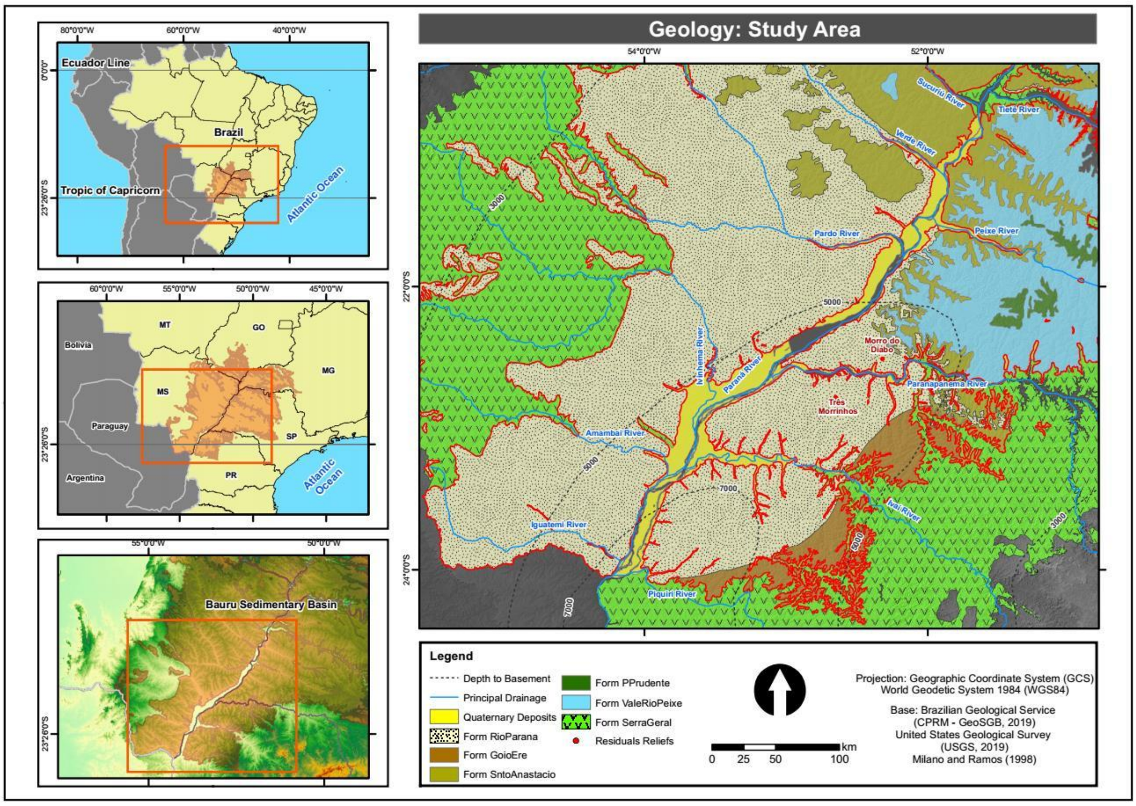

Figure 3.2: Geologic map of the Southern Bauru Sedimentary Basin.

The study area was delimited based on lithological criteria, Caiuá Group greater coverage, south of the Paranapanema River and east of the Paraná River, and by technical criteria of the methodological procedures associated with the ^{10}Be, measurements, since there were already quantifications made by do Couto et al. (2018)[10].

In the study area, main drainage dividers can be observed that delimit important regional watersheds, such as the Ivaí, Paranapanema, and Piquirí River basins. All of these basins flow into the same river, located in the central portion of the Bauru Sedimentary Basin, the Paraná River. This is the tenth largest river in the world

[10] The measurements made by do Couto et al. (2018) were made only in the Ivaí River basin, and the purpose of this chapter encompasses this basin and expands the area analyzed to other large regional basins, as part of the Paranapanema and Piquirí basins.

in discharge and the second largest in the South American continent (Stevaux, 1994), only behind the Amazon River.

Following the regional slope with the lowest elevations in the West portions, these hydrographic basins form the drainage network that feeds the left bank of the Paraná River, with an East-West direction. The less important drainages are conditioned by the Caiuá Group's morphodynamics, however, in the larger rivers, the basaltic-sandstone contact is frequent, with the basalt controlling the local base levels by punctual knickpoints.

Along long interfluves and with low slope, thick Oxisols are observed. As the slope is accentuated in the middle escarpment, there is the concentration of clay, originating Argisols. In the lower escarpments section, in the lower portions of the relief, close to the drainage network there is the presence of quartz sands, forming when structured the Quartzarenic Neosols.

The study area is located in the Paranavaí Plateau, which is characterized by predominantly low dissection, flattened tops, convex slopes, and open V-valleys, typical morphologies of areas where the denudational process is/was intense. The plateau elevations range between 240 and 590 meters above sea level, which indicates a gradient of approximately 350 meters, but with slopes less than 6 degrees predominance, thus constituting a smooth relief, without major significant altimetric variations (Santos *et al*, 2006).

The studied region is in the transition between two climatic zones: the tropical zone with dry winter (Aw) and the humid subtropical zone with hot summer (Cfa) to the south, which gives the characteristic of two well-marked seasons, hot and rainy summer and dry winter with mild temperatures (Alvares et al., 2014).

The original vegetation is a reflection of the other elements that make up the landscape. The current forest remnants that predominate in the region are classified as Seasonal Semideciduous Forest. Forest, as it has four well-defined strata (herbaceous, shrub, low tree, and canopy), Seasonal due to the great influence of seasonality, Semideciduous due to the percentage of deciduous specimens being between 20 and 50% (IBGE, 2012).

3.3.3 MATERIALS AND METHODS

do Couto et al. (2018) sampled 14 first-order watersheds (7 tributaries of the north bank of the Ivaí River and 7 to the south of the same river), with dimensions between 27,9 and 66,8 km². Starting from these sampling points, we sought to expand the spatial scale, and consequently understand the influence of these local watersheds on the evolution of the regional watershed in which they are inserted.

This methodological option chose to concentrate the research in the same region, refining results in the search to expand the scales, instead of seeking new measurements in regions not yet worked by the methodology. It was also noted the importance of understanding the different processes accumulation and their reflections in the landscape, in other words, how some relictual/anomalous relief features may have interfered in the regional morphodynamics in long term, which culminated in the addition of the paleogullies measurement in the analysis.

To understand the palegullies role in the study area evolution, local (1: 60,000) and regional (1: 1,000,000) spatial scales were compared, to understand how local processes can accelerate or mitigate the rate of denudational processes on a wider scale.

The sampling points selection was made without using spatial dimension criteria, as in the work of do Couto et al. (2018), but opting to sample watersheds mouths from larger regional basins, which generated a difference in the size of the sampled watersheds. The total analysis area was also expanded if compared to the paper by do Couto et al. (2018), as it was not limited to sampling and interpretation of tributaries of the Ivaí River only, but of neighboring watersheds that drain into the Paraná, Paranapanema, and Piquirí Rivers as well. This spatial scale expansion allowed conjectures about morphodynamics on a regional scale.

It was sampled 20 points for regional analysis (identified with the letter “P”), covering practically the entire Paraná River left bank at the Bauru Sedimentary Basin southern limit: 2 Piquiri River tributaries samples, 6 Paranapanema River tributaries, 3 Paraná River tributaries, and 9 Ivaí River tributaries (3 on the left margin and 6 on the right margin). Another 5 points were sampled with the specificity of being paleogullies (identified with the letters "PG"), all within the sampled hydrographic basins.

Therefore, there are 25 points with new measurements and another 14 points already published (identified with the letter “C”), which totals 39 points distributed throughout the study area.

Table 3.2 and Figure 3.3 show the location of all sampled points, as well as the respective main watersheds.

Table 3.2. Sample locations and geomorphic catchment parameters from all 39 catchments analyzed (see location in Figure 3.2).

Sample ID[A]	Longitude X (m) (UTM)	Latitude Y (m) (UTM)	Main Watershed	Local/Regional correlation
C1	325948	7363009	South Ivaí	Sandstone - Basalt transition
C2	307445	7402091	South Ivaí	Nearly P4 watershed
C3	306441	7381373	South Ivaí	Inside P4 catchment area
C4	281342	7386119	South Ivaí	Inside P2 catchment area
C5	259072	7389131	South Ivaí	Inside P1 catchment area
C6	233699	7413683	South Ivaí	Between P0 and P1 watersheds
C7	265735	7423722	South Ivaí	Nearly P1 and P2 watersheds
C8	288004	7433853	North Ivaí	Nearly P6 watershed
C9	297223	7434583	North Ivaí	Nearly P7 watershed
C10	329350	7436318	North Ivaí	Inside P26 catchment area
C11	354176	7428103	North Ivaí	Sandstone - Basalt transition
C12	272580	7459226	North Ivaí	Inside P10 catchment area
C13	272215	7435679	North Ivaí	Nearly P10 watershed
C14	250675	7442524	North Ivaí	Nearly P10 watershed
PG1	246925	7465257	North Paraná	Inside P9 catchment area
PG2	285157	7459810	North Ivaí	Inside P6 catchment area
PG3	295089	7458553	North Ivaí	Inside P7 catchment area
PG4	295970	7457730	North Ivaí	Inside P7 catchment area
PG5	299134	7468288	Paranapanema	Inside P11 catchment area
P0	219467	7412267	South Paraná	None
P1	241885	7425840	South Ivaí	Covers C5 catchment area
P2	272175	7412152	South Ivaí	Covers C4 catchment area
P3	202182	7380545	South Paraná	None
P4	292888	7418535	South Ivaí	Covers C3 catchment area
P6	279383	7445177	North Ivaí	Covers PG2 catchment area
P7	292271	7444033	North Ivaí	Covers PG3 and PG4 catchment area
P8	312691	7430592	North Ivaí	None
P9	244133	7467199	North Paraná	Covers PG1 catchment area
P10	262917	7444269	North Ivaí	Covers C12 catchment area
P11	293473	7498765	Paranapanema	Covers PG5 catchment area
P12	316908	7491953	Paranapanema	None
P13	326680	7488470	Paranapanema	Resistant residual relief
P14	339661	7484740	Paranapanema	Possibly Paleo Gullies non mesuareds
P15	368735	7486471	Paranapanema	None
P16	354657	7486189	Paranapanema	None
P23	263757	7333344	Piquirí	None
P24	208511	7340541	Piquirí	None
P25	317333	7427591	North Ivaí	None
P26	318782	7426216	North Ivaí	Covers C10 catchment area

[A] Sample ID: C = do Couto et al. (2018) published data; PG = possibly Paleo Gullies unpublished data; P = this chapter sample points.

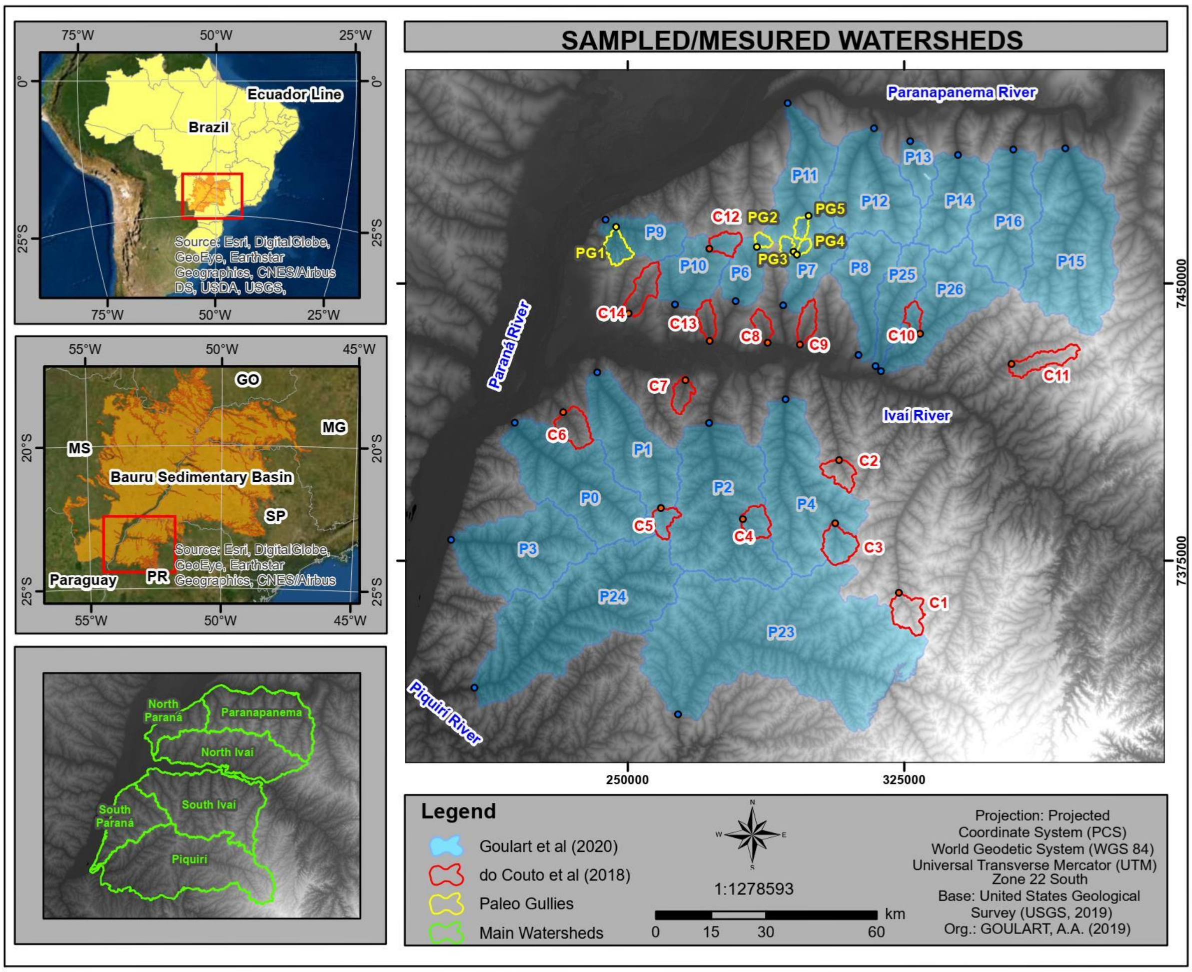

Figure 3.3. Location of the studied area, with the Bauru Sedimentary Basin, the main watersheds and the sampled/measured watersheds according to the sample ID in Table 3.2.

Some morphometric indexes were measured to search for correlations that explain the results of denudation rates in both spatial scales. The following indexes were calculated for each analyzed catchment area: maximum χ (water dividers readjust), maximum K_{sn} (Steepness index), and the hypsometric integral (HI). In addition to descriptive watershed measures such as: the area and volume upstream of the sampling; the maximum elevation; and the mean slope of each measured basin.

An approximate age of the denudation process beginning of the sampled basins was also calculated. From the denudation rate (m/My) and the volume of each basin (m^3), it was possible to estimate when the denudation process (My) started. To calculate the volume, the highest point extraction of the current relief was made, at the edges and inside the sampled basins, which allowed a possible past surface interpolation.

It was considered that the erosive process is constant in time and space (Bierman and Portenga, 2018), and even the local processes action that may have conditioned changes at the base level was abstracted, assuming that it is fixed during the entire period analyzed. Thus, it was considered that these interpolated surfaces served as abstractions used for volume calculations, were generalizations made for the comparative analysis purpose of the calculated totals and not exact paleosurfaces reconstructions. Therefore, it was possible to stipulate the minimum time scale that this chapter could cover, an important result for the association with local/regional proxies.

For the watersheds delimitation, descriptive measures extraction, and morphometric indexes calculations, we used rasters, Digital Elevation Model (DEM), with 30m spatial resolution of the Shuttle Radar Topography Mission (SRTM). The software used to generate the indexes were ArcGIS 10.3 and Matlab 2018, using Topotoolbox scripts (Schwanghart e Scherler, 2014).

Chemical preparation and measurements of ^{10}Be accumulation in sediments were carried out in the *Laboratoire National des Nucléides Cosmogéniques* (LN2C), located at the *Centre de Recherche et d'Enseignement de Géosciences de l'Environnement* (CEREGE), France. The equipment for measuring Accelerated Mass Spectrometry (AMS) used to quantify the results is part of the CEREGE-ASTER infrastructure.

3.3.4 RESULTS AND DISCUSSION

Tables 3.3 and 3.4 show the results of the 25 points sampled analyzed in this paper, in addition to the 14 points already measured by Couto et al. (2018).

The denudation rates results of P catchments derived from the *in situ* cosmogenic ^{10}Be produced were 12.2 ±2.0 [12.5] (20)[11] m/My with a range of 10.0 m/My, varying between 6.5 ±1.1 m/My and 16.5 ±2.7 m/My. While for PG watersheds the results were the highest in the analyzed series, 42.7 ±3.7 [41.6] (5) m/My with a range of 61.8 m/My, varying between 15.6 ±0.9 m/My and 77.4 ±6.5 m/My. The results obtained by do Couto et al. (2018) for C watersheds was 8.6 ±0.3 [7.8] (14) m/My with a range of 12.4 m/My, varying between 3.9 ±0.2 m/My and 16.3 ±0.7 m/My.

The P catchments' average area and volume were calculated in 586.8km² and 37.4km³ respectively. For the PG group, the mean values were the lowest in the series, 20.4km² of area and 0.7km³ of volume. While the basins analyzed by do Couto et al.

---

[11] The results standardization presented was done as follows: AVERAGE ± UNCERTAINTY [MEDIAN] (NUMBER OF SAMPLES) m/My.

(2018), group C, had average area values calculated from 48.9km² and a volume of 1.8km³.

Table 3.3. Geomorphic parameters data

Sample ID[A]	Area (m²)	Volume (m³)	Z Max (m)	Slope Average (degrees)	HI	χ Max	K_{sn} Max	AD[B] (My)
C1	68351042	3186872216	626	4,75	0,5	11424,4	33,9	2,9
C2	48253173	1972327839	519	3,20	0,6	8380,4	23,8	3,5
C3	71786716	3708677226	536	4,14	0,6	9470,3	61,8	4,5
C4	52817735	1958926289	487	4,31	0,5	8388,0	25,9	3,7
C5	37230149	1038963932	502	4,32	0,5	9149,8	18,7	2,9
C6	72972902	3064345782	443	3,87	0,5	6495,4	26,1	4,7
C7	37423232	1163926158	417	3,89	0,5	6236,5	23,7	3,9
C8	31193728	863247657	415	3,92	0,5	5532,3	21,3	3,7
C9	41540400	1035833381	426	3,17	0,5	7748,9	34,5	3,4
C10	28126800	747476400	461	4,00	0,5	6882,5	41,7	3,7
C11	69348354	2359152189	565	3,96	0,5	9636,8	30,9	4,8
C12	39488138	1032831684	497	3,29	0,5	9215,2	43,9	4,5
C13	37473300	1009871433	398	3,11	0,5	6592,4	22,0	4,7
C14	68567263	1911021942	433	3,20	0,4	8491,1	24,3	7,1
PG1	44318682	1597532447	417	6,46	0,5	5428,0	31,0	0,9
PG2	13050000	406551161	504	6,44	0,5	7933,4	14,7	0,5
PG3	15177600	622360211	495	8,26	0,5	7486,5	18,7	2,2
PG4	10719900	316322997	509	7,35	0,5	7867,8	17,2	1,9
PG5	18974700	714483295	499	7,01	0,5	7680,3	22,0	0,5
P0	720074498	48085592073	497	3,34	0,4	6901,3	22,6	5,2
P1	559344006	32898902356	527	3,39	0,5	7319,9	37,3	4,5
P2	1000064757	71936135997	517	4,74	0,4	8004,3	34,9	4,8
P3	647682821	44778560312	498	3,54	0,5	6636,9	22,8	5,0
P4	823697959	57925667469	539	4,33	0,5	8361,4	51,5	5,0
P6	173977557	8473955574	625	4,50	0,4	9086,4	57,3	5,5
P7	231598622	12738315749	442	4,21	0,5	5161,8	24,5	4,2
P8	319673925	17332904093	571	3,79	0,5	8110,7	22,6	4,8
P9	221552676	9549182738	471	4,32	0,5	9397,0	26,4	2,6
P10	297227124	14193684754	537	3,55	0,5	6864,2	20,5	4,6
P11	431891230	26200438320	532	3,61	0,5	6606,0	46,0	5,3
P12	545421459	38525685622	532	3,39	0,5	6214,8	29,5	6,1
P13	114874698	7849052576	518	3,63	0,5	7453,3	26,8	8,1
P14	340301192	24386369964	493	4,22	0,5	7469,4	43,0	4,3
P15	872799409	48729502720	461	4,39	0,5	7382,0	29,1	3,9
P16	491300283	29490775756	502	4,88	0,4	8185,2	29,2	7,0
P23	1990038102	131491828180	534	3,71	0,5	7756,2	28,7	10,2
P24	1207201264	85149119834	521	3,43	0,5	6197,8	35,6	5,8
P25	241588896	12883803040	527	4,04	0,5	7343,3	30,8	4,0
P26	505357370	24652163519	635	3,46	0,4	6586,9	19,5	4,2

Sample ID[A]: C = do Couto et al. (2018) published data; PG = possibly Paleo Gullies unpublished data; P = this chapter sampled points. AD[B]: Approximate age of the denudation process beginning.

The results for the approximate age of the denudation process beginning calculated for P basins were 5.3 ±0.4 [4.9] My, varying between 2.6 and 10.2 My, with a range of 7.6 My. The PG watersheds started the denudation process more recently, 1.2 ±0.4 [0.9] My, varying between 2.2 and 0.5 My, with a range of 1.7 My. For basins C, the average age at the beginning of the denudation process was 4.1 ±0.3 [3.8] My, with a maximum and minimum age of 7.1 and 2.9 My, which reveals a breadth of 4.3 My.

Table 3.4. ^{10}Be in-situ-produced concentrations.

Sample ID	Shielding mean	Stone fator mean	Elevation mean (m)	Quartz Mass (g)	^{9}Be carrier (mg)	$^{10}Be/^{9}Be$ ratio (x10^{-13} atoms)	Denudation Rate (m/My)	Integr. Times (y)
P0	1,000	0,956	359,76	10,6	150,49	0,81	12.9 ± 2.1	27200
P1	1,000	0,961	373,08	22,0	148,62	1,68	13.1 ± 2.2	47646
P2	1,000	0,974	349,00	22,0	147,23	1,51	14.9 ± 2.5	27726
P3	1,000	0,959	402,81	22,1	149,74	1,58	13.9 ± 2.3	38401
P4	1,000	0,996	379,17	22,0	148,13	1,68	14.1 ± 2.3	36919
P6	1,000	0,965	392,32	22,0	147,56	2,44	8.8 ± 1.5	49339
P7	1,000	0,975	390,12	22,0	151,92	1,68	13.0 ± 2.2	37444
P8	1,000	0,974	337,19	22,0	152,85	1,90	11.3 ± 1.9	42204
P9	1,000	0,933	362,83	22,0	154,17	1,31	16.5 ± 2.7	31707
P10	1,000	0,953	381,11	22,0	154,62	1,90	10.4 ± 1.7	45241
P11	1,000	0,962	400,28	22,0	153,77	1,82	11.5 ± 1.9	41892
P12	1,000	0,977	404,94	22,0	155,79	1,83	11.6 ± 1.9	41598
P13	1,000	0,979	412,59	22,0	152,75	2,52	8.5 ± 1.4	50588
P14	1,000	0,986	416,34	22,0	153,38	1,37	16.5 ± 2.7	32916
P15	1,000	0,992	413,23	22,0	154,28	1,49	14.4 ± 2.4	35911
P16	1,000	0,988	434,41	22,0	153,76	2,53	8.6 ± 1.4	49860
P23	1,000	1,050	341,12	22,0	154,44	3,23	6.5 ± 1.1	62542
P24	1,000	0,956	384,41	10,8	154,19	0,85	12.2 ± 2.0	33418
P25	1,000	0,971	390,89	22,0	154,11	1,63	13.3 ± 2.2	39507
P26	1,000	0,976	350,78	22,0	153,90	1,78	11.5 ± 1.9	36064

Sample ID: P = this chapter sampled points.

The highest elevations average for the P basins, was 524.0 ±10.5m, ranging from 635 to 442m, which results in 193m of amplitude. The analysis of the mean of the highest elevations for the PG group was 484.5 ±17.1m, with values between 509 and 417m, which corresponds 92.0 m of amplitude. For the catchments measured by do Couto et al. (2018), C group, the highest points average was 408.4 ±17.50m, with more heterogeneous variations, between 626 and 398m, resulting in 228m of amplitude.

The slope values average for P watersheds were 3.9 ±0.1 [3.8] degrees, with values ranging from 4.9 to 3.3 degrees, which generated an amplitude of 1.5 degrees. The values for the PG catchments were the highest, demonstrating that there are greater declivities in this group, resulting in 7.1 ±0.3 [7.0] degrees, ranging from 8.3 to 6.4 degrees, and amplitude of 1.8 degrees. The slope values for the group C measured areas were very close to the P watersheds, 3.8 ± 0.1 [3.9] degrees, with values ranging from 4.8 to 3.1 degrees, which generated 1.6 degrees of amplitude.

The results for the HI index indicated that there were no significant variations for the 3 groups analyzed, with an index of 0.5 ± 0.01 [0.5], which characterizes a uniform behavior for all analyzed basins.

The analysis of the most susceptible surfaces to be eroded by the drainage network readjustment, maximum χ index, resulted in relatively close average values, homogeneous behavior: 7351.9 ±227.2 [7362.6] for the P watersheds; 7279.2 ±469.3 [7.680.3] for the PG; and 8117.5 ±435.2 [8384.2] for group C.

The K_{sn} index maximum values for the P catchments were 31.9 ± 2.3 [29.1], with variations between 57.3 and 19.5, which results in a 37.8 ranging. The PG basins had the lowest values in the series, with 20.7 ± 2.8 [18.7], varying between 31.0 and 14.7, with 16.3 of amplitude. While group C keeps the trend observed in basins P, with 30.9 ± 3.1 [26.0], alternating between 61.8 and 18.7, resulting in 43.1 of maximum K_{sn} amplitude.

3.3.4.1 Background Denudation Rates

To indicate a regional background denudation rate[12], a geomorphological evolution pattern of the Bauru Sedimentary Basin southern region, just the P basins within the average results were considered. In other words, only the basins that, considering their uncertainty, were within the values calculated for the regional average.

Thus, it was possible to establish a regional background denudation rate, which considers the region evolution in a homogeneous and generic way. The watersheds that are in the pattern (except the P13, P16, and P23, which will be addressed separately) resulted in a 12.9 ±2.1 [13.0] (17) m/My of regional background denudation rate.

The particularities that deviate from the regional pattern, the 3 catchments below the P average, the PG group, and even the C watersheds, answer the processes that occurred at other scales, spatial and temporal, which deserve attention in proposing an explanation for regional morphodynamics.

---

[12] Background rate is a terminology widely used in studies of Ecology and Public Health when the authors refer to patterns, expected trends. These rates are often used in comparison with occasional high rates that are outliers the expected behavior, such as high extinction rates that characterize mass extinction events (Ecology) and disease outbreaks that characterize epidemics (Health).

According to Imeson and Lavee (1998), conceptual or practical erosion models need to address issues of scale, temporal and spatial. According to the authors, the magnitude and the greater or lesser influence of different denudational processes change as the temporal and spatial scales also change.

Therefore, it was not feasible to use all measurements, all 39 basins already measured in the region, as equivalent data in the proposal for the regional background denudation rate. The watersheds particularities that deviate from the background rate pattern and the distinctions in the morphometric indexes will be addressed below, in the chapter course.

3.3.4.2 Nonstandard Watersheds

In the group P results analysis, it was noted that only 3 watersheds were outside the average, considering the average uncertainty. The basins that are out of the pattern, with average values below 10.2 m/My were: P23 with 6.5 ±1.1 m/My, P13 with 8.5±1.4 m/My, and P16 with 8.6 ±1.4 m/My. Among these 3 measurements, the only one that deviates a lot from the observed trend is P23, with at least 2.6 m/My below the average minimum.

This rate may have been influenced by lithology, since this watershed is in the lithological transition from sandstone to basalt, with its upstream located in volcanic lithology areas, outside the study area (approximately 9.2% of the P23 basin area located in the basalts domain). A lithology more resistant to denudational processes, such as the basalt found upstream of the P23 basin, can attenuate the sediments production and transport in a watershed, which consequently will result in ^{10}Be higher concentrations in the sampled sediments and therefore reduce the rate denudation.

The explanation of the denudation rates below the average for the P13 and P16 watersheds is based on the same principle, the presence of *inselbergs* more resistant to the denudational process. Within the P13 catchment is located one of the most significant witness hills in the region, Morro dos Três Irmãos or Três morrinhos. This geomorphological feature found in the P13 basin is a remnant result of the ancient surfaces denudational processes action in its immediate surroundings, but which was maintained due to structural characteristics, silicified sandstones by hydrothermal silica fluids. Currently, this *inselberg*, with elevations of the surface K-T, presents an approximately 130 meters difference in relation to regional surfaces (Fernandes et al., 2013). Altimetric correlations of the Três Morrinhos with the Bauru Basin edges could be observed in swath profiles by Goulart (in press, item 3.2), proving old levels of regional flat surfaces, but due to the magnitude of the Pleistocene denudational processes today they only allow propositions of regional low surfaces.

The Três Morrinhos is not the only inselberg in the region, Fernandes et al. (2013) have already described the presence of some of these remnants in the relief in the Bauru Basin South. Since the sandy deposits silicification in the Caiuá paleodesert occurred through regional fissure systems still in the Cretaceous, we can conjecture about the possible existence of some of these lesser-known *inselbergs* in the region that have not yet been exhumed and described in the scientific literature.

What may have occurred in the P16 basin that attenuated the denudation process was the presence of a similar structure, an old silicified sandy deposit with less vertical amplitude than the inselbergs already identified by Fernandes et al. (2013), but that may have controlled the sediment transport process in the region.

Another possibility that may explain the denudational processes attenuation in the P16 basin, and in the region, is the possible occasional presence of surfaces supported by ferruginous concretions, such as those found and described by Fumiya (2016) in the study area. According to the author, these ferruginous concretions were found mostly in the Ivaí River south, however, as the denudation results show, denudational processes do not occur continuously in time and space across the study area, which indicates that some of these surfaces may also occur in the Ivaí North, however, the denudational process has not yet exposed them as in the Ivaí South.

Small peculiarities such as those described in P23, P13, and P16 can attenuate the denudational process, but when analyzing the regional scale and to propose an evolution pattern, it ends up generalizing features or homogenizing the processes. In proposing to understand regional evolution, the uncertainty is assumed, therefore, that the denudational process is spatially and temporally continuous.

When analyzing the roughness concentration Goulart (in press, item 3.2) found that approximately 2% of the study area was identified as the high class values, classified as moderate dissected terrains. Many of these pixels identified in the classification as moderate dissected terrains corroborate the location of these features that are outside the regional standard, such as the Três Morrinhos. However, it is important to note that the roughness also considers features where, unlike inselbergs that reduce denudation, the process was more intense compared to the surroundings, as in the paleogullies.

Specific geomorphological features measurements in the region, such as in the outcrops of inselbergs, can help explain how these structures or residual surfaces are evolving and how they are integrated into regional morphodynamics.

3.3.4.3 Comparison of P and C Watersheds

Relevant information for comparison is the sampling strategy. According to Couto et al. (2018), the authors choose the first-order watersheds sampling, with sizes between 27.9 and 66.8 km^2, which allows a spatial scale analysis at 1:60,000. Thus, C watersheds reflected a local processes pattern that was extrapolated to the whole region by the authors.

The P group sampling selects significant catchments for the regional context interpretation, which caused the watersheds to vary in dimension from 114.9 to 1990.0 km^2. This distinction directly reflects the spatial scale delimitation, allowing for regional, of 1:1,000,000. Thus, the P basins demonstrated the regional processes action, distributed not punctually as in the C basins, but more homogenized throughout the region.

For comparative effect between groups P and C, the basins that correspond to the same local base level, the Ivaí River basins, were approached (Table 3.2). The trend noted by do Couto et al. (2018) of the basins that drain to Ivaí southern have higher denudation rates, 10.9 ±2.7 m/My, compared to Ivaí northern, 6.4 ±1.30 m/My, it is not confirmed at the regional scale if we consider the average uncertainty. The P group results of the Ivaí South catchments were 14.0 ±2.3 [14.1] (3) m/My, while the results from Ivaí North were 11.4 ±1.9 [11.4] (6) m/My.

This results comparison allows us to affirm that on a local scale, in the first order basins analysis, the denudational processes are more intense in Ivaí South compared to Ivaí North. However, when analyzing the basins on a regional scale, this difference in the denudation process's magnitude is homogenized. As if the greater magnitude of the first order watersheds observed by do Couto et al (2018) were dissipated as the spatial scale is expanded to the larger basins. Consequently, this process's uniformity brings regional averages closer to the "real" trend, while the results by do Couto et al. (2018) tend to respond to specific and local processes that may not reflect the regional trend. Therefore, the statement made by do Couto et al. (2018), of the difference in denudation rate between North and South Ivaí cannot be generalized at the regional scale.

According to Kirkby et al. (2009), the drainage headwaters tend to be the first points of readjustment in case the basin goes through some internal instability, which would corroborate with the magnitude accentuation of the denudational processes. This theoretical proposition can explain this increase in the magnitude of the processes measured by do Couto et al. (2018) compared to the P group results.

In this way, it is also necessary to distinguish the time scale to which these measurements refer. The C group analyzes, on a 1: 60,000 scale, tend to reveal the short-term processes performance, while the P group results, scales 1: 1,000,000, indicate the long-term processes action (Boer, 1992). This is due to the fact that regional patterns tend to take longer to be representative, as they have to be repeated at different points in the same region to be expressive, while local processes can be generated in a few or even just one great magnitude event. This idea reinforces the assertion that the C watersheds results indicate the performance of punctual processes, more recent, when compared with the P group results, regional and of long-term duration.

In general, the difference in morphodynamics between Ivaí North and South tends to be small, if there is any distinction since the landscape characteristics differ little between the two Ivaí River banks. The landscape main elements that interfere in the denudation rate magnitude, base level, lithology, and climate, do not vary significantly between the Ivaí two banks.

As demonstrated by do Couto et al. (2018), there is a great variation between the Ivaí North and South banks with concern to the distance between the watersheds mouth and the interfluve. However, a difference in denudation between the two banks cannot be explained by this factor, since the regional interfluves are at approximately the same elevation level and the base level of both is the Ivaí River. As we can observe in Figure 3.4, the correlation between denudation rates and area in the do Couto et al. (2018) is low (R^2=0,10), since the basins are approximately the same size, but the denudation speed varies. When analyzed on a regional scale, the correlation between denudation rate and basin area is less significant (R^2=0,04), even so, as already exposed, a difference cannot be attributed due to the measurement results from uncertainty of the ^{10}Be.

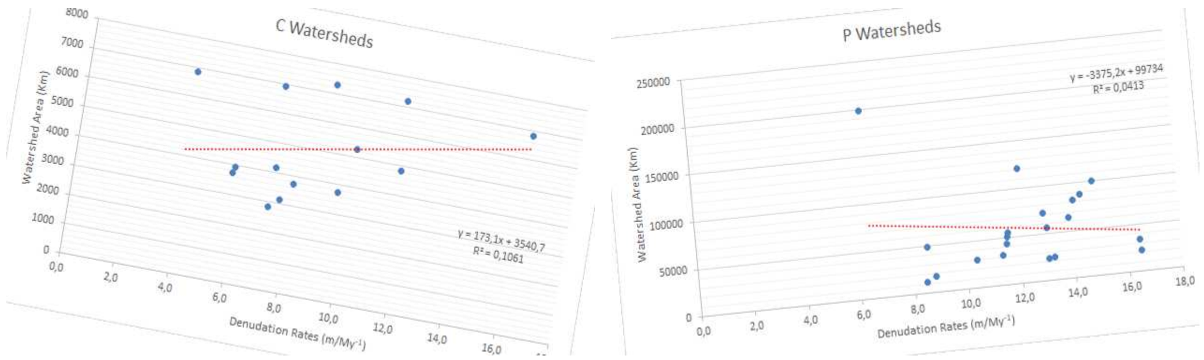

Figure 3.4: Regression plot of the relationship between erosion rate and area, of the C (left) and P (right) watersheds.

In general, it is possible to affirm that there is a correlation between the data from C and P groups. However, the data refinement demonstrates that the results by do Couto et al. (2018) end up overestimating the denunciation action, since at the regional scale there is a tendency to homogenize processes and, consequently, rates.

3.3.4.4 The PG Watersheds

The most dissonant of series results were obtained in the PG group measurements, with denudation rates of 42.7 ±3.7 [41.6] (5) m/My. In comparison with the other basins, the PG group demonstrated that denudation rates are higher than the C and P groups averages, approximately 30 m/My more, almost 3 times the average value calculated for the P watersheds. The maximum denudation measured in the PG watersheds reached 77.4 ±6.5 m/My, which corresponds to an increase of approximately 7 times concerning the group P average.

These values demonstrate that the PG basins responded punctually to evolutionary processes distinct from the processes responsible for general morphodynamics. This idea corroborates with the hypothesis of the existence of possible paleogullies present in this area (Bigarella and Mazuchowski, 1985), with the outliers finding in the area (do Couto, 2014) and with the erosive paleo features presence even before the anthropic occupation in the region (Goulart and Santos, 2014).

The paleogullies result was also not homogeneous even within the PG group. The highest rates were observed at points PG2 and PG5, above 60 m/My, but also high rates, not like the previous ones, were observed within the same group, as at points PG3 and PG4, just below 20 m/My. Which showed that even among paleogullies there are different evolutionary stages, with the denudational process more advanced in some, which have higher rates, and milder in others, in which the rates approach the highest rates seen in group P.

Unlike the P and C groups' behavior, in which the basins larger area and volume, the greater is the denudation rate; in the paleogullies group, which has the smallest areas and volumes, the highest rates could be observed. Proving that this intense erosive process occurs punctually, concentrated in certain locations throughout the study area. This idea is analogous to the statement by Wolman and Gerson (1978), that a specific feature occurrence in space may indicate the recurrence of that feature in the same region in the long term. This regional extrapolation was seen in the region, where some of these paleogullies were identified (Goulart, in press, item 3.2).

The PG basins average slope was the parameter that best explained the trend in the high denudation rates since the paleogullies group was the one with the highest slope values. This trend was also evidenced by Portenga and Biergman (2011), who, when correlating measured watersheds in the world with *in situ* ^{10}Be, concluded that the most significant regressor to explain denudation rates was the slope (R^2=0.33).

However, even in the PG group, the index values did not contrast significantly with the other groups. The K_{sn} and HI results indicate concave longitudinal profiles, suggesting that the watersheds measured in the PG group have already undergone adjustments in the longitudinal river profile, without the slope break present in the tributaries outside the PG basins. These adjustment examples could be seen in the longitudinal profiles of basins P6 (which includes PG2) and P7 (which includes PG3 and PG4) in Figure 3.5, in which the drainages internal to the paleogullies present a more evolved profile, with a relatively concave shape, demonstrating to be more developed, as it has already undergone a readjustment, compared to drainages outside the PGs.

The maximum χ value is not lower in the PG watersheds as was expected at first, since it was judged that due to the high denudation rate found in these basins, they would have a behavior of attacking the surrounding catchments and the divide should migrate, expanding the paleogullies area. The steady state picture showed that, contrary to what the high denudation rates led to suppose, these watersheds have already undergone an adjustment process, being now in balance in the current landscape. This balance could be observed in the field, in the verification of the inexistence of significant current erosive processes inside the PGs basins, or even eroded material large deposits coming from these features downstream of the sampled area for the ^{10}Be measurements.

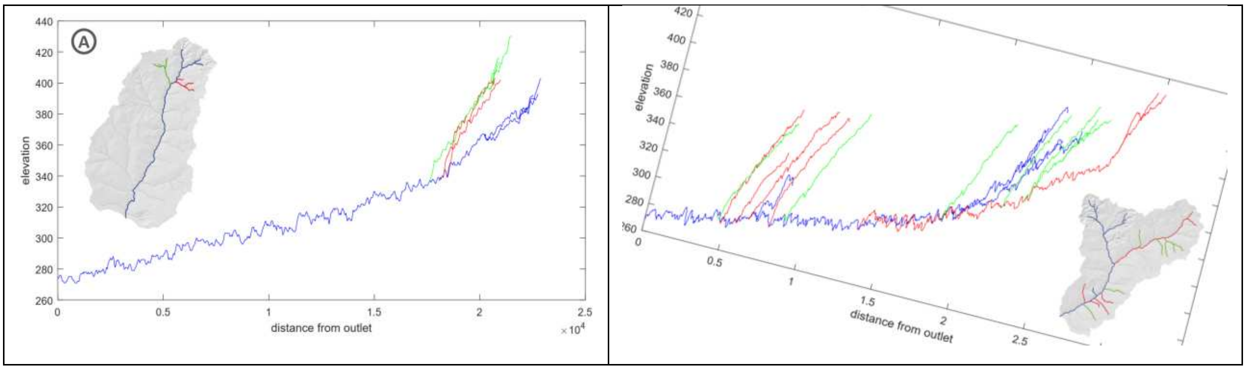

Figure 3.5: Longitudinal profiles of the main drainage in basins P6 (A) and P7 (B), demonstrating the adjustment of the profiles in blue, coming from within the paleogullies areas, in contrast to the green and red profiles that present the slope break in the encounter with the main basin drainage.

It is worth mentioning that the referred steady state presupposes a long-term analysis, with current human interventions without planning[13], in the short term, they can and should quickly reactivate the intense erosive processes of these stabilized features and associated with the sandy soils from the Caiuá Group's lithology, cause erosions that are difficult to contain.

The PG group K_{sn} also did not indicate large variations between the internal values, since there are no significant lithological variations or recent tectonic activities in the study area added to the fact that the regional relief has a little slope, characteristics that would significantly modify this index.

The paleogullies presence only in the Ivaí River northern portion, can be explained by the difference in denudation speed and consequently in the evolutionary stages of the measured watersheds. As, in general, the south Ivaí basins presented higher rates of denudation compared to the north Ivaí basins (do Couto et al., 2018), it was assumed that these paleogullies also existed in the South, however the denudation process generally faster in the South making them coalesce, making it impossible to visualize these features individually. In the Ivaí North, where the denudational process is a little slower, these large erosive features can still be more easily individualized amid relatively flat relief (Fumiya et al., 2016).

---

[13] The discussion of anthropic interference in increasing measured erosion rates was disregarded. Because the ^{10}Be is 1.38 My (Bierman and Portenga, 2018) and the anthropic occupation in the study area occurred only in the last 60, 70 years (Kohlhepp, 2014), it was considered that the anthropic interference in the denudation rate results was insignificant.

The evidence that paleogullies are in equilibrium with the landscape was reiterated when comparing the P basins denudation rates with the PGs basins internal to them. The analysis showed that the PGs basins that induce high rates in the local analysis are invisible in the regional analysis. Especially PG1, PG2, and PG5 increase the denudation rate of the basins in which they are present (except for the PG3 and PG4 paleogullies that seem to be closer to the P basins evolutionary stages), but at the regional level this influence is diluted, homogenizing it among the group P averages. When separately analyzing the basins with more recent evolutionary stages, PG1 (internal to P9), PG2 (internal to P6), and PG5 (internal to P11), a significant correlation was found between denudation rates and area (R^2 = 0.62) and between denudation rates and slope (R^2 = 0.89). The correlation shows the PG basins influence on the P basins evolution. The PG3 and PG4 basins (internal to P7) also influenced the regional basin denudation rate, since the P7 results show that it is in the regional average, but with a denudation speed slightly lower than the PG3 and PG4 results.

It should be noted that, just as the *inselbergs* are not all identified in the region, there are other paleogullies not yet identified and measured with cosmogenic nuclides. Examples of this gap are the areas of high roughness concentration and with a similar physiognomy to the PGs found inside the P14 basin. The P14 basin, even with a high rate of denudation, fits into the expected regional morphodynamic pattern, proving that even possible paleofeatures not identified or measured individually are in line with regional evolution.

3.3.4.5 Main Watersheds Patterns

A data compilation by large regional basins may also reveal new possibilities for interpreting regional morphodynamics. Among this systematization, what attracted the most attention was that the basins that have their base level in the Piquirí River (P23 and P24) have very low denudation rates concerning their size. They are the two largest basins in area and volume of the analyzed series, however the denudation is 9.3 ±1.5 m/My.

The Paranapanema basins (P11, P12, P13, P14, P15, and P16), North Ivaí (P6, P7, P8, P10, P25, and P26), and South Ivaí (P1, P2, and P4) are developing at approximately the same rate, with values of 11..8 ±1.9 m/My, 11.4 ±1.9 m/My, 14.0 ±2.3 m/My respectively. It was decided not to make generalizations about the denudation rate of the basins that drain directly into the Paraná River (P0, P3, and P9), because the sampled points number is low, just 3.

In general, the rates found in the main watersheds in the Bauru Basin southeast have denudation measures much lower than those measured in large river systems across the globe, like the Orinoco Rivers (Venezuela), 66.8 ±7.8 m/My, Ebro (Spain), 70.3 ±8.5 m/My, Red (China), 69.8 ±8.8 m/My, Snake (USA) 89.1 ±8.3 m/My, Columbia (USA) 97.4 ±22.3 m/My, Colorado (USA) 82.2 ±9.8 m/My (Wittmann et al., 2020). This demonstrates that the erosion process in the study area is slow.

3.3.4.6 Approximate Age of the Denudation Process Beginning

The age calculated for the erosion process beginning of the measured basins also showed a standard behavior for groups P and C. The P group is the oldest, with the erosion process starting during the Mio-Pliocene transition, 5.3 My on average. However, with amplitudes ranging from the middle Miocene in the case of the oldest basin, 10.2 My (6.5 ±1.1 m/My denudation rate), and the late Pliocene, 2.6 My (15.5 ±2.7 m/My denudation rate). These values could be attributed to a paleoclimate action with falling temperatures, which marks the Mio-Pliocene transition (Burke et al., 2018). This temperature drop that has been observed since the lower Eocene, although it does not characterize a glacial period, has the potential to catalyze physical erosive processes, as well as several other changes in the landscape.

As the C basins are smaller in area and volume and some are within the P basins, the tendency was for the C basins to be younger, which was confirmed by the erosion process beginning calculations. With an average result of 4.1 My, the C catchments must have started their erosion process in the middle Pliocene, in progressively colder and drier paleoclimate (Burke et al., 2018), compared to the paleoclimate conditions that prevailed during the beginning of the P basins formation.

The C group analysis showed that the oldest basin (C14) begins its erosive process still in the Miocene, 7.1 My (3.9 ±0.2 m/My denudation rate), and the most recent (C1) begins its formation in the upper Pliocene, almost at the transition to the Pleistocene glacial period, 2.9 My (16.3 ±0.7 m/My denudation rate). The minimum ages results of P group erosive processes, corroborating the order of magnitude observed in basins C, were 10.2 My (6.5 ±1.1 m/My denudation rate), early Miocene, for the oldest basin (P23), and 2.6 My (16.5 ±2.7 m/My denudation rate), Plio-Pleistocene transition, for the most recent basin (P9).

Once again behaving outside the pattern found for P and C groups, the results of the PGs basins showed that their formation process is much more recent than the other basins. The average ages at the process beginning, 1.2 My, indicates a formation beginning during the glacial paleoclimate influence, during the Pleistocene. Even the oldest basin in the group (PG3), which started to form 2.2 My (18.6 ±1.1 m/My denudation rate), indicates an age that corroborates the last glaciation beginning, at the Pleistocene beginning. While the most recent basin (PG5) started the formation process only 0.5 My (77.4 ±6.5 m/My denudation rate), the height of the Pleistocene glaciations.

3.3.4.7 Paleoclimatic Implications

These patterns found in the basins denudation rates and ages could be traced to the erosion processes behavior in arid and semi-arid landscapes. Since during the last Pleistocene glaciations, on the South American continent, already present in the current latitudes, drier and colder paleoclimates than the current ones, which consequently also affected the characteristics of the erosive processes at the time.

Therefore, a conceptual evolution analysis in the southeast of the Bauru Sedimentary Basin must consider at least two distinct patterns: a first involving the late Miocene and the Pliocene, with influences on regional evolution; and a second that covers the Pleistocene with more intense denudational processes that occurred during the last glacial period, with local influences on the relief, such as the formation of paleogullies found in the study area.

The evolution first pattern, P and C groups, with Miocene-Pliocene age, corresponds to processes developed in a paleoclimatic framework with temperatures just above the current ones, from 2 to 3 °C (Burke et al., 2018). Thus, this first pattern gave conditions to denudational processes very similar to contemporary ones, possibly with denudation rates similar to the current ones. In the second evolution pattern observed, group PG, with Pleistocene age, the denudational processes intensify concomitantly with the beginning of the last great glaciation, with temperatures on average 5 to 6 ° C below the current ones (Burke et al., 2018). These paleoclimatic characteristics interfere not only in the weathering of the rocks but also in the precipitation amount and its distribution, which tends to increase the denudational processes magnitude and consequently has potential for the gully’s emergence.

For Kirkby et al. (2009) the gullies formation in arid regions occurs when, in intense precipitation events, the ability of water to infiltrate the soil is overcome by runoff. This drains a large volume of material, forcing rapid internal adjustments to the basin, due to the magnitude and the short period of these events, in the preferential outflow channels. This sudden disequilibrium in the sediments production and transportation forces the watershed to readjust itself in a short period, and it can form gullies in a few major events in arid and semi-arid regions, climatic conditions similar to those of the Pleistocene in the South American continent inlands.

Thus, the paleogullies origin, according to Bigarella and Mazuchowski (1985), can be related to the erosion and/or sedimentation episodes of this last great glacial period, responsible for the topographic model sculpture and the colluvium-alluvial deposits nature, especially those of the study area sandstones.

Ratifying the ages and the studied basins formation context, Stevaux (2000) characterizes 4 distinct paleoclimatic phases in the Paraná River basin: a first (4.0 to 0.8My) dry, possible paleoclimate that forms the paleogullies; a second (0.8 to 0.35My) humid, which may have attenuated the denudational process in the area and stabilized the paleogullies, because the most recent was formed 0.5My ago; a third (0.35 to 0.15My) dry, which tends to reactivate some erosive processes and accelerate the denudation rate; and a last one (0.15My that remains until today) humid, stabilizing these features again, as evidenced by the morphometric indexes.

Another conjecture that was possible to be made on a regional scale that explains the probable paleogullies formation in the Pleistocene is in relation to the change in the global and, consequently, regional base level. Changes at the regional base level (Paranapanema, Ivaí, and Piquirí Rivers) must have caused erosion in the drainage headwaters of some basins when Pleistocene paleoclimates were active. What corroborated for the paleogullies appearance in the areas close to the drainage headwaters, as it could be observed in the study area, in the PG group.

According to Kirkby et al. (2009), one of the processes that can form gullies is the main channel fast incision since the change in the local base level tends to accentuate the erosion process. After the incision reaches the new base level, the tendency is for the channel profile to come into balance and for the denudational process to stabilize in the upstream areas. This apparent stability of the current main channels longitudinal profile was showed in the values of χ, K_{sn} and observed in the comparison of the longitudinal profiles, with the PG group drainage network already adjusted in relation to the tributaries external to these watersheds (Figure 3.5). As the global base level was lower than the current one during the Pleistocene, the idea of the paleo features formation related to the last great glacial period, under the influence of a readjustment in its longitudinal profile that would have the first reflections in the drainage headwaters was shown plausible.

Explanations of Pleistocene dynamics studied basins downstream also corroborate the paleogullies formation understanding, such as the change in the riverbed position of the channels that make up the regionally based levels. When studying the Paraná River terraces, Morais et al (2016) found a paleoconfluence between the Ivaí and Paraná Rivers, aged approximately 2.3My, early Pleistocene, 6km upstream of the current confluence. It should also be noted that the authors (Morais et al, 2016) describe a change in the drainage pattern, characterizing the drainage paleochannels as an anastomosed pattern, typical of semi-arid regions where the erosive process occurs in short but high magnitude events, as the events that theoretically were responsible for the paleogullies formation.

3.3.5 FINAL CONSIDERATIONS

Denudation rates measurements of regional, local, and even paleogullies made it possible to analyze the long-term geomorphological evolution of the Bauru Sedimentary Basin southeast region. The background denudation rate, as well as the average values of P and C groups, indicated a slow denudation pattern, as is expected for regions with a low slope. It was noted that paleogullies ended up being integrated into the regional evolutionary pattern, not significantly interfering in the averages of the regional watersheds.

However, the *inselbergs* had a great impact on the regional basins rates, mitigating the denudational process and excluding their respective basins from the regional pattern. This trend outliers could be attributed to a lithological propensity in the area for large and intense denudational processes, in which the pattern is that the basins have, or have had or will have, large gullies that are responsible for the long-term morphodynamics. A trend that makes *inselbergs* the true and unique geomorphological anomalies in the region.

Not only the denudational processes measured magnitude, but the possibility of dating the beginning of these processes indicates two distinct evolutionary patterns, one of the Mio-Pliocene and the other of the Pleistocene. However, both patterns must be considered for the area's current morphology sculpture understanding.

The identification and confirmation of the paleogullies presence in the region reinforce the Pleistocene denudational processes influence in the modeling of the current relief and proves the old processes legacy, which are no longer in force, but which help in the regional morphodynamics understanding. The indexes result showed that the paleogullies are actually in equilibrium, even with denudational rates so high compared to the P and C averages. However, the current relationship of these paleo features with the landscape deserves further investigation, as they end up becoming integrated into the regional landscape. Works with complementary methodologies such as phytoliths assemblies studies inside the paleogullies and other morphometric indexes application can help to understand how the different paleo features formation since they do not behave uniformly, because, as verified, the amplitude at the denudation rates and the PG group ages of the basins suggest different evolutionary stages.

New *in situ* ^{10}Be isotopes measurements can also be made in the investigation of the Piquirí River basin, which presented lower denudation rates, which may also infer a different pattern of regional evolution, raising the hypothesis that this basin is more recent in relation to the Ivaí and Paranapanema watersheds. These new measurements can refine the analysis for landscape evolution models that, if associated with studies that address paleogeographic issues, can help in understanding how the deposition center of the South American continent evolved.

In short, the landscape long-term morphodynamics analysis of the southeast Bauru Sedimentary Basin region revealed a clear cumulative influence of processes that occurred along the Miocene, Pliocene, and Pleistocene. Thus, it was possible to integrate the explanation of the local feature’s evolution, such as inselbergs and paleogullies, with the regional morphodynamics, because when they fit the pattern, the paleo features help to understand regional evolution.

3.3.6 REFERENCES

ALMEIDA, F. F. M. de; BRITO NEVES, B. B. de; CARNEIRO, C. D.R. The origin and evolution of the South American platform. ***Earth-Science Reviews***[S.l.], v. 50, n. 1-2, p. 77-111, 2000.

ALVARES, C.A., STAPE, J.L., SENTELHAS, P.C., GONÇALVES, J.L.M.; SPAROVEK, G. Köppen's climate classification map for Brazil. – **Meteorologische Zeitschrift** 22: 711–728. 2013.

ARZHANNIKOVA, A.; ARZHANNIKOV, S.; BRAUCHER, R.; JOLIVET, M.; AUMAÎTRE, G.; BOURLÈS, D.; KEDDADOUCHE, K. Morphotectonic analysis and 10 Be dating of the Kyngarga river terraces (southwestern flank of the Baikal rift system, South Siberia). **Geomorphology**, 303, 94–105. 2018.

BATEZELLI, A., GOMES, N.S., PERINOTTO, J.A.J. Petrográfica e evolução diagenética dos arenitos da porção norte e nordeste da bacia Bauru (Cretáceo Superior). **Revista Brasileira de Geociências**, v. 35, n.3, p.311-322, 2005.

BIERMAN, P. R.; PORTENGA, E. Beryllium Isotopes. In: White, W.M. (Ed.) **Encyclopedia of Geochemistry**. Springer International Publishing. 2018.

BIGARELLA, J.J. e MAZUCHOWSKI, J.Z. **Simpósio nacional de controle de erosão**. Anais. Maringá, 1985.

BURKE, K. D., WILLIAMS, J. W., CHANDLER, M. A., HAYWOOD, A. M., LUNT, D. J.; OTTO-BLIESNER, B. L. Pliocene and Eocene provide best analogs for near-future climates. **Proceedings of the National Academy of Sciences**, 115(52), 13288-13293. 2018

CHEREM, L. F. S.; VARAJÃO, C. A. C.; BRAUCHER, R.; BOURLÈS, D.; SALGADO, A. A. R.; VARAJÃO, A. C. O papel das capturas fluviais na morfodinâmica das bordas interplanálticas do Sudeste do Brasil. **Revista Brasileira de Geomorfologia**, v. 14, n. 4, p. 299-308, 2013.

DE BOER, D.H. Hierarchies and spatial scale in process geomorphology: a review **Geomorphology** 4 303-18.1992.

de MORAIS, E.S.; dos SANTOS, M.L.; CREMON É.H.; STEVAUX, J.C. Floodplain evolution in a confluence zone: Paraná and Ivaí rivers, Brazil. **Geomorphology**, Volume 257, p. 1-9, 2016.

do COUTO, E.V. **Evolução denudacional de longo prazo e a relação solo-relevo no Noroeste do Paraná**. Tese (Doutorado em Geografia. Universidade Federal do Paraná. Curitiba, 113f. 2014.

do COUTO, E.V.; SANTOS, L.J.C.; SORDI, M.V.; BOURLÈS, D.; BRAUCHER, R.; SALGADO, A.A.R.; LÉANNI, L.; FERREIRA, J.H.D.; ASTER TEAM. Changes of the base levels in the Ivaí and Paraná Rivers confluence zone (Southern Brazil): Denudational reflexes in the evolution of the upstream drainage network. **Zeitschrift für Geomorphologie**. Volume 62 Issue 1 , p.23-40. 2018.

EVENSTAR, L. A.; SPARKS, R. S. J.; COOPER, F. J.; LAWTON, M. N. Quaternary landscape evolution of the Helmand Basin, Afghanistan: Insights from staircase terraces, deltas, and paleoshorelines using high-resolution remote sensing analysis. **Geomorphology**, 311, 37–50. 2018.

FERNANDES L.A.; COIMBRA A.M. O Grupo Caiuá (Ks): revisão estratigráfica e contexto deposicional. **Rev. Bras. Geociências**, 24(3):164-176, 1994.

FERNANDES, L.A. **A cobertura cretácea suprabasáltica no Paraná e Pontal do Paranapanema (SP)**: os grupos Bauru e Caiuá. São Paulo. 129p. (Dissertação de Mestrado, IGc/USP). 1992.

FERNANDES, L.A. Mapa litoestratigráfico da parte Oriental da Bacia Bauru. **Boletim Paranaense de Geociências**, n.55, p. 53-66, 2004.

FERNANDES, L.A.; COIMBRA, A.M.; NETO, M.B. Silicificação hidrotermal neocretácea na porção meridional da Bacia Bauru. Revista do Instituto Geológico, 14(2), 19-26. 1993.

FERNANDES, L.A.; COUTO, E.V.; SANTOS, L.J.C. Três Morrinhos, Terra Rica, PR Arenitos silicificados de dunas do Deserto Caiuá testemunham nível de superfície de aplainamento K-T. In: WINGE, M. et al (edit./org.). Sítios geológicos e paleontológicos do Brasil, vol. III. Brasília. **Serviço Geológico do Brasil – CPRM,** v. III, p. 69-87. 2013.

FERNANDES, L.A.; COUTO, E.V.; SANTOS, L.J.C. Três Morrinhos, Terra Rica, PR Arenitos silicificados de dunas do Deserto Caiuá testemunham nível de superfície de aplainamento K-T. In: WINGE, M. et al (edit./org.). **Sítios geológicos e paleontológicos do Brasil**, vol. III. Brasília. Serviço Geológico do Brasil – CPRM, v. III, p. 69-87.2013.

FUMIYA, M.H.; SANTOS, L.J.C.; MANGUEIRA, C.G.; COUTO, E.V. Emprego do índice de concentração da rugosidade para a identificação de feições morfológicas associadas as crostas ferruginosas no Noroeste do Paraná. **Revista Brasileira de Geomorfologia,** v. 17, nº 3 2016.

FUMIYA, M.H.; SANTOS, L.J.C.; RIFFEL, S.B. Morphostratigraphy of Ferruginous Duricrusts in the Northwest of Paraná. **Revista Brasileira de Geomorfologia**. v.20, n.4. 2019.

GAO, H.; LI, Z.; LIU, F.; WU, Y.; LI, P.; ZHAO, X.; LI, F.; GUO, J.; LIU, C.; PAN, B.; JIA, H. Terrace formation and river valley development along the lower Taohe River in central China. **Geomorphology**. 2019.

GOULART, A.Á.; SANTOS, L.J.C. Evolução temporal e espacial das paleovoçorocas presentes no município de Loanda/PR. **Revista Geonorte**, Edição Especial, v. 10, p. 81-86, 2014.

GRANGER, Darryl E.; SCHALLER, Mirjam. Cosmogenic nuclides and erosion at the watershed scale. **Elements**, v. 10, n. 5, p. 369-373, 2014.

GUERRA, A.T.; GUERRA, A.J.T. **Novo dicionário geológico-geomorfológico**. 6. ed. Rio de Janeiro: Bertrand Brasil, 648 p. 2008.

HECKMANN, T.; HAAS, F.; ABEL, J.; RIMBÖCK, A.; BECHT, M. Feeding the hungry river: Fluvial morphodynamics and the entrainment of artificially inserted sediment at the dammed river Isar, Eastern Alps, Germany. **Geomorphology**. 2017.

Hu, G.; Yi, C.-L.; Liu, J.-H.; Wang, P.; Zhang, J.-F.; Li, S.-H.; Li, D.; Huang, J.; Wang, H.-Y.; Zhang, A.-M.; Shi, L.; Shui, X. Glacial advances and stability of the moraine dam on Mount Namcha Barwa since the Last Glacial Maximum, eastern Himalayan syntaxis. **Geomorphology**, 2020.

HUGHES, P.D. Geomorphology and Quaternary stratigraphy: The roles of morpho-, litho-, and allostratigraphy. **Geomorphology**, vol. 123, no. 3-4, pp. 189-199. 2010.

IBGE - Instituto Brasileiro de Geografia e Estatística. **Manual Técnico da Vegetação Brasileira**. Rio de Janeiro: IBGE, 2012.

IELPI, A. Lateral accretion of modern unvegetated rivers: Remotely sensed fluvial - aeolian morphodynamics and perspectives on the Precambrian rock record. **Geol. Mag**. 154, 609–624. 2017.

IELPI, A. Morphodynamics of meandering streams devoid of plant life: Amargosa River, Death Valley, California. **Geol. Soc**. Am. Bull. 31, 782–802. 2018.

IMESON, A. C.; LAVEE, H. Soil erosion and climate change: the transect approach and the influence of scale. **Geomorphology**, v. 23, n. 2-4, p. 219-227, 1998.

KING, L. A geomorfologia do Brasil oriental. **Rev. Bras. Geogr.**, 18(2), 147-265. 1956.

KIRKBY, M. J.; BRACKEN, L. J. Gully processes and gully dynamics. **Earth Surface Processes and Landforms: The Journal of the British Geomorphological Research Group**, v. 34, n. 14, p. 1841-1851, 2009.

KISS, T.; SÜMEGHY, B.; SIPOS, G. Late Quaternary paleodrainage reconstruction of the Maros River alluvial fan. **Geomorphology**, 204, p.49–60. 2014.

KOHLHEPP, G. **Colonização agrária do norte do Paraná**: processos geoeconômicos e sociogeográficos de desenvolvimento de uma zona subtropical do Brasil sob a influência da plantação de café. 1 ed. Editora da Universidade Estadual de Maringá, Maringá, 2014.

KOMATSU, G.; BRANTINGHAM, P. J.; OLSEN, J. W.; BAKER, V. R. Paleoshoreline geomorphology of Böön Tsagaan Nuur, Tsagaan Nuur and Orog Nuur: the Valley of Lakes, Mongolia. **Geomorphology**, 39(3-4), 83–98. 2001.

LEIGH, D. S. Late Quaternary climates and river channels of the Atlantic Coastal Plain, Southeastern USA. **Geomorphology**, 101(1-2), 90–108. 2008.

LIM, Y.J.; LEVY, J.S.; GOUDGE, T.A.; KIM, W. Ice cover as a control on the morphodynamics and stratigraphy of Arctic deltas. **Geology**; 47 (5): 399–402. 2019.

MADDY, D.; VELDKAMP, A.; DEMIR, T.; AYTAÇ, A.S.; SCHOORL, J.M.; SCAIFE, R.; BOOMER, I.; STEMERDINK, C.; VAN DER SCHRIEK, T.; AKSAY, S.; LIEVENS, C. Early Pleistocene River Terraces of the Gediz River, Turkey: The role of faulting, fracturing, volcanism and travertines in their genesis, **Geomorphology**, Volume 358, 2020.

MARTINOD, J.; REGARD, V.; RIQUELME, R.; AGUILAR, G.; GUILLAUME, B.; CARRETIER, S.; HÉRAIL, G. Pleistocene uplift, climate and morphological segmentation of the Northern Chile coasts (24°S–32°S): Insights from cosmogenic 10Be dating of paleoshorelines. **Geomorphology**, 274, 78–91. 2016.

MASELLI, V.; PELLEGRINI, C.; DEL BIANCO, F.; MERCORELLA, A.; NONES, M.; CROSE, L.; GUERRERO, M.; NITTROUER, J. River Morphodynamic Evolution Under Dam-Induced Backwater: An Example from the Po River (Italy). **Journal of Sedimentary Research**. 88. 1190-1204. 2018.

MASSELINK G.; KROON, A.; DAVIDSON-ARNOTT, R.G.D. Morphodynamics of intertidal bars in wave-dominated coastal settings — A review. **Geomorphology**, Volume 73, Issues 1–2, Pages 33-49, 2006.

MATMON, A., BIERMAN, P. R., LARSEN, J., SOUTHWORTH, S., PAVICH, M.; CAFFEE, M. Temporally and spatially uniform rates of erosion in the southern Appalachian Great Smoky Mountains. Geology, 31(2). 2003.

MATTHEWS, J.A.; WINKLER, S. Schmidt-hammer exposure-age dating (SHD): application to early Holocene moraines and a reappraisal of the reliability of terrestrial cosmogenic-nuclide dating (TCND) at Austanbotnbreen, Jotunheimen, Norway. **Boreas**. 2010:

MORAIS, E.S. de; SANTOS, M.L.; CREMON, E.H.; STEVAUX, J.C. Floodplain evolution in a confluence zone: Paraná and Ivaí rivers, Brazil. **Geomorphology** (Amsterdam), V. 257 , P. 1-9 , 2016.

PORTENGA, E.; BIERMAN, P. Understanding Earth's eroding surface with 10Be. **GSA Today**. 21. P. 4-10. 2011

QUEIROZ NETO, J.P. Solos e paleossolos do Estado de São Paulo e suas interpretações paleogeográficas. In: Congresso Brasileiro De Geologia, 28., Porto Alegre. **Anais**... Porto Alegre, Sociedade Brasileira de Geologia, v.3. p.173-181. 1974.

RIFFEL, S.; VASCONCELOS, P.; CARMO, I.; FARLEY, K. Combined 40Ar/39Ar and (U-Th)/He geochronological constraints on long-term landscape evolution of the

Second Paraná Plateau and its ruiniform surface features, Paraná, Brazil. **Geomorphology**. 233. 52-63. 2015.
SANTOS, L. J. C.; OKA-FIORI, C.; CANALLI, N. E.; FIORI, A. P.; SILVEIRA, C. T.; SILVA, J. M. F.; ROSS, J. L. S. Mapeamento Geomorfológico do Estado do Paraná. **Revista Brasileira de Geomorfologia**, Ano 7, nº 2, p. 03-12, 2006.
SCHWANGHART, W.; SCHERLER, D. Short Communication: TopoToolbox 2 – MATLAB-based software for topographic analysis and modeling in Earth surface sciences. – **Earth Surface Dynamics** 2: 1–7. 2014.
STEVAUX, J.C. Climatic events during the Late Pleistocene and Holocene in the Upper Parana River: Correlation with NE Argentina and South-Central Brazil. **Quatern. Int**., 72:73-85, 2000.
STEVAUX, J.C. The upper Parana river *(*Brazil): geomorphology*,* sedimentology, and paleoclimatology*.* **Quaternary International**, v.21, p.143-161, 1994.
SU, Q.; KIRBY, E.; REN, Z.; ZHANG, P.; ZHANG, H.; MANOPKAWEE, P.; LEI, Q. Chronology of the Yellow River terraces at Qingtong Gorge (NE Tibet): insights into evolution of the Yellow River since the Middle Pleistocene. **Geomorphology**. 2019.
SUMMERFIELD, M. A Tale of Two Scales, or the Two Geomorphologies. **Transactions of the Institute of British Geographers**, 30(4), new series, 402-415. 2005.
VILES, H.A. Technology and geomorphology: Are improvements in data collection techniques transforming geomorphic science? **Geomorphology**. 270. 2016.
WOLMAN, M.G.; GERSON, R. Relative scales of time and effectiveness of climate in watershed geomorphology. **Earth Surf. Process**. 1978.
WU, C., NITTROUER, J.A.; MUTO, T.; NAITO, K.; PARKER, G. Morphodynamic equilibrium of lowland river systems during autoretreat. **Geology**. 2020.
YANG, H.; YANG, X.; HUANG, W.; LI, A.; HU, Z.; HUANG, X.; YANG, H. 10Be and OSL dating of Pleistocene fluvial terraces along the Hongshuiba River: Constraints on tectonic and climatic drivers for fluvial downcutting across the NE Tibetan Plateau margin, China, **Geomorphology**. 2019.
ZARZUELO, C.; LÓPEZ-RUIZ, A.; D’ALPAOS, A.; CARNIELLO, L.; ORTEGA-SÁNCHEZ, M. Assessing the morphodynamic response of human–altered tidal embayments. **Geomorphology**. 320, 127–141. 2018.

4 CONSIDERAÇÕES GERAIS

A análise comparativa dos artigos publicados com taxas de denudação utilizando-se dos isótopos de ^{10}Be feitos no Brasil até o final de 2019 mostrou não haver ainda uma correlação direta com um elemento da paisagem que possa explicar um padrão de denudação em todo o território.

As distintas características que formam as diversas paisagens encontradas no país aparecem pontualmente em cada um dos estudos, como constituintes que influenciam de maneira distinta a magnitude da taxa de denudação. Os fatores mais influentes que recorrentemente aparecem nos trabalhos analisados foram a declividade média e a litologia, mesmo que generalizada, sem considerar especificidades pontuais.

A concentração espacial das publicações nas regiões sul-sudeste, assim como a ausência das coordenadas dos pontos de amostragem nas publicações tornaram a análise mais incerta, dificultando a busca de um padrão de evolução do relevo. Para um melhor entendimento da morfodinâmica no país é necessário a mensuração de taxas de denudação em áreas ainda pouco exploradas, como nas regiões norte e nordeste.

A partir de dados mais distribuídos no território brasileiro, será possível propor um modelo de evolução do relevo que envolva todo o país. Atualmente, apenas algumas regiões, onde os cientistas concentraram seus esforços, como por exemplo a Serra do Mar, podem ser utilizadas para propor grandes sínteses evolutivas do relevo.

Outra região que a partir dessa tese já pode servir de base para modelos evolutivos é o sul da BB. A identificação de *low relief surfaces* foi fundamental para a compreensão de como os ciclos erosivos já descritos na literatura agiram na área de estudo. A aplicação dos índices geomórficos mostraram especificidades relevantes para a interpretação de feições pontuais como os inselbergs e as paleovoçorocas. Essas últimas, erosões pleistocênicas relativamente estáveis atualmente, mostraram um *steady-state* na análise dos índices, o que revelou uma sintonia com a morofodinâmica regional, demonstrando que essas feições tendem a ocorrer de forma natural na região, não sendo anomalias, mas sim um padrão evolutivo esperado para a morfodinâmica do sul da BB.

As mensurações com nuclídeos cosmogênicos complementaram a análise, resultando em médias de taxas de denudação baixas, como se espera de regiões relativamente planas e sem tectonismo recente, como o sul da BB. Os resultados da mensuração das taxas de denudação das paleovoçorocas revelaram que essas feições foram denudadas intensamente durante o Plio-Pleistoceno, porém esses valores altos se homogeneizaram na análise regional, o que revela que ao contrário do imaginado em um primeiro momento, as paleovoçorocas se integram na evolução da paisagem. O que reforça a ideia de que o processo evolutivo natural do relevo na região é o surgimento e posterior coalescência dessas paleo feições erosivas, como explanado na introdução da tese.

A partir desses resultados pode-se conjecturar que: ao contrário do que afirma do Couto (2014) e do Couto et al (2018), não há uma diferença significativa nas taxas de denudação ao Norte e Sul do rio Ivaí. A influência de um tectonismo recente que explicaria diferenças na morfodinâmica regional, conforme explanado por do Couto (2014), não se confirma com os resultados da tese.

As diferenças entre as margens do Ivaí, associadas a presença/ausência atual das paleovoçorocas parece ser melhor explicada pela atuação de paleoclimas quaternários, conforme mostram os resultados das taxas de denudação e da idade aproximada do início do processo erosivo das bacias mensuradas. Fato esse que se reforça não apenas pela intensificação dos processos erosivos durante as flutuações paleoclimáticas, mas também pela variação dos níveis de base das principais drenagens regionais, o que pode ter resultado no aparecimento das paleovoçorocas nos canais de primeira ordem das bacias.

Essa interpretação, não refuta por completo a hipótese inicial da tese, mas demonstra que, assim como observado no item 3.1, a busca por padrões que expliquem as taxas erosivas varia de acordo com especificidades locais, das bacias analisadas. As mensurações feitas por do Couto et al. (2018) superestimaram uma diferença norte e sul, devido ao critério de amostragem, a partir de bacias hidrográficas de primeira ordem. O processo regional se mostrou mais homogêneo, não apresentando a mesma discrepância visualizada pelos autores anteriores.

A diferença de escala, que pode superestimar os resultados, se mostrou ainda mais clara na mensuração das paleovoçorocas. As bacias que possuem essas paleo feições não apresentaram valores distintos dos visualizados na média regional, mas pelo contrário, se integraram nos valores médios sem maiores distinções. Esse fato permitiu a resposta de que as paleovoçorocas fazem parte da evolução natural do sul da BB, onde as grandes bacias ou já apresentaram essas feições que se coalesceram e hoje não podem ser facilmente visualizadas ou que apresentam atualmente essas feições, mas que, diferentemente do ocorrido no Plio-Pleistoceno, hoje as mesmas estão estabilizadas.

Estudos mais detalhados, com reconstituições ambientais da paisagem pleistocênica, como o levantamento de assembléias fitolíticas nas paleovoçorocas, além da aplicação de outros índices morfométricos podem ajudar a entender como as paleovoçorocas foram formadas, uma vez que mesmo entre essas feições não há um comportamento uniforme, o que sugere diferentes estágios evolutivos.

Ao contrário das paleovoçorocas, os inselbergs apresentaram uma influência mais direta nas taxas de denudação, reduzindo a magnitude dos processos denudacionais nas bacias onde são encontrados. Fato esse que não exclui a interpretação regional, apenas os aponta como estruturas que fogem ao padrão de denudação esperado para a região. Sendo assim, há de se propor novas mensurações com nuclídeos cosmogênicos nos inselbergs.

Novas mensurações de taxas denudacionais também podem ser feitas nas bacias que estão fora do padrão esperado. As bacias que drenam para o Piquirí, por exemplo, precisam ser melhor compreendidas, pois estão abaixo dos valores da média regional.

Essas novas medidas podem refinar a análise já existente e até propor modelos preditivos de evolução da paisagem. Associados a estudos que abordam questões paleogeográficas, esses trabalhos podem vir a ajudar a entender como evoluiu o centro de deposição do continente sul-americano durante desde o Mioceno até os dias de hoje.

REFERÊNCIAS GERAIS

Ab'saber A.N. **Os domínios de natureza no Brasil: potencialidades paisagísticas**. São Paulo: Ateliê Editorial, 2003.

Alcantara-Santos, J.C. **Paleogeografia e Paleoambientes do baixo curso do rio Ivaí**- Pr. 81f. Dissertação (Mestrado em Geografia), Universidade Estadual de Maringá, Maringá, Paraná, 2013.

Almeida, F. F. M. de; Brito Neves, B. B. de; Carneiro, C. D.R. The origin and evolution of the South American platform. **Earth-Science Reviews**[S.I.], v. 50, n. 1-2, p. 77-111, 2000.

Arnold, M., Merchel, S., Bourl`es, D. L., Braucher, R., Benedetti, L., Finkel, R. C., Klein, M. The French accelerator mass spectrometry facility ASTER: Improved performance and developments. **Nuclear Instruments and Methods in Physics Research** Section B: Beam Interactions with Materials and Atoms, 268(11-12), 1954-1959. 2010.

Barreto, H. N. **Investigação da Influência dos Processos Denudacionais na Evolução do relevo da Serra do Espinhaço Meridional, Minas Gerais – Brasil**. Tese (Doutorado em Geologia). DEGEO/UFOP. Ouro Preto. 2012.

Barreto, H.N.; Varajão, C.A.C.; Braucher, R.; Bourlès, D.L.; Salgado, A.A.R.; Varajão, A.F.D.C. Denudation rates of the Southern Espinhaço Range, Minas Gerais, Brazil, determined by in situ-produced cosmogenic beryllium-10. **Geomorphology**, Volume 191, Pages 1-13, 2013.

Barretto, A.G.O.P. **História e geografia da pesquisa brasileira em erosão de solo**. 2007. 120f. Dissertação (Mestrado em Agronomia) – Escola Superior de Agricultura Luiz de Queiroz, Piracicaba, 2007.

Bellanca, E.T.; Suertegaray, D.M.A. Sitios arqueológicos e areais no sudoeste do Rio Grande do Sul. **Mercator. Revista de Geografia da UFC**, Fortaleza, v. 2, n. 4, p. 99-114, 2003.

Bierman, P. R.; Portenga, E. Beryllium Isotopes. In: White, W.M. (Ed.) **Encyclopedia of Geochemistry**. Springer International Publishing. 2018.

Bierman, P.; Steig, E. J. Estimating rates of denudation using cosmogenic isotope abundances in sediment. **Earth surface processes and landforms**, 21(2), 125-139. 1996.

Bigarella, J.J.; Mazuchowski, J.Z. **Simpósio nacional de controle de erosão**. Anais. Maringá, 1985.

Bishop, P. Long-term landscape evolution: Linking tectonics and surface processes. **Earth Surface Processes and Landforms**, 32, 329–365. 2007.

Bishop, P.; Hoey, T. B.; Jansen, J. D.; Artza, I. L.: Knickpoint recession rate and catchment area: the case of uplifted rivers in Eastern Scotland, **Earth Surf. Process. Landf.**, 30(6), 767–778, 2005.

Borchers, B., Marrero, S., Balco, G., Caffee, M., Goehring, B., Lifton, N., Stone, J. Geological calibration of spallation production rates in the CRONUS-Earth project. **Quaternary Geochronology,** 31, 188-198. 2016.

Braucher R. Utilisation du 10Be cosmogenique produit in situ pour l'etude da la dynamique des laterites em zone intertropicale. CEREGE, Université d'Aix Marseille III. Aix-en-Provence. **These Doctorat**. 112p. 1998.

Braucher, R., Merchel, S., Borgomano, J., Bourlès, D. Production of cosmogenic radionuclides at great depth: A multi element approach. **Earth and Planetary Science Letters**, 309(1-2), 1-9. 2011.

Brocard, G.Y.; Van Der Beek, P.A.; Bourlès, D.L.; Siame, L.L.; Mugnier, J-L. Long-term fluvial incision rates and postglacial river relaxation time in the French Western Alps from 10Be dating of alluvial terraces with assessment of inheritance, soil development and wind ablation effects. **Earth Planet**. Sc. Lett., 209, 197-214. 2003.

Brown L., M. Pavich, Hickman R. E., Klein J, Middleton R. Erosion of the eastern United States observed with 10Be. **Earth Surf. Process. Landform**., 13: 441-457. 1988.

Brown, E. T., Edmond, J. M., Raisbeck, G. M., Yiou, F., Kurz, M. D., Brook, E. J. Examination of surface exposure ages of Antarctic moraines using in situ produced 10Be and 26Al. **Geochimica et Cosmochimica Acta**, 55(8), 2269-2283. 1991.

Brown, E. T., Stallard, R. F., Larsen, M. C., Raisbeck, G. M., Yiou, F. Denudation rates determined from the accumulation of in situ-produced 10be in the luquillo experimental forest, puerto rico. **Earth and Planetary Science Letters**, 129(1-4), 193–202. 1995.

Brown, E. T., Stallard, R. F., Larsen, M. C., Raisbeck, G. M., Yiou, F. Denudation rates determined from the accumulation of in situ-produced 10be in the luquillo experimental forest, puerto rico. **Earth and Planetary Science Letters**, 129(1-4), 193–202. 1995.

Castro, S.S. Erosão hídrica na alta bacia do rio Araguaia: distribuição, condicionantes, origem e dinâmica atual. **Revista do Departamento de Geografia**, 17: 38-60, 2005.

Cavalcanti, E.R.; Coutinho, S.F.S. Desertification in the northeast of Brazil: the natural resources use and the land degradation. **Sociedade & Natureza** Special Issue: 891 – 900. 2005.

Cherem, L.F.; Varajao, C.; Braucher, R. Bourlès, D.; Salgado, A.; Varajão, A. Long-term evolution of denudational escarpments in southeastern Brazil. **Geomorphology**. 2012.

Chmeleff, J., von Blanckenburg, F., Kossert, K., Jakob, D. Determination of the 10Be half-life by multicollector ICP-MS and liquid scintillation counting. **Nuclear Instruments and Methods in Physics Research**, Section B: Beam Interactions with Materials and Atoms, 268(2), 192–199. 2010.

Corrêa, A.C.B.; Souza, J.O.P.; Cavalcanti, L.C.S. Solos do Ambiente Semiárido In Guerra, A.J.T.; Jorge, M.C.O. (Org.). **Degradação dos solos no Brasil.** Rio de Janeiro: Bertrand Brasil, 2014.

Derrieux, F., Siame, L.L., Bourlès, D.L., Chen, R.F., Braucher, R., Léanni, L., Lee, J.C., Chu, H.T., Byrne, T.B. How fast is the denudation of the Taiwan Mountain belt? Perspectives from in situ cosmogenic 10Be. **Journal of Asian Earth Sciences**, 88, 230-245. 2014.

do Couto, E. V. **Evolução denudacional de longo prazo e a relação solo - relevo no noroeste do Paraná**. Curitiba, Tese (Doutorado em Geografia). Departamento de Geografia, Setor de Ciências da Terra, Universidade Federal do Paraná. 2014.

do Couto, E.V.; Santos, L.J.C.; Sordi, M.V.; Bourlès, D.; Braucher, R.; Salgado, A.A.R.; Léanni, L.; Ferreira, J.H.D.; ASTER TEAM. Changes of the base levels in the Ivaí and Paraná Rivers confluence zone (Southern Brazil): Denudational reflexes in the evolution of the upstream drainage network. **Zeitschrift für Geomorphologie**. Volume 62 Issue 1 , p.23-40. 2018.

Dunai, T. J. **Cosmogenic nuclides**: Principles, concepts and applications in the earth surface sciences. Cambridge University Press. 2010.

Fernandes L.A.; Coimbra A.M. O Grupo Caiuá (Ks): revisão estratigráfica e contexto deposicional. **Rev. Bras. Geociências**, 24(3):164-176, 1994.

Fernandes, L.A. **A cobertura cretácea suprabasáltica no Paraná e Pontal do Paranapanema (SP)**: os grupos Bauru e Caiuá. São Paulo, Dissertação (Mestrado em Geologia) IGc, Universidade de São Paulo. 129p. 1992.

Fernandes, L.A. Mapa litoestratigráfico da parte Oriental da Bacia Bauru. **Boletim Paranaense de Geociências**, n.55, p. 53-66, 2004.

Fernandes, L.A.; de Castro, A.B.; Basicili, G. Seismites in continental sand sea deposits of the late cretaceous Caiuá Desert, Bauru Basin. Brazil. **Sed. Geol.** 199, 51–64. 2007.
Fernandes, L.A.; do Couto, E.V.; Santos, L.J.C. Três Morrinhos, Terra Rica, PR Arenitos silicificados de dunas do Deserto Caiuá testemunham nível de superfície de aplainamento K-T. In: WINGE, M. et al (edit./org.). Sítios geológicos e paleontológicos do Brasil, vol. III. Brasília. **Serviço Geológico do Brasil – CPRM,** v. III, p. 69-87. 2013.
Fidalski, J. Diagnóstico de manejo e conservação do solo e da água na região noroeste do Paraná. **Revista Unimar**, Maringá, v. 19, n.3, p. 845-851, 1997.
Fumiya, M. H. **Gênese dos Ferricretes e sua Relação com Transformações da Paisagem no Noroeste do Paraná**. Tese (Doutorado em Geografia) - Universidade Federal do Paraná, Setor de Ciências da Terra, no curso de Pós-Graduação em Geografia, Curitiba, 2017.
Gonzalez, V.S.; Bierman, P.R.; Fernandes, N.F; Hood, D.H. Long-term background denudation rates of southern and southeastern Brazilian watersheds estimated with cosmogenic 10Be. **Geomorphology**. Volume 268 p.54–63. 2016b.
Gonzalez, V.S.; Bierman, P.R.; Nichols, K.K.; Rood, D.H. Long-term erosion rates of Panamanian drainage basins determined using in situ 10Be. **Geomorphology**. Volume 275. P. 1-15. 2016a.
Gosse J.C., Phillips F.M. Terrestrial in situ cosmogenic nuclides: theory and application. **Quat. Sci. Rev**., 20:1475-1560. 2001.
Goulart, A. Á.; de Oliveira, J. G.; Santos, L. J. C. Utilização do Índice de Concentração de Rugosidade para Identificação de Feições Erosivas na Região Noroeste do Estado do Paraná. In: **Anais do XII Simpósio Nacional de Geomorfologia (SINAGEO)**, UGB. Crato/CE. 2018.
Goulart, A. Á.; Santos, L. J. C. Evolução temporal e espacial das paleovoçorocas presentes no município de Loanda/PR. **Revista Geonorte**, Edição Especial, v. 10, p. 81-86, 2014.
Granger, D. E., Kirchner, J. W., Finkel, R. Spatially averaged long-term erosion rates measured from in situ-produced cosmogenic nuclides in alluvial sediment. **The Journal of Geology**, 104(3), 249–257. 1996.
Granger, D. E., Lifton, N. A., Willenbring, J. K. A cosmic trip: 25 years of cosmogenic nuclides in geology. **GSA Bulletin**, 125(9-10), 1379–1402. 2013.
Granger, D. E.; Schaller, M. Cosmogenic nuclides and erosion at the watershed scale. **Elements**, 10(5), 369–373. 2014.
Guerra, A.J.T. e Cunha, S.B. da (org.). **Geomorfologia**: uma atualização de bases e conceitos. Rio de Janeiro: Bertrand Brasil, 1994.
Guerreiro R.L. **Evolução geomorfológica e paleoambiental dos terraços da margem esquerda do alto rio Paraná**. Rio Claro – SP: Inst. Geoc. e Ciências Exatas. Univ. Est. Paulista. 67p. (Dissert. Mestrado). 2011.
Harel, M.-A.; Mudd, S.M.; Attal, M. Global analysis of the stream power law parameters based on worldwide 10Be denudation rates. **Geomorphology**, Volume 268, Pages 184-196, 2016.
Hergarten, S.; Robl, J.; Stüwe, K. Extracting topographic swath profiles across curved geomorphic features. **Earth Surface Dynamics**, vol. 2, no. 1, p. 97-104. 2014.
Inkpen, R.J.; Stephenson, W.J.; Kirk, R.M.; Hemmingsen, M.A.; Hemmingsen, S.A. Analysis of relationships between micro-topography and short- and long-term erosion rates on shore platforms at Kaikoura Peninsula, South Island, New Zealand. **Geomorphology**. Volume 121, Issues 3–4. P. 266-273. 2010.

Justus, J.O. **Subsídios para interpretação morfogenética através da utilização de imagens de radar.** 204 f. Dissertação (Mestrado em Geografia) – Universidade Federal da Bahia, Salvador. 1985.
Kirby, E., Whipple, K.X. Expression of active tectonics in erosional landscapes.**J. Struct. Geol**. 44, 54–75. 2012.
Korschinek, G.; Bergmaier, A.; Dillmann, I.; Faestermann, T.; Gerstmann, U.; Knie, K.; Lierse von Gostomski, C; Maiti, M.; Poutivtsev, M.; Remmert, A.; Rugel, G.; Wallner, A. Determination of the 10be half-life by hi-erd and liquid scintillation counting. **Geochimica et Cosmochimica Acta Supplement**, 73, A685. 2009.
Lal D. In situ produced cosmogenic isotopes in terrestrial rocks. **Ann. Rev. Earth Planet. Sci.**, 16:355-388. 1988.
Lal, D. Cosmic ray labeling of erosion surfaces: in situ nuclide production. **Earth and Planetary Science Letters**, 104, 424–439. 1991.
Luz, L.M. **Aspectos Paleoambientais do Quaternário Superior na Região de Campo Mourão, Paraná.** Dissertação de Mestrado, Programa de Pós-Graduação em Geografia, área de concentração Análise Ambiental, Universidade Estadual de Maringá, 123p., 2014.
Maack, R. **Geografia física do Estado do Paraná**. Curitiba: José Olympio, 1968.
Martinelli, L. A.; Ometto, J P H B; Ferraz, E. S.; Victoria, R. L.; Camargo, P. B.; Moreira, M. Z. **Desvendando Questões Ambientais com Isótopos Estáveis**. São Paulo: Oficina de Textos, v. 1. 144p. 2009.
Mendonça, F. de A. A erosão urbana de Paranavaí / PR: estudo com base no emprego de fotografias aéreas. Seminário: **Ciências Sociais e Humanas**, Londrina, v. 14, n. 3, p. 151-154, set. 1994.
Merchel, S.; Herpers, U. An update on radiochemical separation techniques for the determination of long-lived radionuclides via accelerator mass spectrometry. **Radiochimica Acta**, 84(4), 215-220. 1999.
Milani, E. J.; Ramos, V. A. Orogenias paleozóicas no domínio sul-ocidental do Gondwana e os ciclos de subsidência da Bacia do Paraná. **Brazilian Journal of Geology**, 28(4):473–484. 1998.
Morais, E.S. de; Santos, M.L.; Cremon, E.H.; Stevaux, J.C. Floodplain evolution in a confluence zone: Paraná and Ivaí rivers, Brazil. **Geomorphology** (Amsterdam), V. 257, P. 1-9, 2016.
Nakashima, P. **Sistemas pedológicos da região noroeste do Estado do Paraná: distribuição e subsídios para o controle da erosão**. São Paulo, Tese (Doutorado em Geografia Física) Faculdade de Filosofia, Letras e Ciências Humanas, Universidade de São Paulo, 1999
Netto, A.L.C. Hidrologia de encosta na interface com a geomorfologia. In. Guerra, A.J.T. e Cunha, S.B. da (org.). **Geomorfologia**: uma atualização de bases e conceitos. Rio de Janeiro: Bertrand Brasil, 1994.
Parolin, M.; Domiciliano, R. T.; Guerreiro, R. L.; Caxambu, M. G. Primeiras considerações palinológicas e paleoclimáticas do Pleistoceno tardio na região de Campo Mourão, Paraná, Brasil. In: XIII CONGRESSO DA ABEQUA, Búzios, RJ **Anais...** 2011.
Parolin, M.; Volkmer-Ribeiro, C.; Stevaux, J.C. Sponge spicules in peaty sediments as paleoenvironmental indicators of the Holocenein the upper Paraná river, Brazil. **Revista Brasileira de Paleontologia** 10 (1), 17-26, 2007. 33, 2007.
Pinese Junior, J.F.; Cruz, L.M.; Rodrigues, S.C. Monitoramento de erosão laminar em diferentes usos da terra, Uberlândia - MG. **Soc. nat. (Online)**, vol.20, n.2, pp.157-175. 2008.

Portenga, E.W.; Bierman, P.R.; Trodick, C.D.; Greene, S.E.; DeJong, B.D.; Rood, D.H.; Pavich, M.J. Erosion rates and sediment flux within the Potomac River basin quantified over millennial timescales using beryllium isotopes. **GSA Bulletin** ; 131 (7-8): 1295–1311. 2019.
Raab, G.; Egli, M.; Norton, K.; Dahms, D.; Brandová, D.; Christl, M.; Scarciglia, F. Climate and relief-induced controls on the temporal variability of denudation rates in a granitic upland. **Earth Surf. Process. Landforms**, 44: 2570–2586. 2019.
Regard, V.; Carretier, S.; Boeglin, J.-L.; Ndam Ngoupayou, J.-R.; Dzana, J.-G.; Bedimo Bedimo, J.-P.; Riotte, J.; Braun, J.-J. Denudation rates on cratonic landscapes: comparison between suspended and dissolved fluxes, and 10Be analysis in the Nyong and Sanaga River basins, south Cameroon. **Earth Surf. Process. Landforms**, 41: 1671–1683. 2016.
Riley, S. J.; DeGloria, S. D.; Elliot, R. A terrain ruggedness index that quantifies topographic heterogeneity, **Intermountain Journal of Sciences**, vol. 5, No. 1-4,1999.
Rodrigues, S.C. Degradação dos solos do cerrado. In: Guerra, A.J.T.; Jorge, M.C.O. (Org.). **Degradação dos solos no Brasil**. Rio de Janeiro: Bertrand Brasil, 2014.
Rodrigues, Sc. Mudanças ambientais na região do Cerrado: Análise das causas e efeitos da ocupação do solo sobre o relevo: O caso da bacia hidrográfica do rio Araguari – MG. **Geousp**, no. 12, p. 105-124. 2002.
Salgado, A.A.R., Rezende, E.A., Bourlès, D., Braucher, R., Da Silva, J.R., Garcia, R.A. Relief evolution of the continental rift of Southeast Brazil revealed by in situproduced 10Be concentrations in river-borne sediments. **J. South America Earth Science**. 67: 89–99. 2016.
Salgado, A.R.; Marent, B.R.; Cherem, L.F.S.; Bourles, D.; Santos, L.J.C.; Braucher, R.; Barreto, H.N. Denudation and retreat of the Serra do Mar escarpment in southern Brazil derived from in situ-produced 10Be concentration in river sediment. **Earth Surf. Process Landf**. 39, 311 e 319. 2014.
Santos, M.; Ladeira, F. S. B.; Batezelli, A. Indicadores geomórficos aplicados à investigação de deformação tectônica: uma revisão. **Revista Brasileira de Geomorfologia.** v. 20, n. 2, p. 287-316. 2019.
Schwanghart, W., Scherler, D. Bumps in river profiles: the good, the bad, and the ugly. **Earth Surface Dynamics Discussions** 1–30. 2017.
Scuderi, L.A. Quantification of long-term erosion rates from root exposure/tree age relationships in an alpine meadow catchment. **Geomorphology**. Volume 283. p. 114-121. 2017.
Sembroni, A.; Molin, P. Long-term drainage system evolution in the Wabe Shebele River basin (SE Ethiopia-SW Somalia). **Geomorphology**. Volume 320, p. 45-63, 2018.
Siame L., Bruacher R., Bourlès D. L. Les nucléides cosmogéniques produits in situ: de noveaux outils em géomorphologie quantitative. **Bull. Soc. Géol. France**., 171(4): 383-396. 2000.
Siame, L. L., M. Sébrier, O. Bellier, D. Bourlès, C. Costa, E. A. Ahumada, C. E. Gardini, and H. Cisneros. Active basement uplift of Sierra Pie de Palo (Northwestern Argentina): Rates and inception from 10Be cosmogenic nuclide concentrations. **Tectonics**, 34, 1129-1153. 2015.
Siame, L.L., Angelier, J., Chen, R.-F., Godard, V., Derrieux, F., Bourlès, D.L., Braucher, R., Chang, K.-J., Chu, H.-T., Lee, J.-C. Erosion rates in an active orogen (NE-Taiwan): Erosion rates in an active orogen (NE-Taiwan): A confrontation of cosmogenic measurements with river suspended loads. **Quaternary Geochronology**, 6 (2), 246-260. 2011.

Siame, L; Braucher, R; Bourles, D.L. Applications of in situ-produced cosmogenic nuclides to quantitative geomorphology. **Bulletin de la Société Géologique de France**, Société géologique de France, 171 (4), pp.383-396. 2000.
Sofia, G. Combining geomorphometry, feature extraction techniques and Earth-surface processes research: The way forward. **Geomorphology**. 2020.
Sordi, M.C.; Salgado, A.A.R.; Siame, L.; Bourlès, D.; Paisani, J.C.; Léanni, L.; Braucher, R.; Couto, E.V.; ASTER Team. Implications of drainage rearrangement for passive margin escarpment evolution in southern Brazil. **Geomorphology** 306, 155–169. 2018.
Souza, D.; Stuart, F.; Rodes, A.; Pupim, F.; Hackspacher, P. Controls on the erosion of the continental margin of southeast Brazil from cosmogenic 10Be in river sediments. **Geomorphology**. 330. 2019.
Stevaux J.C.; Corradini F.A.; Aquino, S. Connectivity processes and riparian vegetation of the upper Paraná River, Brazil. **Journal of South American Earth Sciences** 46: 113-121. 2013.
Stevaux, J.C. Climatic events during the Late Pleistocene and Holocene in the Upper Parana River: Correlation with NE Argentina and South-Central Brazil. **Quatern. Int**., 72:73-85, 2000.
Stevaux, J.C. The upper Parana river (Brazil): geomorphology, sedimentology, and paleoclimatology. **Quaternary International**, v.21, p.143-161, 1994.
Stevaux, J.C.; Martins, D.P.; Meurer, M. Changes in a large regulated tropical river: The Paraná River downstream from the Porto Primavera Dam, Brazil. **Geomorphology**, v.113, p.230-238, 2009.
Stone, J. O. Air pressure and cosmogenic isotope production. **Journal of Geophysical Research**, 105(B10), 23753-23759. 2000.
Strahler, A. M. Hypsometric (area-altitude curve) analysis of erosional topography. **Geol. Soc. Amer**., Bull., Vol. 63, p. 1117- 1142, 1952.
Suertegaray, D.M.A. Erosão nos campos sulinos: arenização no sudoeste do Rio Grande do Sul. **Revista Brasileira de Geomorfologia**, Goiânia, v. 12, número especial p. 61-74, 2011.
Suertegaray, D.M.A.; Verdum, R. Desertification in the tropics. In: UNESCO (Org.) **Encyclopedia of life support systems (EOLSS)**. Paris: UNESCO Publishing, 2008.
Telbisz, T.; Kovács, G.; Székely, B.; Szabó, J. Topographic swath profile analysis: a generalization and sensitivity evaluation of a digital terrain analysis tool. **Zeitschrift Für Geomorphologie**, 57(4), 485–513. 2013.
Tricart, J. **Ecodinâmica.** Rio de Janeiro: IBGE, Diretoria Técnica, SUPREN, 1977
Van Binh, D.; Kantoush, S.; Sumi, T. Changes to long-term discharge and sediment loads in the Vietnamese Mekong Delta caused by upstream dams, **Geomorphology**. 2019.
Vasconcelos, P.; Farley, K.; Stone, J.; Piacentini, T.; Fifield, L. Stranded landscapes in the humid tropics: Earth's oldest land surfaces. **Earth and Planetary Science Letters**. 519. 152-164. 2019
Vasconcelos, T.L.; Souza, S.F.; Duarte, C.C.; Meliani, P.F.; Araújo, M.S.B.; Corrêa, A.C.B. Estudo Morfodinâmico em área do Semi-Árido do Nordeste Brasileiro: Um Mapeamento Geomorfológico em Micro-Escala. **Revista de Geografia**. Recife: UFPE – DCG/ NAPA, v.24, nº 3, p. 34-48. set/dez, 2007.
Verdum, R.; Streck, E.; Vieira, L.F.S. Degradação dos solos no Rio Grande do Sul. In: Guerra, A.J.T.; Jorge, M.C.O. (Org.). **Degradação dos solos no Brasil.** Rio de Janeiro: Bertrand Brasil, 2014.

Vieira, A.F.G.; Abreu, N.R.P. Histórico das voçorocas em Manaus-Amazonas-Brasil. **Revista Geonorte**, Edição Especial, v. 10, p. 41-45, 2014.
Viles, H.A. Technology and geomorphology: Are improvements in data collection techniques transforming geomorphic science? **Geomorphology**. 270. 2016.
von Blanckenburg, F. The control mechanisms of erosion and weathering at basin scale from cosmogenic nuclides in river sediment. **Earth and Planetary Science Letters**, 237(3-4), 462–479. 2005.
von Blanckenburg, F.; Willenbring, J. K. Cosmogenic nuclides: Dates and rates of earth-surface change. **Elements**, 10(5), 341-346. 2014.
Willett, S. D., McCoy, S. W., Perron, J. T., Goren, L. and Chen, C.-Y. Dynamic Reorganization of River Basins, **Science**, 343(6175), 2014.
Wobus, C.W.; Whipple, K.X.; Kirby, E.; Snyder, N.P.; Johnson, J.; Spyropolou, K.; Crosby, B.T.; Sheehan, D. Tectonics from topography: procedures, promise and pitfalls. In: Willett, S.D.; Hovius, N.; Brandon, M.T.; Fisher, D.M. (Eds.), **Tectonics, Climate and Landscape Evolution**: Geological Society of America, Special Paper, 398, pp. 55-74. 2006.
Wolff, R.; Hetzel, R.; Strobl, M. Quantifying river incision into low-relief surfaces using local and catchment-wide ^{10}Be denudation rates. **Earth Surf. Process. Landforms**, 43: 2327– 2341. 2018.